7-2021

Characterization of Iron-Sulfur Cluster Biogenesis in Methanogenic Archaea

Thomas Modlin Deere
University of Arkansas, Fayetteville

Characterization of Iron-Sulfur Cluster Biogenesis in Methanogenic Archaea

A dissertation submitted in partial fulfillment
of the requirements for the degree of
Doctor of Philosophy in Cell and Molecular Biology

by

Thomas Modlin Deere
Yale University
Bachelor of Arts in Molecular, Cellular, and Developmental Biology, 2009

July 2021
University of Arkansas

This dissertation is approved for recommendation to the Graduate Council.

_____
Daniel Lessner, Ph.D.
Dissertation Director

_____
Paul Adams, Ph.D.
Committee Member

_____
Mack Ivey, Ph.D.
Committee Member

_____
Timothy Kral, Ph.D.
Committee Member

_____
David McNabb, Ph.D.
Committee Member

ABSTRACT

Iron-sulfur (Fe-S) clusters are among the oldest cofactors on the planet, used by proteins in almost all forms of life on Earth to carry out processes ranging from energy transfer to DNA replication. Among the organisms believed to use these Fe-S proteins more extensively than almost any others are the methanogens, an ancient lineage of archaeal microbes that produce methane as a required product of their metabolism. Methane, the primary component of commercial natural gas, is both a potent greenhouse gas and an important fossil fuel. It can also be renewably produced as a biofuel. Biogenic methane is almost entirely a product of archaea carrying out methanogenesis, a metabolic process with an absolute requirement for Fe-S clusters at multiple steps. They are also believed to be the lineage in which nitrogen fixation began, an activity that uses multiple Fe-S proteins to convert nitrogen gas into ammonia, which can be used by microbes and plants for growth. Despite this heavy reliance on Fe-S proteins, we know very little about how Fe-S clusters are generated in these methanogens. This process is well understood in bacteria and eukaryotes, but what little we know about archaeal Fe-S biogenesis suggests that the mechanisms in these organisms may not work the way they do in the other two domains. This dissertation presents several different but related projects undertaken to gain a deeper understanding of Fe-S cluster biogenesis in methanogenic archaea. Methanogens contain homologs of proteins known to function in Fe-S cluster biogenesis in bacteria and eukaryotes, including components of the ISC and SUF systems, as well as an ApbC Fe-S carrier protein. To test the hypothesis that these proteins have similar roles in methanogens, I employed biochemical and genetic approaches to assess the function of these homologs in the model methanogen *Methanosarcina acetivorans*. The primary avenue of investigation was a characterization of heterologously expressed putative ISC-type Fe-S cluster biogenesis proteins, and an assessment

of the effects of deleting the genes encoding them, from *M. acetivorans*. Another subject of study was the putative Fe-S carrier protein ApbC, whose gene I also deleted. Finally, I demonstrated the feasibility of a CRISPR/Cas9 genome editing system that was recently developed for *M. acetivorans* by deleting the genes for a putative SUF-type Fe-S biogenesis system. My results demonstrate that *M. acetivorans* contains a functional ISC system but that the system is not essential. However, the results support the ISC system playing an important role in nitrogen fixation, potentially supplying Fe-S clusters to nitrogenase, but only when cysteine is the sulfur source. ApbC is also not essential but seems to be important for growth with certain sulfur sources, especially the thiosulfate ion. Deletion of SUF failed to produce any phenotype indicating SUF is not the primary Fe-S cluster biogenesis system in methanogens. Taken together, these results suggest that despite the evidence from bacteria and eukaryotes, and counter to the conclusions a bioinformatic approach would indicate, the ISC, ApbC, and perhaps even SUF cluster biogenesis systems individually appear surprisingly dispensable in methanogens.

ACKNOWLEDGMENTS

I could not have achieved this work without the unflagging efforts of my colleagues and collaborators, and I must thank them for their parts in helping me to this finish line. While I came into this program with an undergraduate degree in Molecular, Cellular, and Developmental Biology, I think it's fair to say I would have had no idea what I was doing in the laboratory without the wisdom and patience of Dr. Faith Lessner. She and my then-fellow graduate student, Dr. Matt "Skippy" Jennings, taught me the esoteric arts of working with methanogens, a body of knowledge I am privileged to pass on to the best of my abilities to newer members of the lab whenever I have the chance. For further help, be it as sounding boards, extra pairs of hands, or generous providers of purified protein, I am grateful to Drs. Addison McCarver, Ahmed Dhamad, and Carly Engel, graduate students Ryan Sheehan, Melissa Chanderban, Jasleen Saini, and Jadelyn Hoerr, as well as undergraduates Chris Hill, Adam Ratliff, and Madison Martinez.

Our collaborators in the laboratory of Prof. Evert Duin at Auburn University have been invaluable in helping me with EPR spectroscopy, and I doubt I could have learned my way around a gas chromatograph without the patient assistance of Erik Pollock in the University of Arkansas Stable Isotope Laboratory. The systems and tools developed by Prof. Williams Metcalf and his research group at the University of Illinois, Urbana-Champaign have made my genetic work possible.

Above all, I want to thank my advisor, Prof. Dan Lessner. He has helped me at every step along the winding road of my Ph.D. studies, buoying my spirits when experiments didn't pan out, tempering unrealistic expectations when I got ahead of myself, and giving me a nudge when I grew complacent or distracted. He taught me to think like a scientist, and I hope I can do the same for others as I move into the next phase of my career.

DEDICATION

It has been my great fortune to be surrounded by love and support in my life, and I can say that what is good in me I owe to my parents, Beth and David Deere. They have never stopped believing in me, even in times when I've felt like a failure, I always knew they couldn't see me that way. I've had the benefit of a strong-minded and protective big sister, and knowing that I can call on Molly for help or advice whenever I need it is a true comfort.

My wife Debbie brightens my life in a way that I can't fully express with words. I am reminded every day of how lucky I am to have her in my life, and she more than anyone has kept me level through the trials of my doctoral studies. My daughters Juliet and Sarah have been constant, adorable companions since they joined my life, distracting and inspiring me, and I'm so incredibly grateful for them. I love them fiercely, and I can't wait to see what great things they will do, even if they decide not to go into science.

To all of you, my loved ones, I dedicate this labor of love and not infrequent frustration.

TABLE OF CONTENTS

LIST OF PUBLISHED PAPERS

Chapter I - Deere TM, Prakash D, Lessner FH, Duin EC, Lessner DJ. *Methanosarcina acetivorans* contains a functional ISC system for iron-sulfur cluster biogenesis. *BMC Microbiology*. 2020 20(1):323.
(https://bmcmicrobiol.biomedcentral.com/articles/10.1186/s12866-020-02014-z)
doi: 10.1186/s12866-020-02014-z.

INTRODUCTION

As science has engaged with the questions of life's origins on Earth and how they have influenced its subsequent development down to modern biology, a key focus has been interactions with the early-Earth environment, especially its atmospheric and marine conditions. Striking differences from present-day conditions include the likely absence of gaseous oxygen, especially prior to around 2.5 billion years ago (Bekker *et al*., 2004). Early oceans likely also went through periods of relatively high concentrations of reduced ionic species including iron (Fe^{2+}) and sulfur (S^{2-}). This anoxic, iron- and sulfide-rich marine environment would likely have favored the spontaneous formation of various pyrites (iron sulfide compounds that can precipitate out of solution, especially upon oxidation) as well as iron-sulfur clusters (nanocrystalline structures frequently abbreviated as [Fe-S]). This chemical process can occur abiotically and has been invoked in one popular theory of the origins of metabolism in life on Earth, the so-called "Iron-Sulfur World" first proposed by Günter Wächtershäuser (Wächtershäuser, 1990). The iron-sulfur clusters themselves are excellent surfaces for reduction-oxidation ("redox") reactions in which molecules gain and lose electrons due to the ability of the iron atoms in [Fe-S] to reversibly change oxidation states (Johnson *et al*., 2005). As proteins developed and diversified, incorporating [Fe-S] to catalyze redox reactions not easily accommodated by proteins alone would have also conferred the ability to link protein secondary and tertiary structure to the status of the cluster bound by an Fe-S protein (Beinert *et al*., 1997). This incorporation is achieved by binding the iron atoms of an [Fe-S] with amino acid side-chains as depicted in **Figure 1.** Employing numerous Fe-S proteins involved in processes ranging from DNA replication and repair to central metabolism, allowing these activities to be coupled to sensing the oxidation/reduction (redox) state of the cell and availability of elements required to build [Fe-S], is a strategy that would have served prokaryotic life well on early Earth.

Genomic analysis indicates that modern anaerobes still code for many more Fe-S proteins than do aerobes (Major *et al*., 2004).

There are numerous types of [Fe-S], broadly identified by the number of Fe and S atoms making up the cluster. The simplest widely seen form is an essentially planar [2Fe-2Fe], but the most widely conserved Fe-S protein types incorporate a [4Fe-4S] arranged in a cubane structure with Fe and S atoms arranged at alternating vertices (**Figure 1**). In vitro experiments support interconversion between these forms, for instance tracking with spectroscopy and chromatography the assembly of first one and then a second [2Fe-2S] cluster, followed by a reductive coupling synthesis of a single [4Fe-4S] cluster, all in the same protein complex (Agar *et al*., 2000). Larger cluster forms are occasionally seen, e.g. [8Fe-8S] or [8Fe-7S], presumably also formed initially from smaller-order [Fe-S]. Special metal-sulfide clusters can include the addition or substitution of other metal atoms in addition to or in place of Fe atoms; characterized examples include molybdenum (Mo), vanadium (V), and nickel (Ni) (Fontecave, 2006). In many cases, [Fe-S] can also be modified by removal of one or more atoms (either Fe or S), or by covalent attachment of ligands such as cyanide or homocysteine moieties (Fontecilla-Camps *et al*., 2007, Hu & Ribbe, 2011). Whatever the form of the [Fe-S] in question, its attachment to the Fe-S protein that coordinates it is via covalent bonds between Fe atoms composing the cluster and amino acid side chains in the protein. The most common arrangement involves four L-cysteine side chains whose organic sulfhydryl (thiol) groups must be in their reduced form to be free to coordinate a cluster. The spacing of these cysteine residues in the protein primary structure is generally highly conserved in particular motifs, with the bacterial ferredoxin $CXXCXXC(X)_nCP$ fold serving as a prototypical example (Child *et al*., 2018). Important deviations from this pattern can include fewer coordinating residues or other amino acids, e.g. L-

histidine or L-aspartic acid side chains, providing the coordinating ligand for the Fe atoms of [Fe-S] (Johnson *et al*., 2005). The nature and pattern of which residues occur in the primary structure appear to determine many of the characteristics of the [Fe-S] cluster bound by an Fe-S protein. For example, aconitase, a critically important enzyme in the tricarboxylic (TCA), sometimes called the Krebs or citric acid, cycle binds a [4Fe-4S] that is required for catalytic activity. Aconitase is easily deactivated by oxidation and prone to loss of one Fe under these conditions, converting its cluster to [3Fe-4S], due in part to the absence of a fourth coordinating cysteine side-chain (Beinert *et al*., 1996).

The redox properties of [Fe-S] may account for the versatility of this prosthetic group and its application to so many enzymatic and regulatory processes. Since the transition metal Fe can commonly occupy either of the Fe^{2+} or Fe^{3+} oxidation states, and in the environment of a coordinated Fe-S cluster sulfur is typically restricted to a state of S^{2-}, a typical bacterial ferredoxin [Fe-S] could theoretically occupy any integer charge state from $[4Fe\text{-}4S]^{0}$ through $[4Fe\text{-}4S]^{4+}$, but the latter is not seen. Generally speaking, such clusters are observed transitioning from $[4Fe\text{-}4S]^{+}$ to $[4Fe\text{-}4S]^{2+}$ and back (Johnson *et al*., 2005). Such one electron transfer events can occur either intramolecularly, e.g. with another [Fe-S] or a flavin, or intermolecularly, as is the function of typical ferredoxins. Precise properties such as the midpoint reduction potential of a given [Fe-S] are tuned by the protein environment, including amino acid side chains not directly involved in coordinating the cluster but still located nearby in the tertiary or quaternary folds. Numerous [Fe-S] actually bridge across protein subunits, with coordinating side chain ligands provided by different molecules (Hu & Ribbe, 2013). The changes in oxidation states and overall charge are associated with changes in the spin states of an [Fe-S], which can be of integer and half-integer values. This allows certain clusters in specific states (more precisely,

superexchanges between Fe atoms) to be characterized using a technique called electron paramagnetic resonance (EPR) spectroscopy. Oxidized [Fe-S], for instance $[4Fe\text{-}4S]^{2+}$, are often EPR-silent due to their spin states (Hagen, 2018).

Abiotic [Fe-S] formation is a relatively slow and unregulated process, necessitating the development of biologically-guided cluster biogenesis for reliable formation of properly-constituted clusters. Early understanding of how [Fe-S] are assembled in cells arose naturally in research of organisms known to use multiple metal-sulfur proteins in processes such as biological dinitrogen (N_2) fixation, or diazotrophy. The free-living aerobic bacterium *Azotobacter vinelandii* was shown to possess a suite of genes whose disruption virtually eliminates the ability to grow diazotrophically, even when the genes coding for nitrogenase (the protein complex responsible for fixing dinitrogen) were undisturbed (Kennedy & Dean, 1992). Given their association with the larger cluster of genes involved in diazotrophy in *A. vinelandii*, the *nif* (nitrogen fixation) operon, these genes, particularly *nifS* and *nifU*, have come to be considered the core of the "NIF" system of [Fe-S] biogenesis. Sequence homology searches revealed the presence of NifS/NifU-like protein-coding genes elsewhere in the *A. vinelandii* genome, leading to the discovery and elucidation of a more generalized, "housekeeping" system of Fe-S biogenesis, the "ISC" (iron-sulfur cluster) system (Zheng *et al*., 1998, Outten *et al*., 2004). This Fe-S biogenesis system is broadly conserved among bacteria and eukaryotes, including model organisms like *Escherichia coli*. The Isc core components (IscS/IscU) were similar to their Nif counterparts, with some important differences (**Figure 2**). IscU resembles the N-terminal domain of NifU, and IscS has similar enzymatic activity to NifS, but neither of the Isc proteins can confer full nitrogen fixation activity when its Nif counterpart has been deleted. Further sequence homology analysis, supported by genetic and biochemical characterization,

soon led to the discovery of a third system for Fe-S biogenesis found in numerous bacteria and eukaryotic plastids, the so-called "SUF" (sulfur assimilation, or mobilization) system (Takahashi & Tokumoto, 2002). Common to all three characterized systems, NIF, ISC, and SUF, are two core components (**Figure 3**): a cysteine desulfurase protein (NifS, IscS, or SufS) that catalyzes the cleavage of the sulfhydryl group from L-cysteine molecules, and a scaffold (NifU, IscU, or $SufB_xC_2(D)$) upon which [Fe-S] can be assembled (Agar *et al.*, 2000, Frazzon *et al*., 2002, Layer *et al*., 2007). The mechanism of the cysteine desulfurase "S" proteins involves the formation of a bound persulfide intermediate with the aid of a pyridoxal 5'-phosphate (PLP) prosthetic group. In terms of sulfur chemistry, this bound atom is in an S^0 oxidation state, and so is considered part of the larger pool of sulfane sulfur in the cell. This intermediate enzyme-bound structure links Fe-S cluster biogenesis to more general sulfur metabolism within cells. The biosyntheses of molybdenum cofactors, and also 2-thiouridine in tRNA's, relies upon a "sulfur relay" system whose first input is a persulfide, typically bound to IscS (Black & Dos Santos, 2015, Leimkühler *et al*., 2017).

Direct transfer of a mature [Fe-S] from scaffold to target apo-protein is well-documented in numerous model systems, but this process can be accelerated or mediated by various accessory proteins. The ISC system in particular makes use of a pair of chaperone proteins called HscA and HscB that are homologous to the general heat-shock proteins DnaK and DnaJ, to stimulate transfer of [Fe-S] to target proteins such as ferredoxins (Chandramouli & Johnson, 2006). Also widely conserved are Fe-S carrier proteins that can accept [Fe-S] from a scaffold, or perhaps even serve as an alternative scaffold, before delivering the mature cofactor to an apo-protein. These carriers are sorted into the "A" types, e.g. IscA or SufA, and the ApbC homologs (Pinske & Sawers, 2012, Boyd *et al*., 2008[a], Boyd *et al*., 2008[b]). Eukaryotic [Fe-S] biogenesis

and transfer incorporates an even greater array of accessory proteins, and in most cases entire complementary systems at work in the nucleus, cytosol, mitochondria, and plastids (Grosche *et al*., 2018; Lill *et al*., 2006). The prokaryotic systems studied to date generally function with a much smaller suite of components as described above. What is largely unknown at this time is what this biogenesis machinery looks like specifically in the non-bacterial prokaryotes of domain Archaea.

Archaea were first proposed as a distinct phylogenetic lineage by Carl Woese and George Fox in 1977 based on the sequence of rDNA coding for the 16S subunit of the ribosome, demonstrating a fundamental difference within the prokaryotes, until then considered a monophyletic bacterial "Kingdom" (Woese & Fox, 1977). The current three-domain model of life on Earth incorporates this distinction, though others have been elucidated since that further support the separation of the domains Bacteria, Archaea, and Eukaryota. Alongside their cell organization and metabolic pathways that parallel those of bacteria, and their DNA/RNA polymerases and ribosomes bearing significant homology to those of eukaryotes, archaea possess a number of unique features. Phospholipids from archaeal cell membranes feature glycerol-1-phosphate moieties ether-linked to isoprene chains that can sometimes be fused tail-to-tail, converting a phospholipid bilayer into a stratified monolayer. Cell membrane phospholipids from bacteria and eukaryotes typically contain glycerol-3-phosphate moieties ester-linked to fatty acid chains. How this "lipid divide" came to be is still an open question (Villanueva *et al*., 2017, Imachi *et al*., 2020). Many archaea grow under conditions even more hot, acidic, or hypersaline than those known to harbor extremophilic bacteria, and it is postulated that their unique lipid envelope may confer additional protection in these environments (Caforio & Driessen, 2017). These differences between the domains do not extend to reliance on Fe-S proteins for

metabolism and regulation, a seemingly unifying property of all three domains of life. Anaerobic archaea appear to encode large numbers of predicted Fe-S proteins, in particular the methanogens (Sousa *et al.*, 2013, Major *et al*., 2004).

Methanogens are a variegated group of prokaryotes comprising seven orders of strict anaerobes whose central metabolism relies upon the reduction of carbon species to methane. The primordial methanogens are thought to have arisen roughly 3.5 Ga (Wolfe & Fournier, 2018), likely originally conserving energy by coupling the oxidation of dihydrogen (H_2) to protons with the reduction of carbon dioxide (CO_2) to methane (CH_4), called the "hydrogenotrophic" pathway. A process of evolutionary diversification over ensuing eons has yielded expanded metabolic complexity in some lineages of methanogens. So-called "basal" methanogens in orders Methanobacteriales, Methanococcales, and Methanopyrales are restricted to hydrogenotrophic methanogenesis, occasionally using formate as an electron donor in place of H_2. Two of the four "derived" orders, Methanocellales and Methanomicrobiales, broadly preserve the hydrogenotrophic pathway, with the added ability to reduce methylated compounds such as methanol and methylamines to methane, oxidizing some molecules of the organic carbon compound to CO_2 to generate reducing equivalents necessary for reduction of other methyl groups to CH_4. This "methylotrophic" pathway is also mostly conserved in the other two derived orders, Methanomassiliicoccales and Methanosarcinales, with some caveats. Methanomassiliicoccales, like isolated members of Methanobacteriales and Methanosarcinales, are unable to reduce methylated compounds to CH_4 using the oxidation of methylated compounds to provide electrons, instead relying on H_2 oxidation for reducing equivalents (Lang *et al*., 2015). Methanosarcinales possess a third distinct pathway for methanogenesis, in which the two-carbon compound acetate is disproportionated, with the carbonyl group being oxidized

to CO_2 to provide reducing equivalents for the methyl group to be reduced to CH_4. This "aceticlastic" pathway is restricted to this one order of cytochrome-containing methanogens; members of genus *Methanosaeta* even rely upon this pathway exclusively. Members of genus *Methanosarcina* generally possess all three pathways of methanogenesis, particularly so the freshwater strains (**Figure 4**). Marine strains of this genus have proved unable to oxidize H_2 to reduce CO_2, though the genes for the entire pathway are preserved (Guss *et al*., 2009). While growth on H_2/CO_2 is infeasible, these marine Methanosarcinales can dissimilate carbon monoxide (CO), oxidizing some equivalents to CO_2 to reduce another to CH_4 in a scheme reminiscent of the methylotrophic pathway. *Methanosarcina acetivorans* is a particularly well-studied example of this phenomenon, and it happens to code for more of certain classes of Fe-S proteins than almost any other known organism (Major *et al*., 2004).

While methane is a diffusible waste product for methanogens, the molecule itself serves as an important electron donor for numerous organisms, both aerobic and anaerobic. It is also a major fuel source for human industry, as methane is the dominant alkane component of the natural gas used to cook in and heat countless homes. Methane is additionally a potent contributor to anthropogenic climate change via the greenhouse effect, showing a 96-fold higher radiative forcing effect per molecule over a 20-year time scale versus CO_2 (Alvarez *et al.*, 2018, Etminan *et al.*, 2016). From a geochemical perspective, methanogenesis drives an important part of the global carbon cycle, ensuring that fermentation products such as organic acids like acetic acid do not accumulate in anaerobic environments, which could alter environmental pH and potentially sink carbon out of availability to less reducing biomes closer to the atmosphere. Instead, methane oxidation by consortia of bacteria and archaea reducing nitrates and sulfates

links the global carbon cycle to the nitrogen and sulfur cycles (Haroon *et al*., 2013, McGlynn *et al*., 2015).

The anaerobic environment in which methanogens and numerous other prokaryotes grow has important implications for iron and sulfur chemistries. In the reducing interior of cells, common metabolic enzymes catalyzing redox reactions can interact with the dioxygen molecule (O_2), as well as reduced iron species such as Fe^{2+}, in a cascade of reactions referred to as Fenton chemistry. The products include reactive oxygen species (ROS) that can not only destroy [Fe-S] but also damage vital molecules such as DNA (**Figure 5**) (Imlay, 2003). In environments where encounters with O_2 are rare, there is relatively little risk in broad use of cofactors containing reduced iron, and the ion itself is likely comparatively plentiful. Reduced sulfur species such as S^{2-} and HS^- are also more likely to be encountered in a low-O_2 habitat, as more oxidized sulfur species are utilized as electron acceptors for central metabolism by sulfate-reducing bacteria (SRB). SRB (as well as archaea with similar metabolic pathways) are thought to be at least as ancient as methanogens and they can establish syntrophic relationships with each other, so methanogens likely evolved under conditions in which the sulfur component of [Fe-S] was readily available (Plugge *et al*., 2011).

As important as Fe-S proteins are methanogens, the current state of knowledge regarding [Fe-S] biogenesis in methanogens, and in Archaea more broadly, is quite limited. Sequence homology analysis of the relevant genomes fully sequenced to date suggest that the Suf system may be essentially universal, leading to speculation this core system is primordial for the entire domain (Liu *et al*., 2010, Boyd ES *et al*., 2014). Intriguingly, these same analyses suggest that ApbC is similarly universal to the domain, but the housekeeping Isc system is only sparsely distributed among archaea. In fact, many of these prokaryotes appear to lack cysteine

desulfurases altogether, a prediction borne out by methanogens such as *Methanococcus* spp. being unable to grow using L-cysteine as a sole sulfur source (Whitman *et al*., 1982). There is detectable desulfurization of cysteine in cell-free lysates from these species, so there is likely some unknown enzyme catalyzing this reaction, either at some level insufficient for growth and reproduction or as part of a process that somehow renders this sulfur unavailable for general use. What is known is that cysteine cannot serve as the sulfur source either for methionine synthesis or [Fe-S] biogenesis in the model methanogen *Methanococcus maripaludis* (Liu *et al*., 2010). Inorganic sulfide is incorporated, either directly or via more mediated processes, into [Fe-S] and likely also other pathways for biosynthesis of sulfur-containing compounds, possibly through a sulfur-relay like system involving persulfides bound to unknown proteins (Liu *et al*., 2012).

If the sequence homology results to date are reflective of evolutionary history in the domain Archaea, a minimal Suf system composed of the two proteins SufB and SufC, typically arranged in the genome as an operon *sufCB*, may be sufficient to function as a scaffold for [Fe-S] biogenesis *in vivo*, with inorganic sulfide providing the sulfur components to a B_2C_2 scaffold complex. ApbC is likely able to function as a carrier protein or alternative scaffold in archaea, as *apbC* genes from archaea of the orders Methanococcales and Sulfolobales, recombined into *Salmonella enterica*, were shown to correct a growth defect arising from deletion of the native copy of *apbC* (Boyd *et al*., 2009). Even more direct evidence has confirmed that ApbC from *M. maripaludis* is capable of transferring [4Fe-4S] *in vitro*, and that it is not an essential gene in that methanogen (Zhao *et al*., 2020). Isc homologs, as noted, appear less widely distributed among archaea, though in certain clades microbes are likelier than not to code for an IscS-like cysteine desulfurase and an IscU-like [Fe-S] scaffold. The four "derived" orders of methanogens described above tend to code for at least one copy each of the core Isc genes, typically arranged

as *iscSU*, and among *Methanosarcina* spp. the genes appear more than once in the chromosome. Among the three "basal" orders, only members of Methanobacteriales code for IscSU, and only sporadically. No archaeon yet isolated and sequenced appears to lack both the Isc and Suf systems.

If the Suf system is indeed primordial in archaea, the question of the origins of the Isc system in this domain must be addressed. The sequences of archaeal *iscS* and *iscU* compared to those of bacterial genes suggest the possibility of horizontal gene transfer (HGT) from bacteria. For instance methanogen Isc proteins closely resemble those of bacteria in order Clostridiales. Methanogens have been identified growing in syntrophic communities with these bacteria (Weimer & Zeikus, 1979). In fact, HGT from this same clade of organisms is theorized to have bestowed upon archaea in Methanosarcinales the ability to metabolize acetate as a growth substrate, though this hypothesis is a subject of some dispute (Fournier & Gogarten, 2008, Barnhart *et al*., 2015). The relative enrichment of Isc genes in the cytochrome-containing Methanosarcinales raises intriguing possibilities with respect to the evolution of [Fe-S] biogenesis in response to environmental factors, given that cytochromes are one of the key vulnerabilities for cellular toxicity from excess free sulfide (Pietri *et al*., 2011, Fu *et al*., 2018). Significantly, no archaea appear to code for true genuine NifS and untruncated NifU as they are depicted in **Figure 2**. The nitrogenase complex is known to bind multiple Fe-S clusters, and it is unclear how these are assembled in methanogens since there are no predicted NifS/NifU genes.

The classic bacterial nitrogenase is a two-component metalloprotein complex, comprising the "iron (Fe) protein" coded for by *nifH*, and the "molybdenum-iron (MoFe) protein" coded for by *nifD* and *nifK*. The Fe protein is a $NifH_2$ homodimer, while the MoFe protein is a NifDK heterodimer, in both cases coordinating [Fe-S] when mature and functional. The Fe protein

(dinitrogenase reductase) contains a conventional [4Fe-4S] that lends the protein its activity as a reductase of the MoFe protein (dinitrogenase), with reducing equivalents provided by a ferredoxin or flavodoxin (Yang *et al*., 2016). Electrons are transferred to the MoFe protein, arriving at an atypical [8Fe-7S] called the "P cluster." This cluster bridges the NifDK subunits and resembles two [4Fe-3S] cubanes bridged by a sulfur atom (Hu & Ribbe, 2013). The P cluster further transfers electrons to an even more unusual metallocofactor at the catalytic site of MoFe protein, referred to as the iron-molybdenum cofactor (FeMoCo) or "M cluster." The M cluster [$MoFe_7S_9C$-homocitrate], is directly involved in the delivery of electrons to the substrate dinitrogen molecule. Four cycles of two-electron delivery at this site is sufficient to reduce one N_2 molecule to two molecules of ammonia per the overall reaction:

$$N_2 + 8H^+ + 8e^- + 16ATP \rightarrow 2NH_3 + H_2 + 16ADP + 16P_i$$

This enzyme complex is now frequently referred to as the Mo nitrogenase, after the Mo-containing M cluster, because two natural nitrogenase variants were subsequently described with either vanadium (V) or iron (Fe) taking the place of Mo in the M cluster (Boyd & Peters, 2013). These are encoded by the *vnf* and *anf* operons, respectively, and the dinitrogenases include an extra "G" subunit. VnfDGK and AnfDGK show altered kinetics and stoichiometry compared to NifDK. V nitrogenase follows the overall reaction scheme (Rehder, 2000):

$$N_2 + 12H^+ + 12e^- + 24ATP \rightarrow 2NH_3 + 3H_2 + 24ADP + 24P_i$$

The Fe nitrogenase catalyzes the most energetically costly overall reaction (Harris *et al*., 2018):

$$N_2 + 24H^+ + 24e^- + 48ATP \rightarrow 2NH_3 + 9H_2 + 48ADP + 48P_i$$

The nitrogenase complex, especially the Fe protein, is especially sensitive to oxygen, so nitrogen fixation must occur in anaerobic environments or the enzyme complex must be protected from O_2. Biological nitrogen fixation is theorized to have begun 2.2-2.5 Ga, at a time when marine

environments were still largely anaerobic. Given the poor solubility parameters of molybdenum ions in anaerobic solutions, intuition led some to speculate that one of the "alternative" (V or Fe) nitrogenases must have arisen first, with the improved energetics of the Mo nitrogenase becoming available later. However, molecular phylogeny suggests that Mo nitrogenase is the original form, with V and Fe nitrogenases evolving later (Boyd & Peters, 2013). Furthermore, this original nitrogenase is hypothesized to have developed within the methanogen lineage, and while the three nitrogenase systems have been most thoroughly characterized from bacteria, all three can be found in domain Archaea, solely in the methanogenic orders (Boyd *et al*., 2015, Dos Santos *et al*., 2012). This distribution does not map to the distribution of the *nifSU*-like *iscSU* genes, either negatively or positively. For instance, both the basal methanogen *M. maripaludis* (codes for SUF only) and the derived methanogen *Methanosarcina barkeri* (codes for ISC and SUF) possess *nif* genes and are capable of diazotrophic growth (Kessler *et al*., 1998, Murray & Zinder, 1984).

This dissertation examines the biogenesis of [Fe-S] clusters in methanogenic archaea by employing a combination of genetic and biochemical approaches. The model used for *in vivo* study and as the genetic source of the proteins used is *Methanosarcina acetivorans* C2A (in addition to the pseudo-wildtype strain WWM73 for genetic manipulations). The reasons for this choice are several: this methanogen codes for multiple putative Isc & Suf protein systems as well as the ApbC carrier protein, it appears to possess all three known nitrogenases (Mo, V, and Fe), it is metabolically flexible (uses all three known pathways of methanogenesis), and is genetically tractable thanks to a system designed by Prof. William Metcalf and others, and already in wide use in our research laboratory (Sowers *et al*., 1984, Galagan *et al.*, 2002; Metcalf *et al*., 1997). The genetic system allows for targeted deletion of genes of interest, as well as complementation

in trans. The nitrogenase complex presents an especially attractive Fe-S protein target system given the conditional nature of its expression.

The putative Isc gene clusters in *M. acetivorans* are minimal as compared to the well-characterized ISC system in *E. coli*, and this pattern of simplicity seems to be typical for archaea (**Figure 6**). The same can be said of the putative Nif, Vnf, and Anf gene clusters (**Figure 7**). Taking into account the information currently available regarding [Fe-S] biogenesis in various methanogenic archaea as well as the potential for specialization given its apparent redundancy in cluster building systems, we have proposed a theoretical model of cluster biogenesis and delivery in *M. acetivorans*: (**Figure 8**). This dissertation presents my work to verify or reject various aspects of this model by answering a number of research questions:

1. Does *Methanosarcina acetivorans* use an ISC system to synthesize and deliver [Fe-S] to apo-proteins? Is it essential?

2. Are other systems for Fe-S cluster biosynthesis and delivery active in *M. acetivorans*? ISC systems are our primary focus, but what is the importance of SUF and/or ApbC?

3. How does *M. acetivorans* generate a functional nitrogenase without a NIF system of [Fe-S] biogenesis? Are the ISC and/or SUF systems involved?

References

Agar, J.N., C. Krebs, J. Frazzon, B.H. Huynh, D.R. Dean, & M.K. Johnson, (2000) IscU as a scaffold for iron-sulfur cluster biosynthesis: sequential assembly of [2Fe-2S] and [4Fe-4S] clusters in IscU. *Biochemistry.* 39: 7856-62.

Alvarez, R.A., D. Zavala-Araiza, D.R. Lyon, D.T. Allen, Z.R. Barkley, A.R. Brandt, K.J. Davis, S.C. Herndon, D.J. Jacob, A. Karion, E.A. Kort, B.K. Lamb, T. Lauvaux, J.D. Maasakkers, A.J. Marchese, M. Omara, S.W. Pacala, J. Peischl, A.L. Robinson, P.B. Shepson, C. Sweeney, A. Townsend-Small, S.C. Wofsy, & S.P. Hamburg, (2018) Assessment of methane emissions from the U.S. oil and gas supply chain. *Science*. 361: 186-188.

Barnhart, E.P., M.A. McClure, K. Johnson, S. Cleveland, K.A. Hunt, & M.W. Fields, (2015) Potential Role of Acetyl-CoA Synthetase (acs) and Malate Dehydrogenase (mae) in the Evolution of the Acetate Switch in Bacteria and Archaea. *Sci Rep*. 5: 12498.

Beinert, H., M.C. Kennedy, & C.D. Stout, (1996) Aconitase as Iron-Sulfur Protein, Enzyme, and Iron-Regulatory Protein. *Chem Rev*. 96: 2335-2374.

Beinert, H., R.H. Holm, & E. Münck, (1997) Iron-sulfur clusters: nature's modular, multipurpose structures. *Science*. 277: 653-9.

Bekker, A., H.D. Holland, P.-L. Wang, D. Rumble 3rd, H.J. Stein, J.L. Hannah, L.L. Coetzee, & N.J. Beukes, (2004) Dating the rise of atmospheric oxygen. *Nature*. 427: 117-20.

Black, K.A. & P.C. Dos Santos, (2015) Abbreviated Pathway for Biosynthesis of 2-Thiouridine in Bacillus subtilis. *J Bacteriol*. 197: 1952-62.

Boyd, E.S. & J.W. Peters, (2013) New insights into the evolutionary history of biological nitrogen fixation. *Front Microbiol*. 4: 201.

Boyd, E.S., K.M. Thomas, Y. Dai, J.M. Boyd, & F.W. Outten, (2014) Interplay between oxygen and Fe-S cluster biogenesis: insights from the Suf pathway. *Biochemistry*. 53: 5834-47.

Boyd, E.S., A.M.G. Costas, T.L. Hamilton, F. Mus, & J.W. Peters, (2015) Evolution of molybdenum nitrogenase during the transition from anaerobic to aerobic metabolism. *J Bacteriol*. 197: 1690-9.

Boyd, J.M., A.J. Pierik, D.J.A. Netz, R. Lill, & D.M. Downs, (2008) Bacterial ApbC can bind and effectively transfer iron-sulfur clusters. *Biochemistry*. 47: 8195-202.

Boyd, J.M., J.A. Lewis, J.C. Escalante-Semerena, & D.M. Downs, (2008) Salmonella enterica requires ApbC function for growth on tricarballylate: evidence of functional redundancy between ApbC and IscU. *J Bacteriol*. 190: 4596-602.

Boyd, J.M., R.M. Drevland, D.M. Downs, & D.E. Graham, (2009) Archaeal ApbC/Nbp35 homologs function as iron-sulfur cluster carrier proteins. *J Bacteriol*. 191: 1490-7.

Caforio, A. & A.J.M. Driessen, (2017) Archaeal phospholipids: Structural properties and biosynthesis. *Biochim Biophys Acta Mol Cell Biol Lipids*. 1862: 1325-1339.

Chandramouli, K. & M.K. Johnson, (2006) HscA and HscB stimulate [2Fe-2S] cluster transfer from IscU to apoferredoxin in an ATP-dependent reaction. *Biochemistry*. 45: 11087-95.

Child, S.A., J.M. Bradley, T.L. Pukala, D.A. Svistunenko, N.E. Le Brun, & S.G. Bell, (2018) Electron transfer ferredoxins with unusual cluster binding motifs support secondary metabolism in many bacteria. *Chem Sci*. 9: 7948-7957.

Dos Santos, P.C., D.C. Johnson, B.E. Ragle, M.-C. Unciuleac, & D.R. Dean, (2007) Controlled expression of nif and isc iron-sulfur protein maturation components reveals target specificity and limited functional replacement between the two systems. *J Bacteriol*. 189: 2854-62.

Dos Santos, P.C., Z. Fang, S.W. Mason, J.C. Setubal, & R. Dixon, (2012) Distribution of nitrogen fixation and nitrogenase-like sequences amongst microbial genomes. *BMC Genomics*. 13: 162.

Etminan, M., G. Myhre, E.J. Highwood, & K.P. Shine, (2016) Radiative forcing of carbon dioxide, methane, and nitrous oxide: A significant revision of the methane radiative forcing. *Geophys Res Lett*. 43: 12,614-23

Fontecave, M., (2006) Iron-sulfur clusters: ever-expanding roles. *Nat Chem Biol*. 2: 171-4.

Fontecilla-Camps, J.C., A. Volbeda, C. Cavazza, & Y. Nicolet, (2007) Structure/function relationships of [NiFe]- and [FeFe]-hydrogenases. *Chem Rev*. 107: 4273-303.

Fournier, G.P. & J.P. Gogarten, (2008) Evolution of acetoclastic methanogenesis in Methanosarcina via horizontal gene transfer from cellulolytic Clostridia. *J Bacteriol.* 190: 1124-7.

Frazzon, J. & D.R. Dean, (2003) Formation of iron-sulfur clusters in bacteria: an emerging field in bioinorganic chemistry. *Curr Opin Chem Biol*. 7: 166-73.

Frazzon, J., J.R. Fick, & D.R. Dean, (2002) Biosynthesis of iron-sulphur clusters is a complex and highly conserved process. *Biochem Soc Trans*. 30: 680-5.

Fu, L.-H., Z.-Z. Wei, K.-D. Hu, L.-Y. Hu, Y.-H. Li, X.-Y. Chen, Z. Han, G.-F. Yao, & H. Zhang, (2018) Hydrogen sulfide inhibits the growth of Escherichia coli through oxidative damage. *J Microbiol*. 56: 238-245.

Galagan, J.E., C. Nusbaum, A. Roy, M.G. Endrizzi, P. Macdonald, W. FitzHugh, S. Calvo, R. Engels, S. Smirnov, D. Atnoor, A. Brown, N. Allen, J. Naylor, N. Stange-Thomann, K.

DeArellano, R. Johnson, L. Linton, P. McEwan, K. McKernan, J. Talamas, A. Tirrell, W. Ye, A. Zimmer, R.D. Barber, I. Cann, D.E. Graham, D.A. Grahame, A.M. Guss, R. Hedderich, C. Ingram-Smith, H.C. Kuettner, J.A. Krzycki, J.A. Leigh, W. Li, J Liu, B. Mukhopadhyay, J.N. Reeve, K. Smith, T.A. Springer, L.A. Umayam, O. White, R.H. White, E. Conway de Macario, J.G. Ferry, K.F. Jarrell, H. Jing, A.J. Macario, I. Paulsen, M. Pritchett, K.R. Sowers, R.V. Swanson, S.H. Zinder, E. Lander, W.W. Metcalf, & B. Birren, (2002) The genome of Methanosarcina acetivorans reveals extensive metabolic and physiological diversity. *Genome Res.* 12: 532-42.

Grosche, C., A. Diehl, S.A. Rensing, & U.G. Maier, (2018) Iron-Sulfur Cluster Biosynthesis in Algae with Complex Plastids. *Genome Biol Evol*. 10: 2061-2071.

Guss, A.M., G. Kulkarni, & W.W. Metcalf, (2009) Differences in hydrogenase gene expression between Methanosarcina acetivorans and Methanosarcina barkeri. *J Bacteriol*. 191: 2826-33.

Hagen, W.R., (2018) EPR spectroscopy of complex biological iron-sulfur systems. *J Biol Inorg Chem*. 23: 623-634.

Haroon, M.F., S. Hu, Y. Shi, M. Imelfort, J. Keller, P. Hugenholtz, Z. Yuan, & G.W. Tyson, (2013) Anaerobic oxidation of methane coupled to nitrate reduction in a novel archaeal lineage. *Nature*. 500: 567-70.

Harris, D.F., Z.-Y. Yang, D.R. Dean, L.C. Seefeldt, & B.M. Hoffman, (2018) Kinetic Understanding of N 2 Reduction versus H 2 Evolution at the E 4(4H) Janus State in the Three Nitrogenases. *Biochemistry*. 57: 5706-5714.

Hu, Y. & M.W. Ribbe, (2011) Biosynthesis of Nitrogenase FeMoco. *Coord Chem Rev*. 255: 1218-1224.

Hu, Y. & M.W. Ribbe, (2013) Nitrogenase assembly. *Biochim Biophys Acta*. 1827: 1112-22.

Imachi, H., M.K. Nobu, N. Nakahara, Y. Morono, M. Ogawara, Y. Takaki, Y. Takano, K. Uematsu, T. Ikuta, M. Ito, Y. Matsui, M. Miyazaki, K. Murata, Y. Saito, S. Sakai, C. Song, E. Tasumi, Y. Yamanaka, T. Yamaguchi, Y. Kamagata, H. Tamaki, & K. Takai, (2020) Isolation of an archaeon at the prokaryote-eukaryote interface. *Nature*. 577: 519-525.

Imlay, J.A., (2003) Pathways of oxidative damage. *Annu Rev Microbiol*. 57: 395-418.

Johnson, D.C., D.R. Dean, A.D. Smith, & M.K. Johnson, (2005) Structure, function, and formation of biological iron-sulfur clusters. *Annu Rev Biochem.* 74: 247-81.

Kennedy, C. & D. Dean, (1992) The nifU, nifS and nifV gene products are required for activity of all three nitrogenases of Azotobacter vinelandii. *Mol Gen Genet*. 231: 494-8.

Kessler, P.S., C. Blank, & J.A. Leigh, (1998) The nif gene operon of the methanogenic archaeon Methanococcus maripaludis. *J Bacteriol*. 180: 1504-11.

Lang, K., J. Schuldes, A. Klingl, A. Poehlein, R. Daniel, & A. Brunea, (2015) New mode of energy metabolism in the seventh order of methanogens as revealed by comparative genome analysis of "Candidatus methanoplasma termitum". *Appl Environ Microbiol*. 81: 1338-52.

Layer, G., S.A. Gaddam, C.N. Ayala-Castro, S. Ollagnier-de Choudens, D. Lascoux, M. Fontecave, & F.W. Outten, (2007) SufE transfers sulfur from SufS to SufB for iron-sulfur cluster assembly. *J Biol Chem*. 282: 13342-50.

Leimkühler, S., M. Bühning, & L. Beilschmidt, (2017) Shared Sulfur Mobilization Routes for tRNA Thiolation and Molybdenum Cofactor Biosynthesis in Prokaryotes and Eukaryotes. *Biomolecules*. 7: 5.

Lill, R., R. Dutkiewicz, H.-P. Elsässer, A. Hausmann, D.J.A. Netz, A.J. Pierik, O. Stehling, E. Urzica, & U. Mühlenhoff, (2006) Mechanisms of iron-sulfur protein maturation in mitochondria, cytosol and nucleus of eukaryotes. *Biochim Biophys Acta*. 1763: 652-67.

Liu, Y., L.L. Beer, & W.B. Whitman, (2012) Sulfur metabolism in archaea reveals novel processes. *Environ Microbiol*. 14: 2632-44.

Liu, Y., M. Sieprawska-Lupa, W.B. Whitman, & R.H. White, (2010) Cysteine is not the sulfur source for iron-sulfur cluster and methionine biosynthesis in the methanogenic archaeon Methanococcus maripaludis. *J Biol Chem.* 285: 31923-9.

Major, T.A., H. Burd, & W.B. Whitman, (2004) Abundance of 4Fe-4S motifs in the genomes of methanogens and other prokaryotes. *FEMS Microbiol Lett.* 239: 117-23.

McGlynn, S.E., G.L. Chadwick, C.P. Kempes, V.J. Orphan, (2015) Single cell activity reveals direct electron transfer in methanotrophic consortia. *Nature*. 526: 531-5.

Metcalf, W.W., J.K. Zhang, E. Apolinario, K.R. Sowers, & R.S. Wolfe, (1997) A genetic system for Archaea of the genus Methanosarcina: liposome-mediated transformation and construction of shuttle vectors. *Proc Natl Acad Sci USA.* 94: 2626-31

Murray, P.A. & S.H. Zinder, (1984) Nitrogen fixation by a methanogenic archaebacterium. *Nature*. 312: 284–6.

Outten, F.W., O. Djaman, & G. Storz, (2004) A suf operon requirement for Fe-S cluster assembly during iron starvation in Escherichia coli. *Mol Microbiol*. 52: 861-72.

Pietri, R., E. Román-Morales, & J. López-Garriga, (2011) Hydrogen sulfide and hemeproteins: knowledge and mysteries. *Antioxid Redox Signal*. 15: 393-404.

Pinske, C. & R.G. Sawers, (2012) A-type carrier protein ErpA is essential for formation of an active formate-nitrate respiratory pathway in Escherichia coli K-12. *J Bacteriol*. 194: 346-53.

Plugge, C.M., W. Zhang, J.C.M. Scholten, & A.J.M. Stams, (2011) Metabolic flexibility of sulfate-reducing bacteria. *Front Microbiol*. 2: 81.

Rehder, D., (2000) Vanadium nitrogenase. *J Inorg Biochem*. 80: 133-6.

Sousa, F.L., T. Thiergart, G. Landan, S. Nelson-Sathi, I.A. Pereira, J.F. Allen, N. Lane, & W.F. Martin, (2013) Early bioenergetic evolution. *Philos Trans R Soc Lond B Biol Sci.* 368: 20130088.

Sowers, K.R., S.F. Baron, & J.G. Ferry, (1984) Methanosarcina acetivorans sp. nov., an Acetotrophic Methane-Producing Bacterium Isolated from Marine Sediments. *Appl Environ Microbiol*. 47: 971-8.

Takahashi, Y. & U. Tokumoto, (2002) A third bacterial system for the assembly of iron-sulfur clusters with homologs in archaea and plastids. *J Biol Chem*. 277: 28380-3.

Villanueva, L., S. Schouten, & J.S.S. Damsté, (2017) Phylogenomic analysis of lipid biosynthetic genes of Archaea shed light on the 'lipid divide'. *Environ Microbiol*. 19: 54-69.

Wächtershäuser, G., (1990) Evolution of the first metabolic cycles. *Proc Natl Acad Sci U S A*. 87: 200-4.

Weimer, P.J. & J.G. Zeikus, (1979) Acetate assimilation pathway of Methanosarcina barkeri. *J Bacteriol*. 137: 332-9.

Whitman, W.B., E. Ankwanda, & R.S. Wolfe, (1982) Nutrition and carbon metabolism of Methanococcus voltae. *J Bacteriol*. 149: 852-63.

Woese, C.R. & G.E. Fox, (1977) Phylogenetic structure of the prokaryotic domain: the primary kingdoms. *Proc Natl Acad Sci U S A*. 74: 5088-90.

Wolfe, J.M. & G.P. Fournier, (2018) Horizontal gene transfer constrains the timing of methanogen evolution. *Nat Ecol Evol*. 2: 897-903.

Yang, Z.-Y., R. Ledbetter, S. Shaw, N. Pence, M. Tokmina-Lukaszewska, B. Eilers, Q. Guo, N. Pokhrel, V.L. Cash, D.R. Dean, E. Antony, B. Bothner, J.W. Peters, & L.C. Seefeldt, (2016) Evidence That the Pi Release Event Is the Rate-Limiting Step in the Nitrogenase Catalytic Cycle. *Biochemistry*. 55: 3625-35.

Zhao, C., Z. Lyu, F. Long, T. Akinyemi, K. Manakongtreecheep, D. Söll, W.B. Whitman, D.J. Vinyard, & Y. Liu, (2020) The Nbp35/ApbC homolog acts as a nonessential [4Fe-4S] transfer protein in methanogenic archaea. *FEBS Lett*. 594: 924-932.

Zheng, L., V.L. Cash, D.H. Flint, & D.R. Dean, (1998) Assembly of iron-sulfur clusters. Identification of an iscSUA-hscBA-fdx gene cluster from Azotobacter vinelandii. *J Biol Chem*. 273: 13264-72.

APPENDIX

Figures

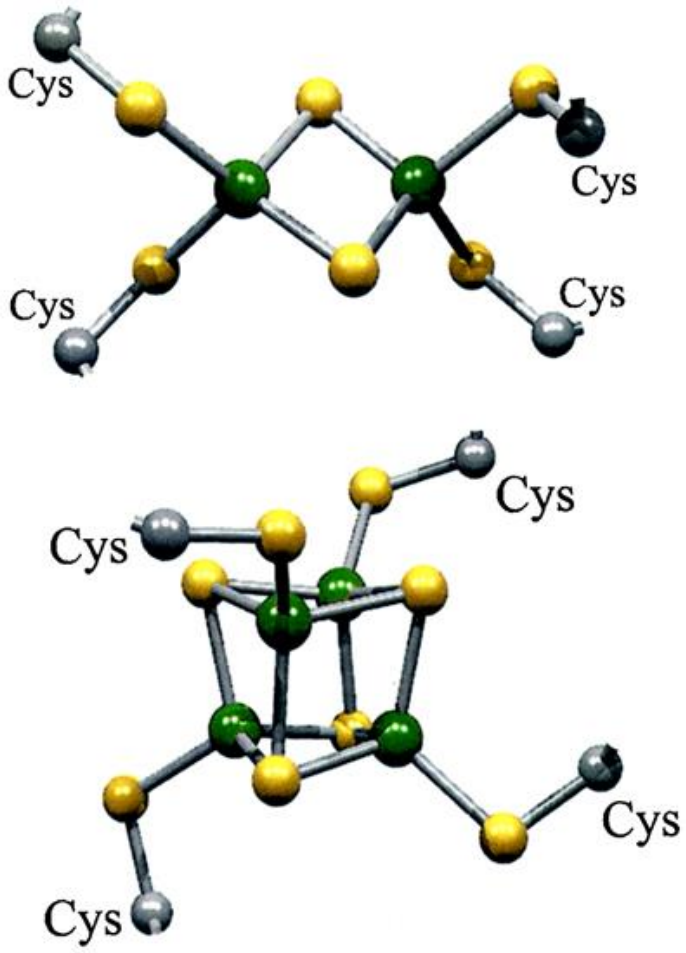

Figure 1. Typical iron-sulfur clusters. **Top.** A planar [2Fe-2S] cluster. **Bottom.** A cubane [4Fe-4S] cluster. In both images, green spheres represent Fe atoms, while yellow spheres represent S atoms. Yellow spheres attached to gray spheres (C atoms) represent the thiol side-chains of cysteine residues, as indicated. Figure adapted from Frazzon & Dean, 2003.

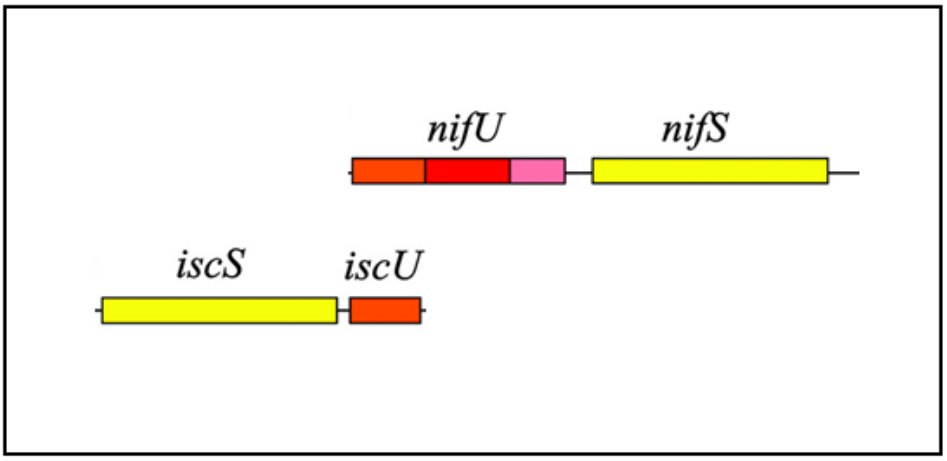

Figure 2. Core NIF and ISC Fe-S biogenesis genes in *Azotobacter vinelandii*. The sequence encoding the [Fe-S]-binding N-terminal domain of NifU is colored orange, as is the homologous gene encoding IscU beneath it. The other domains of NifU are believed to confer specificity for [Fe-S] delivery to the other Nif proteins. Figure adapted from Dos Santos *et al*., 2007.

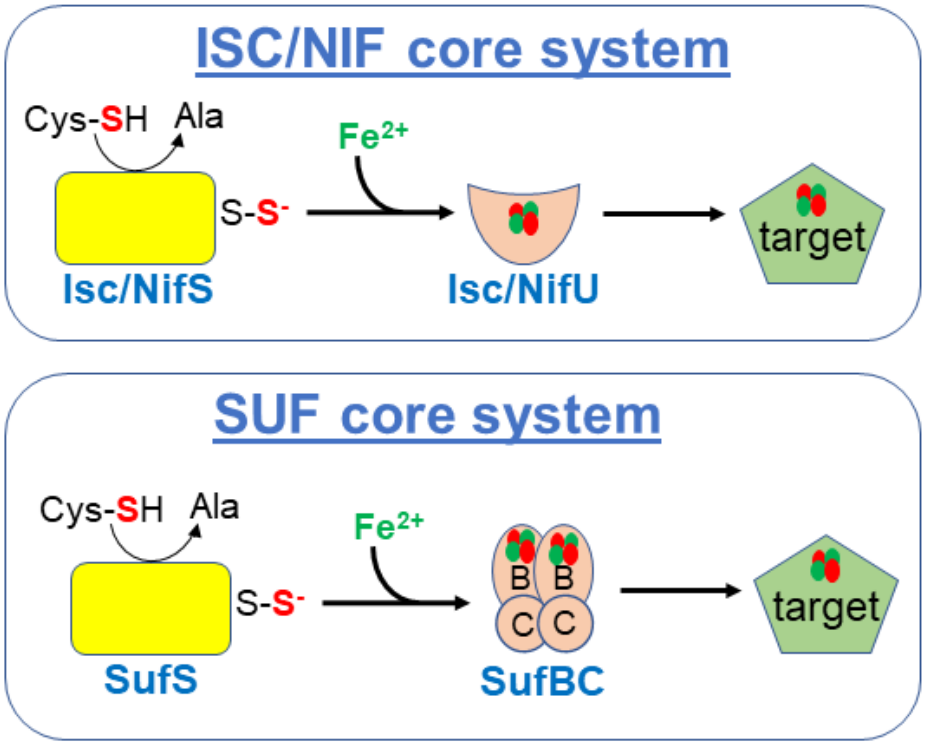

Figure 3. Systems of Fe-S cluster biogenesis. Typical ISC and NIF systems (top) cleave sulfur from cysteine using an S protein, then assemble [Fe-S] on a U protein. Typical SUF systems (bottom) differ in that [Fe-S] is assembled on a tetrameric B_2C_2 (or alternatively BC_2D) scaffold.

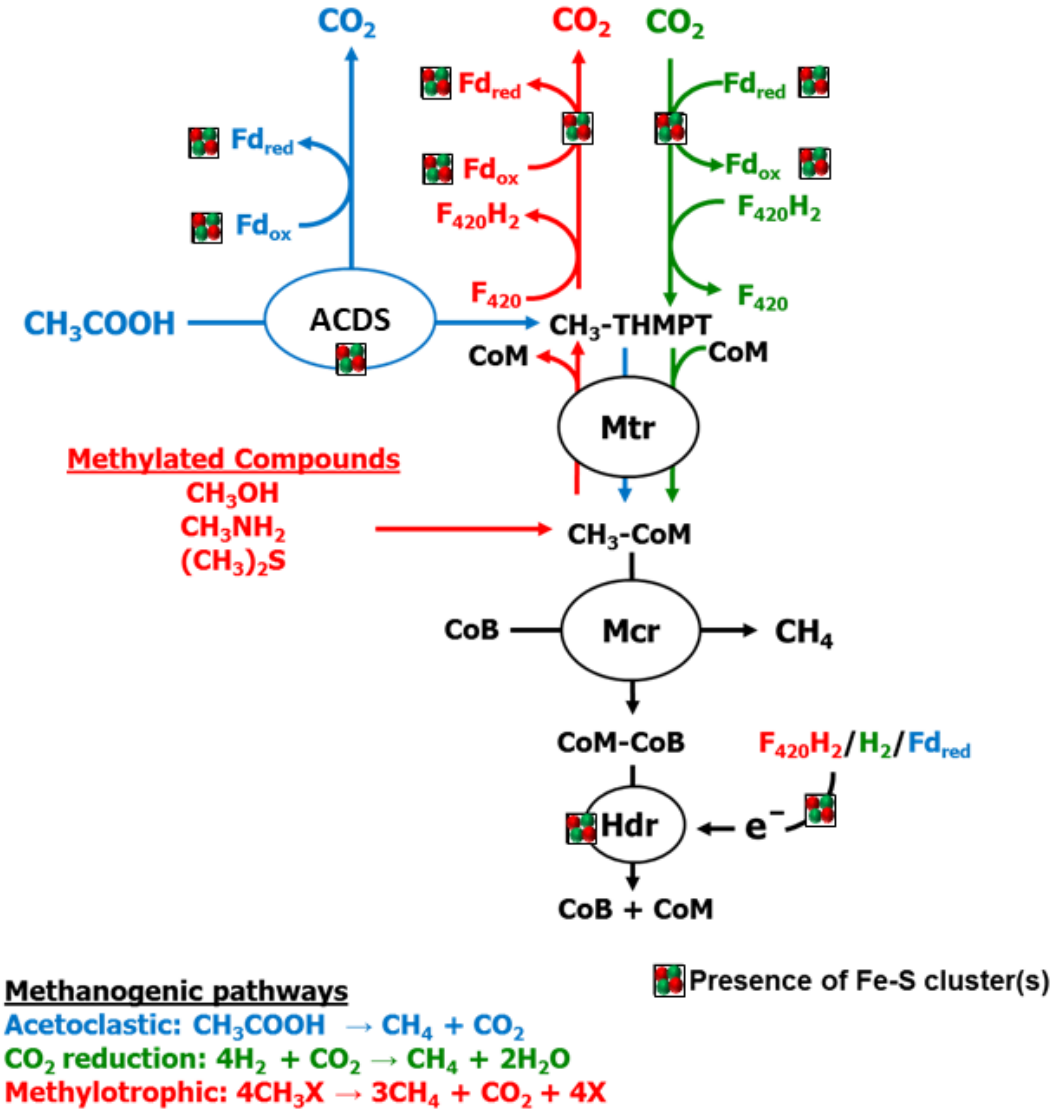

Figure 4. The three central pathways of methanogenesis. Enzymes and substrates shared across all three pathways are colored black, while pathway-specific steps are color-coded as indicated. Proteins and complexes binding at least one [Fe-S] are marked. Abbreviations: coenzyme F_{420} (F_{420}); ferredoxin (Fd); carbon monoxide dehydrogenase/acetyl-CoA synthase (ACDS); tetrahydromethanopterin (THMPT); coenzyme M (CoM); THMPT:coenzyme M methyltransferase (Mtr); coenzyme B (CoB); methyl-coenzyme M reductase (Mcr); heterodisulfide reductase (Hdr).

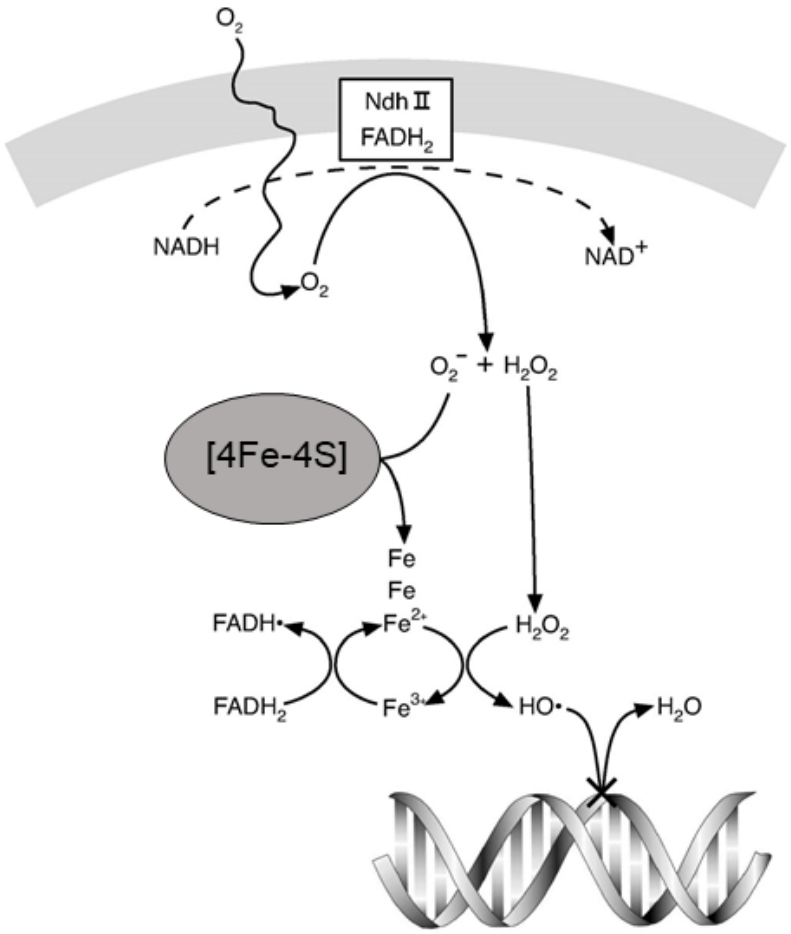

Figure 5. Fenton reactions generate reactive oxygen species (ROS) that damage [Fe-S] and DNA. Adapted from Imlay, 2003.

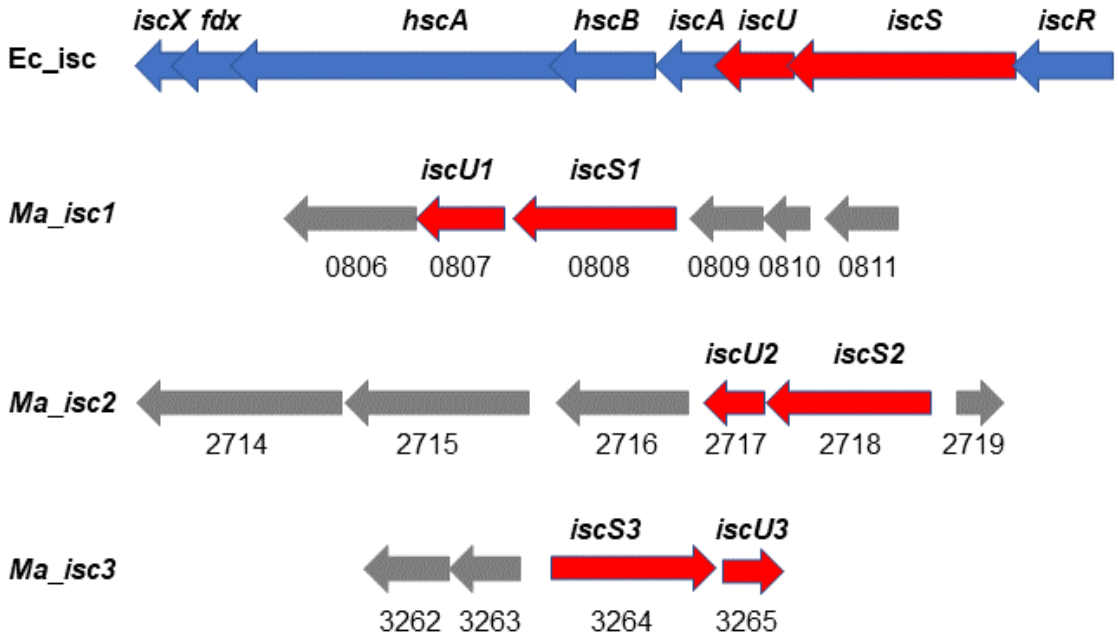

Figure 6. Arrangement of the gene clusters containing *iscS* and *iscU* in *E. coli* and *M. acetivorans* C2A. Gray arrows represent genes not homologous to Isc gene cluster in *E. coli*, predicted to have functions not related to Fe-S cluster assembly.

Figure 7. The putative Nif, Vnf, and Anf gene clusters in *M. acetivorans* (Ma). Numbers above arrows (genes) are the locus tags and below each is the predicted protein. Note: the amino acid sequences of VnfH1 and VnfH2 are identical.

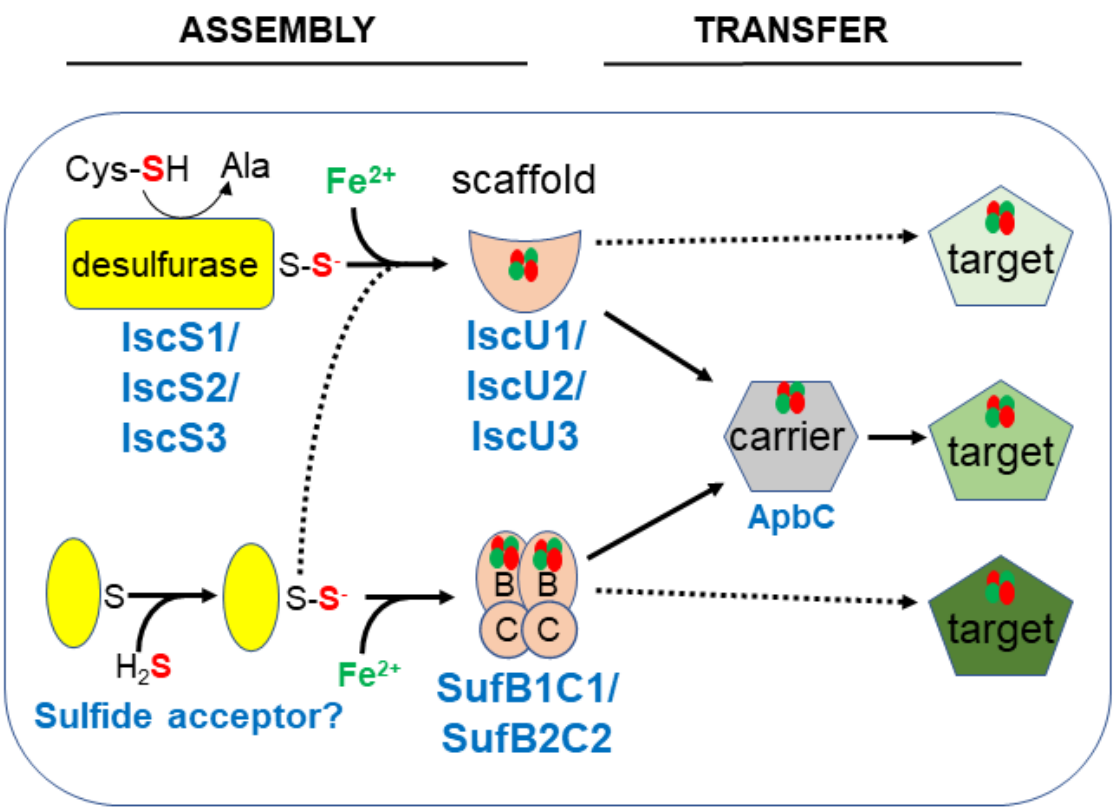

Figure 8. Proposed model of Fe-S cluster biogenesis and delivery in *Methanosarcina acetivorans*. ISC is used when cysteine is the sulfur source, SUF when growing on inorganic sulfide. The potential for interaction between the systems exists, but has not been demonstrated. ApbC may serve as an intermediate [Fe-S] carrier and delivery protein.

Chapter I

Methanosarcina acetivorans contains a functional ISC system for iron-sulfur cluster biogenesis

Thomas M. Deere,

Divya Prakash, Faith H. Lessner, Evert C. Duin, and Daniel J. Lessner

Cell and Molecular Biology Program, University of Arkansas,

Fayetteville, AR 72701 USA

Introduction

Iron-sulfur (Fe-S) clusters are ubiquitous protein cofactors that are involved in numerous cellular processes, such as respiration, photosynthesis, DNA repair, and regulation. A primary function of Fe-S clusters in proteins is to mediate the transfer of electrons during oxidation-reduction reactions (Johnson *et al.*, 2005). As such, Fe-S proteins serve critical roles in energy-conservation pathways in almost all organisms and in steps leading to the production of valuable metabolic products, including biofuels (e.g. H_2) (Bandyopadhyay *et al.*, 2010, Chandrayan *et al*, 2012). Simple Fe-S clusters include [2Fe-2S], [3Fe-4S], and [4Fe-4S] clusters, with the [4Fe-4S] cluster being the most prevalent (Johnson *et al.*, 2005, Sousa *et al.*, 2013). The metabolism of many organisms also relies on enzymes that use more complex Fe-S clusters, such as those found in the biotechnology relevant enzymes hydrogenase, carbon monoxide dehydrogenase, and nitrogenase (Peters *et al.*, 1995, Peters *et al.*, 2015, Ragsdale, 2000). For example, nitrogenase contains a [8Fe-7S] cluster and a Mo-8Fe-9S-C-homocitrate cluster, in addition to [4Fe-4S] clusters (Hu & Ribbe, 2016).

Although Fe-S clusters in proteins are typically oxygen-labile, aerobes rely on Fe-S proteins as obligate components of respiratory systems (Johnson *et al.*, 2005). However, Fe-S proteins are far more abundant in strict anaerobes, specifically those that grow by respiration. Among anaerobes, methanogenic archaea (methanogens) and acetogenic bacteria (acetogens) are predicted to contain the highest number of [4Fe-4S] cluster proteins, indicating that this cluster is critical for methanogenesis and acetogenesis (Sousa *et al.*, 2013, Major *et al.*, 2004). Methanogenesis is a critical step in the global carbon cycle and in the production of methane as a biofuel. Numerous Fe-S proteins are involved in methanogenesis (Ferry, 1999, Thauer, 2012, Thauer *et al.*, 2008). For example, [4Fe-4S] cluster-containing ferredoxin serves as a primary

electron carrier and [4Fe-4S] cluster-containing heterodisulfide reductase plays a central role, including in electron bifurcation (Costa *et al.,* 2010, Hedderich *et al.,* 2005). Recently, the bifurcating hydrogenase/heterodisulfide reductase complex was shown to be a dimer of protomers containing 22 [4Fe-4S] clusters, while the bifunctional formyl-methanofuran dehydrogenase complex, which catalyzes the reversible reduction of CO_2 to formyl-methanofuran, was shown to contain a remarkable 46 electronically coupled [4Fe-4S] clusters (Wagner *et al.,* 2016). Many additional [4Fe-4S] proteins are involved in the metabolism of methanogens, including several biosynthesis enzymes and regulatory proteins. Several information processing enzymes in methanogens also harbor [4Fe-4S] clusters, such as RNA polymerase (Lessner *et al.,* 2012). In addition, methanogens, along with related anaerobic methanotrophs, are the only archaea that possess nitrogenase and are therefore capable of nitrogen fixation (Boyd *et al.,* 2011, Dos Santos *et al.,* 2012, Dekas *et al.,* 2009). Despite methanogenesis having an absolute requirement for Fe-S proteins, the factors and mechanisms used by methanogens to assemble and traffic simple and complex Fe-S clusters remain largely unknown.

Two generalized systems (ISC and SUF) are known to function in the biogenesis of Fe-S clusters in bacteria and eukaryotes. A third system (NIF) is specific to biogenesis of the simple and complex Fe-S clusters in the components of nitrogenases found in bacteria (Ayala-Castro *et al.,* 2008, Couturier *et al.,* 2013, Fontecave *et al.,* 2008, Roche *et al.,* 2013). For general Fe-S cluster biogenesis, bacteria typically have ISC but may have SUF alone or both ISC and SUF systems (e.g. *Escherichia coli*). ISC is the primary system in *E. coli,* whereas SUF appears important during times of increased oxidative stress and/or Fe limitation (Ayala-Castro *et al.,* 2008). In eukaryotes, the ISC system functions in mitochondria, and the SUF system is primarily

present in chloroplasts (Roche *et al.,* 2013, Blanc *et al.,* 2014). The core components of all three systems include a pyridoxal 5'- phosphate (PLP)-dependent cysteine desulfurase (IscS, SufS, or NifS) that liberates sulfur from cysteine, forming a persulfide, followed by sulfur transfer to an Fe-containing scaffold (IscU, SufB(D)C, or NifU). The Fe-S cluster is assembled on the scaffold and subsequently delivered to target apo-proteins, often with the help of accessory and/or carrier proteins. Other accessory proteins may also be involved in cluster assembly (Ayala-Castro *et al.,* 2008, Fontecave & Ollagnier-de-Choudens, 2008, Roche *et al.,* 2013). The core scaffold of the SUF system (SufBC) appears universally encoded in the genomes of archaea, and many archaeal genomes also encode homologs of the minimal components of the ISC system (IscS and IscU) (Boyd *et al.,* 2014). The functional role(s) of these components in archaea are poorly understood.

All sequenced methanogens contain at least one *sufBC* gene cluster, typically arranged as *sufC* then *sufB* (Boyd *et al.,* 2014). Thus, SufBC may serve as a general Fe-S cluster scaffold in all methanogens. Many sequenced methanogen genomes also encode homologs of IscS and IscU, typically arranged as *iscSU*. Methanogen genomes do not encode NifS or NifU, indicating that methanogens lack a nitrogenase-specific Fe-S cluster biogenesis system. To begin to understand the role and importance of IscSU to methanogens, we report here the genetic and biochemical characterization of IscSU from the genetically tractable methanogen *Methanosarcina acetivorans*.

Materials and Methods

***M. acetivorans* growth**. *M. acetivorans* strain WWM73 was obtained from Dr. Bill Metcalf (Guss *et al.,* 2008) and was used as the parent strain for all experiments. All strains of *M. acetivorans* (Table 5) were grown in HS medium containing 125 mM methanol as a carbon and energy source as previously described (Jennings *et al.,* 2016, Sowers *et al.,* 1993). Each liter of

HS medium contains 23.4 g NaCl, 3.8 g $NaHCO_3$, 1.0 g KCl, 11.0 g $MgCl_2*6H_2O$, 0.3 g $CaCl_2*2H_2O$, 1.0 g NH_4Cl, 0.5 g L-cysteine, 5 mL of 1 M KH_2PO_4 at pH=7.4, 1 mL of 0.1% w/v resazurin, 10 mL of Wolfe's Mineral Solution (supplemented with 0.024 g/L $NiCl_2*H_2O$ in the stock), and 2 mL of a 5x concentrated Wolfe's Vitamin Solution (Wolin *et al.*, 1963). HS medium was made anoxic and dispensed into Balch tubes within an anaerobic chamber (Coy Laboratories) containing 75% N_2, 20% CO_2, and 5% H_2. Standard culture conditions include 0.025% w/v Na_2S*9H_2O added from a sterile, anoxic stock just prior to inoculation. To examine growth with different sulfur sources, 1.5 mM DTT was added to HS medium (HS_{DTT} medium) in lieu of cysteine prior to autoclaving, and 3 mM L-cysteine and/or 1mM sodium sulfide were added from sterile anoxic stock solutions prior to inoculation. Growth was monitored by measuring the optical density at 600 nm (OD_{600}) of the culture tubes using a spectrophotometer (Thermo Fisher, Genesys 10 Bio).

Expression of recombinant *M. acetivorans* IscS2, IscU2, and aconitase in *E. coli*. The genes *iscS2* (MA2718) and *iscU2* (MA2717) were amplified by PCR from *Methanosarcina acetivorans* genomic DNA isolated from wild-type strain C2A using standard guanidine thiocyanate lysis, protein precipitation, and isopropanol extraction. *Nde*I and *Xho*I recognition sites were added at the 5' and 3' ends of the PCR product, respectively. The putative *acnA* aconitase gene (MA0250) was similarly amplified, but with an *Nhe*I site rather than *Nde*I. All PCR products were generated using Phusion HF polymerase (New England Biolabs) with reagent concentrations per the manufacturer's instructions. Annealing temperatures of 60 °C for *iscS2* and *iscU2*, and 67 °C for *acnA*, were used (primers listed in Table 5). The PCR products were digested with *Nde*I or *Nhe*I and *Xho*I and ligated using T4 DNA ligase (New England Biolabs) with pET28a that had been similarly digested, resulting in each gene fused to a

thrombin-cleavable His_6-tag. All enzymes were from New England Biolabs and reactions were carried out per manufacturer's instructions. Sub-cloning efficiency *E. coli* DH5α competent cells (Invitrogen) were transformed with the ligation reactions and cells harboring plasmids with *iscU2*, *iscS2*, and *acnA* were identified by restriction digests and confirmed by DNA sequencing (Eurofins). For expression of each N-terminal His_6-tagged recombinant protein, *E. coli* Rosetta (DE3) pLacI was separately transformed with the plasmids containing *iscU2* (pDL201), *iscS2* (pDL202), and *acnA* (pDL204).

E. coli Rosetta (DE3) pLacI harboring pDL201, pDL202, or pDL204 were grown in LB medium containing 50 µg/mL kanamycin and 17 µg/mL chloramphenicol with shaking at 37 °C. At an optical density at 600 nm (OD_{600}) of 0.6, 0.5 mM IPTG was added, and the temperature was lowered to 25 °C for the IscS2-expression culture or 16 °C for the IscU2- and AcnA-expression cultures. The AcnA-expression culture was also supplemented with 0.5 M D-sorbitol at induction to inhibit inclusion body formation. After 18 hours, cells were harvested by centrifugation and frozen at -80 °C.

Purification of recombinant proteins. For purification of IscS2, thawed cells were resuspended in buffer A (20 mM Tris pH 8.0, 500 mM NaCl, 10% glycerol) containing a few crystals of DNase I and approximately 1 mM benzamidine HCl hydrate. Cells were lysed by two passages through a French pressure cell at >110 MPa. Lysates were centrifuged at 41,000 x *g* and 4 °C for 35 minutes. The supernatant was passed through a 0.45 µm filter and loaded on a chromatography column containing 5 mL of Ni^{2+}-agarose resin (Genscript) pre-equilibrated with 25 mL of buffer A. The column was sequentially washed with 50 mL buffer A, 25 mL buffer A containing 10 mM imidazole, and 25 mL buffer A. The column was then incubated in 5 mL buffer A containing 50 U of thrombin (Promega) at 25 °C for 16 hr. Protein was eluted from the

column by the addition of 10 mL of buffer A followed by 10 mL buffer A containing 250 mM imidazole. Thrombin was removed using a 1 mL HiPrep benzamidine column (GE Healthcare) following the manufacturer's instructions. Purified IscS2 was exchanged into storage buffer (50 mM Tris pH 8.0, 150 mM NaCl, 10% glycerol) using a PD-10 column (GE Healthcare) and stored at -80 °C until use.

For purification of IscU2, all steps were performed anaerobically under an atmosphere of 95% N_2, 5% H_2 in an anaerobic chamber (Coy Laboratories). Thawed cells were resuspended in buffer B (20 mM Tris pH 8.0, 2 M NaCl, 10% glycerol) containing a few crystals of DNase I and benzamidine HCl hydrate. Cells were lysed by two passages through a French pressure cell at >110 MPa. Lysates were centrifuged at 41,000 x *g* and 4 °C for 35 minutes. The supernatant was passed through a 0.45 µm filter and loaded on a 5 mL Ni^{2+}-agarose resin chromatography column pre-equilibrated with 25 mL of buffer B. The column was sequentially washed with 50 mL buffer B, 25 mL buffer B containing 10 mM imidazole, 25 mL buffer B, and 25 mL buffer A. The column was then incubated in 5 mL buffer A containing 50 U of thrombin at 25 °C for 16 hr. Protein was eluted from the column by the addition of 10 mL of buffer A followed by 10 mL buffer A containing 250 mM imidazole. Thrombin was removed using a 1 mL HiPrep benzamidine column (GE Healthcare) following the manufacturer's instructions. The partially purified protein was loaded onto a HiPrep 16/60 Sephacryl S-200 gel filtration column using a Biologic LP system (Bio-Rad) housed within the anaerobic chamber. The column was run at a flow rate of 0.5 ml min^{-1} with 50 mM Tris pH 8.0, 150 mM NaCl, 10% glycerol, 2 mM DTT. Fractions containing only IscU2, as determined by SDS-PAGE, were pooled, concentrated, and desalted into storage buffer (50 mM Tris pH 8.0, 150 mM NaCl, 10% glycerol) using a PD-10 column. Purified IscU2 was stored under N_2 at -80 °C.

For the purification of AcnA all steps were performed anaerobically under an atmosphere of 95% N_2, 5% H_2 in an anaerobic chamber (Coy Laboratories). Thawed cells were resuspended in buffer C (20 mM Tris, pH 8.0, 500 mM NaCl) containing a few crystals of DNase I and benzamidine HCl hydrate. Cells were lysed by three passages through a French pressure cell at >110 MPa. Lysates were centrifuged at 41,000 x *g* and 4 °C for 35 minutes. The supernatant was passed through a 0.45 µm filter and loaded on a 5 ml Ni^{2+}-agarose resin chromatography column pre-equilibrated with 25 ml of buffer C. The column was sequentially washed with 50 mL buffer C, 25 mL buffer C containing 50 mM imidazole, and 25 mL buffer C. The column was then incubated in 5 mL Buffer C containing 50 U of thrombin (Promega) at 25 °C for 16 hr. Protein was eluted from the column by the addition of 10 mL of buffer C containing 75 mM imidazole. The partially purified protein was loaded onto a HiPrep 16/60 Sephacryl S-200 gel filtration column and eluted under the same conditions as for IscU2. Fractions containing AcnA, as determined by SDS-PAGE, were pooled, concentrated, and buffer-exchanged into buffer D (20 mM Bis-Tris, pH 6.8). A 1 mL HiTrap Q XL ion exchange column (GE Healthcare) was pre-equilibrated with buffer D and loaded with partially purified AcnA. The column was washed with 20 mL of buffer C containing 200 mM NaCl, then with buffer C containing stepwise-increasing concentrations of NaCl (220-300 mM in 20 mM increments). The flow rate was 1 mL min^{-1}. Fractions containing only AcnA, as determined by SDS-PAGE, were pooled, concentrated, and desalted into storage buffer (50 mM Tris pH 8.0, 150 mM NaCl) using a PD-10 column. Purified AcnA was stored under N_2 at -80 °C.

Recombinant IscS2, IscU2, and AcnA were each separately purified at least twice, and similar results were observed with each preparation. Results are included from a single preparation unless noted otherwise. All protein concentrations were determined by the Bradford assay

(Bradford, 1976) using bovine serum albumin as a standard. Protein purity was analyzed by SDS-PAGE using a 10% gel for AcnA, 12% gel for IscS2, and 15% gel for IscU2. A Broad Range (10-230 kDa) prestained protein ladder (New England Biolabs) was used to approximate the molecular weight of each protein. SDS-PAGE gels were stained with Coomassie Brilliant Blue solution, then destained prior to imaging.

Reconstitution of IscS2 with PLP. IscS2 (150 μM) was incubated with 3 mM PLP in 50 mM Tris pH 7.2, 150 mM NaCl, at 25 °C for 3 hours. Unbound PLP was removed from the IscS2/PLP mix by desalting into storage buffer (50 mM Tris pH 8.0, 150 mM NaCl, 10% glycerol) using a PD-10 column. This sample of IscS2 was designated $IscS2^{PLP}$.

IscU2 Fe-S cluster reconstitution. Two methods were used to examine IscsU2 Fe-S cluster reconstitution. All steps were performed inside an anaerobic chamber. Chemical reconstitution was carried out during a purification of IscU2. After removal of thrombin, partially pure IscU2 (~33 mg of protein) was diluted in 50 mL of 50 mM Tris pH 8.0, 150 mM NaCl, 10% glycerol, followed by the addition of 2 mM β-mercaptoethanol, 138 μM ferrous ammonium sulfate, and 138 μM sodium sulfide. The reaction mix was incubated at 4 °C for 16 hr and then concentrated to 2.5 mL using a stirred-cell concentrator (5 kDa MW cutoff). IscU2 was purified from the reaction mix by size-exclusion chromatography as described above and designated $IscU2^{C\text{-}FeS}$. IscS2-dependent Fe-S cluster reconstitution of IscU2 was performed by incubating 160 μM IscU2 in 100 mM Tris pH 7.4 containing 8 μM IscS2, 2 mM DTT, 1.6 mM ferrous ammonium sulfate, and 1.6 mM L-cysteine for 1 hour at 25 °C. The reaction mix was desalted into storage buffer using a PD-10 column, and aliquots were stored under N_2 at -80°C.

Determination of the oligomeric state of IscS2 and IscU2. The oligomeric state of IscS2 and IscU2 was determined by size-exclusion chromatography using a HiPrep 16/60 Sephacryl S-200

gel filtration column. The column was run at a flow rate of 0.5 ml min^{-1} with 50 mM Tris pH 8.0, 150 mM NaCl, 10% glycerol, 2 mM DTT, and calibrated with standard proteins (Low molecular weight standards, Sigma-Aldrich): β-amylase (200 kDa), alcohol dehydrogenase (150 kDa), bovine serum albumin (66 kDa), carbonic anhydrase (29 kDa), and cytochrome *c* (12.4 kDa).

Cysteine desulfurase assay. Cysteine desulfurase activity was determined by measuring production of sulfide from L-cysteine using the methylene blue method (Beinert, 1983). Assays were performed with 5 µM IscS2 in 50 mM Tris pH 7.5, 1 mM DTT in the presence or absence of 50 µM PLP. Reactions were initiated by the addition of 1 mM L-cysteine in a total reaction of 1 mL and were incubated at 25°C for 20 minutes in sealed vials. The reaction was stopped after 20 min by the addition of zinc acetate and sodium hydroxide. The mixtures were developed, and absorbance measured at 670 nm.

Similar assays were performed on *M. acetivorans* WWM73 cell-free lysates. Cell cultures were grown to an OD_{600} between 0.6-0.8, and cells were pelleted in sealed anoxic bottles at 11,000 x *g* for 10 minutes at 4 °C. Cell pellets were resuspended in 50 mM Tris pH 8.0 containing, 1 mM benzamidine, 1 mM phenylmethylsulfonyl fluoride, transferred to vials, and stored under N_2 at -80 °C until use. Cells were lysed by sonication in an anaerobic chamber, centrifuged at 16,000 x *g* for 10 min., and the supernatant saved. L-cysteine desulfurase activity was measured using crude lysate (0.16 to 0.34 mg) as described above. Reaction mixtures were incubated at 37 °C for 45 minutes before termination by adding 100 µL 20 mM N,N'-Dimethyl-p-phenylenediamine dihydrochloride in 7.3 M HCl and 100 µL 30 mM $FeCl_3$ in 1.2 M HCl using gas-tight syringes. Color developed over 30 minutes, then solutions were quickly vented, spun at 16,000 x *g*, and absorbances read at 670 nm.

Spectroscopy. UV-visible spectra of IscS2 and IscU2 were recorded using a Cary 60 spectrophotometer (Agilent Technologies) housed within an anaerobic chamber. CW EPR spectra were measured at X-band (9 GHz) frequency on a Bruker EMX spectrometer, fitted with the ER-4119-HS high sensitivity perpendicular-mode cavity. The Oxford Instrument ESR 900 flow cryostat in combination with the ITC4 temperature controller was used for measurements in the 4 K to 300 K range using a helium flow. All spectra were recorded with a field modulation frequency of 100 kHz, modulation amplitude of 0.6 mT, and a frequency of 9.386 GHz. Sample-specific conditions are indicated in the figure legends.

Determination of Fe-S cluster and persulfide content in lysate. Acid-labile and persulfide (sulfane) sulfur concentrations were determined in cell-free lysates from strains WWM73 and DJL60 grown on different sulfur sources using the methylene blue method as above. Cell-free lysate was prepared as described above for L-cysteine desulfurase assays. Soluble protein (0.195 to 0.335 mg) was directly assayed by the methylene blue method (acid-labile sulfur) or was incubated at 37°C with 1 mM DTT for 60 minutes in sealed vials prior to sulfide determination to assay reductant-labile (persulfide) sulfur. The persulfide concentration was determined by subtracting the amount of acid-labile sulfur determined in the absence of DTT. Control samples containing DTT without lysate did not produce detectable sulfur.

Aconitase reconstitution assays. AcnA (56 µM) was rendered to the apo-form by anaerobic incubation on ice with 50 molar excess (2.8 mM) EDTA, 20 molar excess (1.12 mM) potassium ferricyanide in 50 mM Tris pH 7.2, 150 mM NaCl. After 15 minutes of incubation, apo-AcnA was desalted using a NAP5 column (GE Healthcare) and stored under N_2 at -80 °C in 50 mM Tris pH 7.2, 150 mM NaCl until use.

Apo-AcnA was mixed with a 10-fold molar excess of IscU2$^{S\text{-}FeS}$ (or with a 40-fold molar excess of ferrous ammonium sulfate and sodium sulfide, or buffer in control reactions) in 50 mM Tris pH 7.2, 150 mM NaCl, 1 mM DTT and allowed to incubate at room temperature in a sealed anaerobic chamber for up to thirty minutes. Samples of these cluster-transfer (or control) incubations were added to activity assay mixtures to achieve final concentrations of 50 mM Tris pH 8, 0.8 µM AcnA, 20 mM sodium citrate, 250 µM $NADP^+$, 1 mM manganese sulfate, and 0.5 units/mL porcine isocitrate dehydrogenase (ICDH). The assay mixtures were immediately read anaerobically for absorbance at 340 nm over 8 minutes in a spectrophotometer. Samples of AcnA that had incubated with IscU2$^{S\text{-}FeS}$ (or controls) for 5 minutes, 15 minutes, and 30 minutes were analyzed.

Aconitase activity was also measured in *M. acetivorans* WWM73 cell lysates, as above. Lysate supernatant was used in place of aconitase. Lysate was divided into aliquots and incubated for three hours at room temperature, with some maintained in an anaerobic chamber while another aliquot was exposed to ambient oxygen. After three hours, the aerobically exposed sample was quickly made anoxic again by vacuuming and purging with nitrogen. Aliquots of the samples were incubated with IscU2 or IscU2$^{S\text{-}FeS}$, or controls, in 50 mM Tris pH 7.2, 150 mM NaCl for 15 minutes, then aconitase/ICDH assays were performed as above.

Generation of a *M. acetivorans* iscSU2 deletion mutant. The pseudo-wildtype parent strain, WWM73, and plasmid vectors for genetic manipulation were generously provided by Prof. William Metcalf from the University of Illinois, and are listed in Table 5. The *iscSU2* deletion mutant was generated using pJK301 and methods similar to those previously described (Welander & Metcalf, 2008). Briefly, homologous regions upstream (US) and downstream (DS) of *iscS2U2* were amplified by PCR, using primers containing *Apa*I and *Hind*III recognition sites

for the US region and *Bam*HI, and *Spe*I for the DS region. Each PCR product was digested with the appropriate restriction enzymes and sequentially ligated into similarly digested pJK301. Restriction digestion, ligation, and transformation were all carried out as described above. The complete *iscS2U2* knockout plasmid (pDL214) was confirmed by DNA sequencing (Eurofins). Unless otherwise noted, all procedures described below were performed in an anerobic chamber (Coy Laboratories). *M. acetivorans* strain WWM73 was transformed with approximately 2 µg of pDL214 linearized by digestion with *Not*I, using the liposomal transfection method as previously described (Metcalf *et al.*, 1997). Transformants were selected by spread plating on HS agar plates (0.8% w/v noble agar) containing 125 mM methanol and 2 µg/mL puromycin. The plates were placed in a canning jar along with a vial containing 2 ml of 2.5 % sodium sulfide. The jar was sealed and incubated at 35 °C in a standard incubator. Well-isolated colonies were inoculated into HS medium supplemented with 125 mM methanol and 2 µg/mL puromycin. Deletion of *iscS2U2* and replacement with the *pac-hpt* cassette from the pJK301 was confirmed in selected transformants by sequencing PCR products generated with primers listed in Table S1 and genomic DNA isolated from transformants. Once confirmed, the *iscSU2* deletion strain was designated as *M. acetivorans* strain DJL60.

Results

***M. acetivorans* contains three distinct *iscSU* gene clusters**. The genome of *M. acetivorans* contains three *isc* gene clusters, each arranged as *iscSU*, and lacking the additional genes found in bacteria, such as in the well-characterized *isc* operon of *E. coli* (**Fig. 1**) (Galagan *et al.*, 2002). We have designated the three *iscSU* clusters in *M. acetivorans* as *isc1*, *isc2*, and *isc3*, based on gene annotation order. The *iscS1* and *iscU1* genes are clustered with four additional genes of unknown function. A similar gene arrangement is found in other *Methanosarcina* species

including *Methanosarcina barkeri* and *Methanosarcina mazei*. The *iscS2* and *iscU2* genes are clustered with genes encoding enzymes involved in methionine and NAD biosynthesis. A similar gene arrangement is present in many Methanomicrobia, including *M. barkeri.* The genes encoding IscS3 and IscU3 are not clustered with additional genes. A similar gene cluster is found in both *M. barkeri* and *M. mazei*.

IscS1, IscS2, and IscS3 share 45-61 % sequence identity to each other, and each is similar in molecular weight and sequence identity to well-characterized IscS from *E. coli* (**Table 1**). The PLP-binding and active site residues identified in *E. coli* IscS are conserved in the *M. acetivorans* IscS homologs, except for PLP-binding residues in IscS1 (**Table 1 and Fig. 2**) (Mihara & Esaki, 2002). IscU1, IscU2, and IscU3 share 49-68% sequence identity to each other, and each protein also has > 50% sequence identity to *E. coli* IscU (**Table 1**). The Fe-S cluster binding/transfer and Hsp70 chaperone (HscA)-interacting residues (LPPVK) identified in *E. coli* IscU are conserved in the three *M. acetivorans* IscU proteins (Blanc *et al.,* 2014, Bonomi *et al.,* 2011). However, one of the cysteines involved in Fe-S cluster binding by *E. coli* IscU is replaced with histidine in *M. acetivorans* IscU3 (**Table 1 and Fig. 3)**. Outside of methanogens, *M. acetivorans* IscS and IscU homologs have highest sequence identity (50-68%) to putative IscS and IscU proteins found in Clostridia (e.g. *Ruminiclostridium thermocellum*), consistent with some genes in *Methanosarcina* acquired from *Clostridia* via horizontal transfer (Fournier & Gogarten, 2008). These results indicate that *M. acetivorans* possesses three distinct copies of the core components of the ISC system. However, some of the functionally important residues in *E. coli* IscS and IscU are not conserved in IscS1 and IscU3, respectively, Furthermore, only IscS2 and IscU2 have been consistently detected in the proteome of *M. acetivorans* (Lessner *et al.,* 2006, Li *et al.,* 2007, Li *et al.,* 2005[a], Li *et al.,* 2005[b]), indicating that IscS2 and IscU2 may serve

as the primary ISC system. Thus, IscS2 and IscU2 were chosen for initial biochemical and genetic characterization.

IscS2 is a cysteine desulfurase. Recombinant IscS2 was over-produced in *E. coli* and purified to homogeneity (**Fig. 4A**). Purified IscS2 was pale-yellow and exhibited an UV-visible spectrum with an absorbance maximum at 420 nm (**Fig. 4B**), consistent with the presence of PLP (Zheng *et al.,* 1993). Purified IscS2 was able to remove sulfur from L-cysteine (**Table 2**) confirming IscS2 is a cysteine desulfurase. To determine if the cysteine desulfurase activity of IscS2 is dependent on PLP and if recombinant IscS2 contained full incorporation of PLP, assays were performed in the presence and absence of PLP (**Table 2**). A 57 % increase in the cysteine desulfurase activity of IscS2 was observed when PLP was added to the assay. IscS2 reconstituted with PLP ($IscS2^{PLP}$) exhibited the same specific activity both in the absence and presence of additional PLP. An increase in the absorbance at 420 nm was also observed with $IscS2^{PLP}$ (**Fig. 4B**). These data are consistent with full incorporation of PLP in $IscS2^{PLP}$. $IscS2^{PLP}$ was used in all subsequent experiments. Size-exclusion chromatography of $IscS2^{PLP}$ revealed the purified protein exists as a homodimer (**Fig. 4C**), similar to previously characterized IscS (Mihara & Esaki, 2002, Zheng *et al.,* 1993). Taken together, these results reveal that IscS2 is a PLP-dependent cysteine desulfurase.

IscU2 is capable of binding Fe-S clusters. Recombinant IscU2 was expressed in *E. coli* and purified to homogeneity under anoxic conditions (**Fig. 5A**). Purified IscU2 was pale-red and exhibited an UV-visible spectrum with minor absorbance maxima at 360 nm and 438 nm (**Fig. 5B**). As-purified IscU2 contained both iron and acid-labile sulfide (**Table 3**). However, the A_{438}/A_{280} ratio and the iron/sulfide content was low indicating that a substantial portion of purified IscU2 was devoid of Fe-S clusters. IscU devoid of cluster (apo-IscU) typically exists as

a monomer and subsequently dimerizes upon incorporation of [2Fe-2S] clusters. The two [2Fe-2S] clusters in dimeric IscU can then reductively couple to form a single [4Fe-4S] cluster (Agar *et al.,* 2000, Chandramouli *et al.,* 2007). Size-exclusion chromatography of as-purified IscU2 yielded a major peak consistent with monomeric IscU2 and a minor peak consistent with dimeric IscU2 (**Fig. 5C**), indicating that the majority of as-purified IscU2 is in the apo-form. To test the ability of IscU2 to bind Fe-S clusters, IscS2-dependent and chemical-dependent reconstitution of Fe-S clusters in IscU2 were performed. IscS2-dependent reconstituted IscU2 ($IscU2^{S\text{-}FeS}$) was generated by the anoxic incubation of as-purified IscU2 with cysteine, iron and a catalytic amount of IscS2. Chemical-dependent reconstituted IscU ($IscU2^{C\text{-}FeS}$) was generated by the anoxic incubation of as-purified IscU2 with a molar excess of sodium sulfide and iron. A substantial increase in the iron and acid-labile sulfur content and the A_{438}/A_{280} ratio was observed for both $IscU2^{S\text{-}FeS}$ and $IscU2^{C\text{-}FeS}$ (**Table 3**), consistent with an increase in Fe-S clusters in both samples. The UV-visible spectra of $IscU2^{S\text{-}FeS}$ and $IscU2^{C\text{-}FeS}$ were similar and showed a substantial increase in the absorbance at 360 nm and 438 nm (**Fig. 5B**). Size-exclusion chromatography revealed $IscU2^{C\text{-}FeS}$ was dimeric (**Fig. 5C**), demonstrating that Fe-S cluster binding causes dimerization of IscU2. The UV-visible spectra and levels of iron and sulfur in $IscU2^{S\text{-}FeS}$ and $IscU2^{C\text{-}FeS}$ are consistent with the presence of a two [2Fe-2S] clusters or a single [4Fe-4S] cluster per dimer.

EPR analysis of the as-purified IscU2 did not produce a signal under the conditions tested (data not shown), likely due to the low Fe-S cluster content. However, both $IscU2^{S\text{-}FeS}$ and $IscU2^{C\text{-}FeS}$ generated EPR spectra upon the addition of dithionite (**Fig. 6**). Both reduced samples showed a similar EPR signal that can be attributed to $[4Fe\text{-}4S]^{+}$ clusters, consistent with reductive coupling of the [2Fe-2S] clusters into a single [4Fe-4S] in dimeric IscU2 (Agar *et al.,*

2000). From the presence of signals at around g = 2 (330 mT) and higher g values (lower field values) it can be concluded that the clusters display several different spin states. The signal in the 300-400 mT region are due to S = 1/2 species. The peak at g = 4.3 is due to the spin ±3/2 doublet of an S = 5/2 species with E/D=0.333. This peak can be due to a 4Fe cluster or adventitiously bound iron. The peaks at g = 5.09 and 6.23 are due to the spin ±1/2 doublet of an S = 5/2 species with E/D=0.032, the peak at g = 5.56 is due to the same spin state but is due to the spin ±3/2 doublet. The peak at g = 7.52 is due to the spin ±1/2 doublet of a S = 7/2 species with E/D = 0. The as-such sample (**Fig 6A, trace C**) does not show signals due to $[4Fe\text{-}4S]^{2+}$ since in that redox state the spin is 0. The sharp signal at around 330 mT is due to a $[3Fe\text{-}4S]^{1+}$ species. The multitude of spin states point towards a highly variable environment for the clusters present in the binding site on IscU2. These results are consistent with IscU2 as an Fe-S cluster scaffold protein, whereby IscS2 can catalyze the formation of [4Fe-4S] clusters in apo-IscU2 in the presence of iron and cysteine.

***M. acetivorans* contains a [4Fe-4S] cluster aconitase.** Aconitase is a member of the dehydratase family of enzymes that requires a [4Fe-4S] cluster for activity and is the most common acceptor protein used in Fe-S cluster transfer assays (Ayala-Castro *et al.,* 2008). The activity of aconitase can be measured spectrophotometrically in a coupled assay with isocitrate dehydrogenase, whereby the reduction of $NADP^+$ with isocitrate is measured at 340 nm (Gardner & Fridovich, 1992). IscU from several organisms is documented to transfer clusters to apo-aconitase (Tian *et al.*, 2014, Unciuleac *et al.,* 2007, Wollers *et al.,* 2010). Given the substantial information on cluster transfer to aconitase by IscU, aconitase is an ideal acceptor protein to initially assess cluster transfer from IscU2. *M. acetivorans* encodes a single aconitase homolog (MA0250), and *M. acetivorans* cell lysate contains detectable aconitase activity (5.2 nmol

NADPH min^{-1} mg^{-1} protein) as measured by the coupled assay. Recombinant MA0250 was expressed in *E. coli* and purified to homogeneity (**Fig. 7A**). As-purified MA0250 lacked aconitase activity. However, after chemical reconstitution with iron and sulfide, purified MA0250 exhibited robust aconitase activity (100 nmol NADPH min^{-1} mg^{-1} protein) and a broad absorbance maximum around 400 nm in UV-visible spectrum, consistent with the presence of a [4Fe-4S] cluster (**Fig. 7B**). These results reveal that MA0250 is an aconitase (designated here as AcnA) with activity dependent on the presence of a [4Fe-4S] cluster.

Cluster-loaded IscU2 can restore the activity of *M. acetivorans* apo-aconitase. Anoxic incubation of apo-AcnA with $IscU2^{S\text{-}FeS}$ resulted in rapid and complete recovery of aconitase activity, whereas incubation with iron and sulfide, at the same molar concentration as found in $IscU2^{S\text{-}FeS}$, did not restore any activity to apo-AcnA over the same timeframe (**Fig. 8**). The ability of cluster loaded IscU2 to restore aconitase activity was also examined using cell lysate. Consistent with AcnA containing an oxygen-labile [4Fe-4S] cluster required for activity, exposure of cell lysate to air resulted in a complete loss of aconitase activity, even when the cell lysate was made anoxic again (**Table 4**). The addition of as-purified IscU2 during the anoxic incubation of air-exposed lysate also did not restore aconitase activity. However, anoxic incubation of air-exposed cell lysate with $IscU2^{S\text{-}FeS}$ partially restored aconitase activity (**Table 4**). Overall, these data demonstrate that cluster-loaded IscU2 is capable of transferring Fe-S clusters to apo-AcnA, consistent with IscU2 as an Fe-S cluster scaffold.

Deletion of *iscSU2* impacts sulfur metabolism in *M. acetivorans*. The results from the biochemical characterization of recombinant IscS2 and IscU2 reveal properties consistent with each protein functioning in Fe-S cluster biogenesis. To determine the importance of IscS2 and IscU2 to *M. acetivorans* physiology, a mutant strain (DJL60) was generated with *iscSU2* deleted

and replaced with the *pac-hpt* genes (**Fig. 9A**). The mutant was isolated using HS medium supplemented with both cysteine and sulfide. PCR (**Fig. 9B**) and DNA sequencing verified the DJL60 mutant. Thus, neither IscS2 nor IscU2 are essential to *M. acetivorans*.

To test the impact of the loss of IscSU2 on *M. acetivorans*, first the growth of strain DJL60 with cysteine, sulfide, or cysteine + sulfide was compared to the parent strain WWM73. Growth studies were performed in HS medium supplemented with 1.5 mM dithiothreitol (DTT), designated here as HS_{DTT} medium, to maintain similar redox conditions with the different sulfur sources. DTT cannot be used as a sulfur source by *M. acetivorans* (Rauch & Perona, 2016). The growth profiles of strains WWM73 and DJL60 were similar with the different exogenous sulfur sources (**Fig. 10**). However, compared to strain WWM73, strain DJL60 exhibited slightly slower and more variable growth when cysteine was present, especially when cysteine was the only sulfur source.

To determine the impact of the loss of IscSU2 on sulfur metabolism of *M. acetivorans* with the different exogenous sulfur sources, cysteine desulfurase activity, Fe-S cluster levels and persulfide content in lysate from strain DJL60 and WWM73 cells were determined. Importantly, lysate from strain DJL60 grown under all conditions exhibited significantly less cysteine desulfurase activity than strain WWM73 lysate (**Fig. 11A**), consistent with IscS2 as a functional *in vivo* cysteine desulfurase. However, cysteine desulfurase activity was not completely abolished in strain DJL60 indicating additional enzymes (e.g. IscS3) contribute to the total cysteine desulfurase activity. Interestingly, lysate from *Methanococcus maripaludis*, whose genome does not encode a cysteine desulfurase, contains some cysteine desulfurase activity from an unknown source (Liu *et al.*, 2010). No significant difference was observed in the Fe-S cluster content in strain DJL60 and WWM73 lysate across all sulfur conditions (**Fig. 11B**). However,

the persulfide content in strain DJL60 was significantly lower in lysate from cysteine and cysteine + sulfide grown cells compared to lysate from WWM73 cells (Fig. 7C). Overall, these results confirm IscS2 as an *in vivo* cysteine desulfurase and link IscSU2 to sulfur metabolism in *M. acetivorans*.

Discussion

Methanogens are metabolic specialists; all species are dependent on methanogenesis for growth (Thauer *et al.,* 2008). Methanogenesis has an obligate requirement for Fe-S cluster proteins. An understanding of the protein machinery used by methanogens for the *de novo* synthesis of Fe-S clusters may lead to improved methods to increase or inhibit methanogenesis. The results presented here reveal that *M. acetivorans* harbors functional IscS and IscU, the minimal components of the ISC-type Fe-S cluster biogenesis system, that serve as the general system in numerous bacteria and in mitochondria. It is reasonable to conclude that other methanogens whose sequenced genomes encode IscSU also utilize a minimal ISC system for Fe-S cluster biogenesis.

The absence of IscSU in some methanogens is likely due to physiological differences resulting from environmental constraints. Members of the Methanococcales, Methanopyrales, and some species of Methanobacteriales lack *iscSU* (Boyd *et al.,* 2014, Lyu & Lu, 2018). These species appear to lack any cysteine desulfurase, suggesting that cysteine may not serve as the direct sulfur donor for Fe-S cluster biogenesis. Indeed, experimental evidence revealed that *M. maripaludis* uses sulfide, instead of cysteine, as the sulfur donor for Fe-S cluster biogenesis (Liu *et al.,* 2010). This was the first evidence of a substrate, other than cysteine, serving as the sulfur donor for Fe-S cluster biogenesis in any organism. *Methanococcus* spp. live in sulfide-rich environments and are dependent primarily on sulfide as an exogenous source of sulfur and do not

use cysteine (Whitman *et al.*, 1982). Like all methanogens, *M. maripaludis* encodes SufBC. It seems likely that methanogen SufBC does not partner with a cysteine desulfurase but receives sulfur from sulfide for the assembly of an Fe-S cluster. The mechanisms and factors involved in directing sulfide to Fe-S cluster biogenesis machinery are unknown in *Methanococcus*, but presumably involve an unknown protein factor(s) to traffic sulfur from sulfide to SufBC.

Most species of the Methanomicrobia contain at least one copy of *iscSU*, in addition to *sufCB* (Boyd *et al.*, 2014). All *Methanosarcina* spp. possess *iscSU* (Lyu & Lu, 2018). *Methanosarcina* spp. are the most metabolically diverse methanogens capable of producing methane with H_2/CO_2, methylated compounds, and acetate. *Methanosarcina* are one of only two genera capable of metabolizing acetate, which accounts for two-thirds of all biogenic methane produced (Thauer *et al.*, 2008). *Methanosarcina* also have the largest genomes and are the most oxygen tolerant methanogens (Galagan *et al.*, 2002, Angel *et al.*, 2012). Unlike *Methanococci*, *Methanosarcina* can use cysteine, in addition to sulfide, as an exogenous sulfur source. The acquisition of IscSU, in addition to SufBC, may aid in the metabolic diversity and aerotolerance of *Methanosarcina* by conferring the ability to use cysteine as an exogenous sulfur source and as a direct sulfur source for the biogenesis of Fe-S clusters in more oxidizing environments with limited sulfide.

M. acetivorans and related Methanosarcinales contain multiple copies of *iscSU*. *M. acetivorans* IscSU1-3 may be functionally redundant, which is supported by residual cysteine desulfurase activity and normal Fe-S cluster content in strain DJL60. However, IscS1 and IscU3 lack some of the residues required for the function of *E. coli* IscS and IscU, indicating these orthologs could be non-functional. Alternatively, each ortholog may serve a different function in Fe-S cluster biogenesis. Recently, the structure of a recombinant [2Fe-2S] cluster-containing

IscS-IscU complex from *Archaeoglobus fulgidus* was solved (Marinoni *et al.*, 2012). *A. fulgidus* is an anaerobic archaeon that is closely related to methanogens. Interestingly, *A. fulgidus* IscS lacks cysteine desulfurase activity due to a substitution of a catalytically essential lysine with aspartate. In the solved structure, *A. fulgidus* IscS provides a cysteine ligand to the [2Fe-2S] cluster in IscU, suggesting it plays a role in cluster assembly as a ligand, but not by providing sulfur (Marinoni *et al.*, 2012, Pagnier *et al.*, 2015, Yamanaka *et al.*, 2013). Like *A. fulgidus* IscS, IscS1 lacks the catalytically essential lysine (**Fig. S2**) indicating it may function as *A. fulgidus* IscS. Expression of recombinant IscS1 in *E. coli* led to the formation of inclusion bodies, indicating it may require co-expression with IscU1 for stabilization (data not shown).

Aerobic bacteria and eukaryotes typically have complex ISC and SUF systems that involve several accessory factors, whereas methanogens appear to use only the minimal components, IscSU and SufBC, respectively. It was proposed that the SUF system increased in complexity as additional factors were needed to control iron and sulfur trafficking to synthesize Fe-S clusters in cells that live in more oxidizing environments (Boyd *et al.*, 2014). The same may be true for the ISC system. For example, the *M. acetivorans isc* gene clusters lack any of the additional genes found in the *E. coli isc* operon, including *hscA* and *hscB,* which are essential to ISC-dependent Fe-S cluster biogenesis in *E. coli*. HscA and HscB are chaperones that specifically interact with IscU to accelerate Fe-S cluster transfer to target apo-proteins. HscA specifically binds to the IscU LPPVK motif to elicit conformational changes in IscU dependent on the hydrolysis of ATP (Bonomi *et al.*, 2011, Chandramouli & Johnson, 2006). Surprisingly, *M. acetivorans* IscSU1-3 all contain a variant of the LPPVK motif (**Table 1**), yet the genome of *M. acetivorans* does not encode homologs of HscA or HscB. It is possible that unrelated chaperones fulfill the role of HscA and HscB. However, it was recently shown that several point

mutations in IscU suppress the essential role of HscA and HscB in *E. coli* (Tanaka *et al.,* 2016). Given that *M. acetivorans* cluster-loaded IscU2 rapidly restored the *in vitro* activity of apo-aconitase in the absence of additional factors, it seems more likely that chaperones are not involved in ISC-dependent Fe-S cluster biogenesis in *M. acetivorans*, despite the presence of the LPPVK motif in IscU1-3.

Finally, the results indicate a cysteine-specific function for *M. acetivorans* IscSU2. Deletion of *iscSU2* resulted in decreased *in vivo* cysteine desulfurase activity. Although a decrease in Fe-S cluster content was not observed in strain DJL60 grown with cysteine, it is possible that IscU1 and/or IscU3 serve as Fe-S cluster scaffolds in the absence of IscU2. Cysteine desulfurase serves as the central hub for trafficking sulfur in bacteria and eukaryotes. Importantly, a decrease in the persulfide content of DJL60 cells compared to wild type cells was only observed when cysteine was provided as an exogenous sulfur source, indicating IscS2 participates in trafficking sulfur from cysteine, but is not involved when sulfide is the sole sulfur source. Based on results presented here and with *M. maripaludis* (Liu *et al.,* 2010, Liu *et al.,* 2012), cells of *M. acetivorans* may primarily use IscSU for Fe-S cluster biogenesis and sulfur trafficking when provided cysteine, and primarily use SufBC for Fe-S cluster biogenesis when cells are provided sulfide.

This study provides the first experimental evidence that methanogens possess functional components of the ISC system for Fe-S cluster biogenesis. Biochemical analyses demonstrated that *M. acetivorans* IscS is a cysteine desulfurase and that IscU2 is an Fe-S cluster scaffold. Importantly, IscSU2 can provide Fe-S clusters to target apo-proteins. Deletion of *iscSU2* revealed that IscSU2 is not essential to Fe-S cluster biogenesis in *M. acetivorans*. However, loss of IscSU2 impacts sulfur metabolism. These results provide new insight into the mechanisms of

Fe-S cluster biogenesis in methanogens, which may aid in the development of methods to enhance or inhibit methanogenesis, due to the obligate requirement for Fe-S proteins.

List of abbreviations

ICDH: isocitrate dehydrogenase

AcnA: aconitase

Fe-S: iron-sulfur

HS: high-salt

DTT: dithiothreitol

PLP: pyridoxal 5'- phosphate

References

Agar, J.N., C. Krebs, J. Frazzon, B.H. Huynh, D.R. Dean, & M.K. Johnson, (2000) IscU as a scaffold for iron-sulfur cluster biosynthesis: sequential assembly of [2Fe-2S] and [4Fe-4S] clusters in IscU. *Biochemistry.* 39: 7856-62.

Angel, R., P. Claus, & R. Conrad, (2012) Methanogenic archaea are globally ubiquitous in aerated soils and become active under wet anoxic conditions. *ISME J.* 6: 847-62.

Ayala-Castro, C., A. Saini, & F.W. Outten, (2008) Fe-S cluster assembly pathways in bacteria. *Microbiology and molecular biology reviews.* 72: 110-25.

Bandyopadhyay, A., J. Stockel, H. Min, L.A. Sherman, & H.B. Pakrasi, (2010) High rates of photobiological H2 production by a cyanobacterium under aerobic conditions. *Nature communications.* 1: 139.

Beinert, H. (1983) Semi-micro methods for analysis of labile sulfide and of labile sulfide plus sulfane sulfur in unusually stable iron-sulfur proteins. *Analytical biochemistry.* 131: 373-8.

Blanc, B., C. Gerez, & S. Ollagnier de Choudens, (2014) Assembly of Fe/S proteins in bacterial systems: Biochemistry of the bacterial ISC system. *Biochimica et biophysica acta*. 1853: 1436-47.

Bonomi, F., S. Iametti, A. Morleo, D. Ta, & L.E. Vickery, (2011) Facilitated transfer of IscU-[2Fe2S] clusters by chaperone-mediated ligand exchange. *Biochemistry.* 50: 9641-50.

Boyd, E.S., T.L. Hamilton, & J.W. Peters, (2011) An alternative path for the evolution of biological nitrogen fixation. *Frontiers in microbiology.* 2: 205.

Boyd, E.S., K.M. Thomas, Y. Dai, J.M. Boyd, & F.W. Outten, (2014) Interplay between oxygen and Fe-S cluster biogenesis: insights from the Suf pathway. *Biochemistry.* 53: 5834-47.

Bradford, M.M., (1976) A rapid and sensitive method for the quantitation of microgram quantities of protein utilizing the principle of protein-dye binding. *Anal. Biochem.* 72: 248-254.

Chandramouli, K. & M.K. Johnson, (2006) HscA and HscB stimulate [2Fe-2S] cluster transfer from IscU to apoferredoxin in an ATP-dependent reaction. *Biochemistry.* 45: 11087-95.

Chandramouli, K., M.C. Unciuleac, S. Naik, D.R. Dean, B.H. Huynh, & M.K. Johnson, (2007) Formation and properties of [4Fe-4S] clusters on the IscU scaffold protein. *Biochemistry.* 46: 6804-11.

Chandrayan, S.K., P.M. McTernan, R.C. Hopkins, J. Sun, F.E. Jenney Jr., & M.W. Adams, (2012) Engineering hyperthermophilic archaeon Pyrococcus furiosus to overproduce its cytoplasmic [NiFe]-hydrogenase. *J Biol Chem.* 287: 3257-64.

Costa, K.C., P.M. Wong, T. Wang, T.J. Lie, J.A. Dodsworth, I. Swanson, J.A. Burn, M. Hackett, & J.A. Leigh, (2010) Protein complexing in a methanogen suggests electron bifurcation and electron delivery from formate to heterodisulfide reductase. *Proc Natl Acad Sci U S A.* 107: 11050-5.

Couturier, J., B. Touraine, J.F. Briat, F. Gaymard, & N. Rouhier, (2013) The iron-sulfur cluster assembly machineries in plants: current knowledge and open questions. *Frontiers in plant science.* 4: 259.

Dekas, A.E., R.S. Poretsky, & V.J. Orphan, (2009) Deep-sea archaea fix and share nitrogen in methane-consuming microbial consortia. *Science.* 326: 422-6.

Dos Santos, P.C., Z. Fang, S.W. Mason, J.C. Setubal, & R. Dixon, (2012) Distribution of nitrogen fixation and nitrogenase-like sequences amongst microbial genomes. *BMC Genomics.* 13: 162.

Ferry, J.G., (1999) Enzymology of one-carbon metabolism in methanogenic pathways. *FEMS Microbiol Rev.* 23: 13-38.

Fontecave, M. & S. Ollagnier-de-Choudens, (2008) Iron-sulfur cluster biosynthesis in bacteria: Mechanisms of cluster assembly and transfer. *Arch Biochem Biophys.* 474: 226-37.

Fournier, G.P. & J.P. Gogarten, (2008) Evolution of acetoclastic methanogenesis in Methanosarcina via horizontal gene transfer from cellulolytic Clostridia. *J Bacteriol.* 190: 1124-7.

Galagan, J.E., C. Nusbaum, A. Roy, M.G. Endrizzi, P. Macdonald, W. FitzHugh, S. Calvo, R. Engels, S. Smirnov, D. Atnoor, A. Brown, N. Allen, J. Naylor, N. Stange-Thomann, K. DeArellano, R. Johnson, L. Linton, P. McEwan, K. McKernan, J. Talamas, A. Tirrell, W. Ye, A. Zimmer, R.D. Barber, I. Cann, D.E. Graham, D.A. Grahame, A.M. Guss, R. Hedderich, C. Ingram-Smith, H.C. Kuettner, J.A. Krzycki, J.A. Leigh, W. Li, J Liu, B. Mukhopadhyay, J.N. Reeve, K. Smith, T.A. Springer, L.A. Umayam, O. White, R.H. White, E. Conway de Macario, J.G. Ferry, K.F. Jarrell, H. Jing, A.J. Macario, I. Paulsen, M. Pritchett, K.R. Sowers, R.V. Swanson, S.H. Zinder, E. Lander, W.W. Metcalf, & B. Birren, (2002) The genome of Methanosarcina acetivorans reveals extensive metabolic and physiological diversity. *Genome Res.* 12: 532-42.

Gardner, P.R. & I. Fridovich, (1992) Inactivation-reactivation of aconitase in Escherichia coli. A sensitive measure of superoxide radical. *J Biol Chem.* 267: 8757-63.

Guss, A.M., M. Rother, J.K. Zhang, G. Kulkarni, & W.W. Metcalf, (2008) New methods for tightly regulated gene expression and highly efficient chromosomal integration of cloned genes for *Methanosarcina* species. *Archaea.* 2: 193-203.

Hedderich, R., N. Hamann, & M. Bennati, (2005) Heterodisulfide reductase from methanogenic archaea: a new catalytic role for an iron-sulfur cluster. *Biol Chem.* 386: 961-70.

Hu, Y. & M.W. Ribbe, (2016) Biosynthesis of the Metalloclusters of Nitrogenases. *Annu Rev Biochem.* 85: 455-83.

Jennings, M.E., F.H. Lessner, E.A. Karr, & D.J. Lessner, (2016) The [4Fe-4S] clusters of Rpo3 are key determinants in the post Rpo3/Rpo11 heterodimer formation of RNA polymerase in Methanosarcina acetivorans. *MicrobiologyOpen.* 6: e00399.

Johnson, D.C., D.R. Dean, A.D. Smith, & M.K. Johnson, (2005) Structure, function, and formation of biological iron-sulfur clusters. *Annu Rev Biochem.* 74: 247-81.

Lessner, D.J., L. Li, Q. Li, T. Rejtar, V.P. Andreev, M. Reichlen, K. Hill, J.J. Moran, B.L. Karger, & J.G. Ferry, (2006) An unconventional pathway for reduction of CO2 to methane in CO-grown Methanosarcina acetivorans revealed by proteomics. *Proc Natl Acad Sci U S A.* 103: 17921-6.

Lessner, F.H., M.E. Jennings, A. Hirata, E.C. Duin, & D.J. Lessner, (2012) Subunit D of RNA polymerase from Methanosarcina acetivorans contains two oxygen-labile [4Fe-4S] clusters: implications for oxidant-dependent regulation of transcription. *J Biol Chem.* 287: 18510-23.

Li, L., Q. Li, L. Rohlin, U. Kim, K. Salmon, T. Rejtar, R.P. Gunsalus, B.L. Karger, & J.G. Ferry, (2007) Quantitative proteomic and microarray analysis of the archaeon Methanosarcina acetivorans grown with acetate versus methanol. *J Proteome Res.* 6: 759-71.

Li, Q., L. Li, T. Rejtar, B.L. Karger, & J.G. Ferry, (2005) Proteome of Methanosarcina acetivorans Part II: comparison of protein levels in acetate- and methanol-grown cells. *J Proteome Res.* 4: 129-35.

Li, Q., L. Li, T. Rejtar, B.L. Karger, & J.G. Ferry, (2005) Proteome of Methanosarcina acetivorans Part I: an expanded view of the biology of the cell. *J Proteome Res.* 4: 112-28.

Liu, Y., M. Sieprawska-Lupa, W.B. Whitman, & R.H. White, (2010) Cysteine is not the sulfur source for iron-sulfur cluster and methionine biosynthesis in the methanogenic archaeon Methanococcus maripaludis. *J Biol Chem.* 285: 31923-9.

Liu, Y., L.L. Beer, & W.B. Whitman, (2012) Sulfur metabolism in archaea reveals novel processes. *Environ Microbiol.* 14: 2632-44.

Lyu, Z. & Y. Lu, (2018) Metabolic shift at the class level sheds light on adaptation of methanogens to oxidative environments. *ISME J.* 12: 411-423.

Major, T.A., H. Burd, & W.B. Whitman, (2004) Abundance of 4Fe-4S motifs in the genomes of methanogens and other prokaryotes. *FEMS Microbiol Lett.* 239: 117-23.

Marinoni, E.N., J.S. de Oliveira, Y. Nicolet, E.C. Raulfs, P. Amara, D.R. Dean, & J.C. Fontecilla-Camps, (2012) (IscS-IscU)2 complex structures provide insights into Fe2S2 biogenesis and transfer. *Angewandte Chemie.* 51: 5439-42.

Metcalf, W.W., J.K. Zhang, E. Apolinario, K.R. Sowers, & R.S. Wolfe, (1997) A genetic system for Archaea of the genus Methanosarcina: liposome-mediated transformation and construction of shuttle vectors. *Proc Natl Acad Sci USA.* 94: 2626-31

Mihara, H. & N. Esaki, (2002) Bacterial cysteine desulfurases: their function and mechanisms. *Applied microbiology and biotechnology.* 60: 12-23.

Pagnier, A., Y. Nicolet, & J.C. Fontecilla-Camps, (2015) IscS from Archaeoglobus fulgidus has no desulfurase activity but may provide a cysteine ligand for [FeS] cluster assembly. *Biochimica et biophysica acta*. 1853: 1457-63.

Peters, J.W., K. Fisher, & D.R. Dean, (1995) Nitrogenase structure and function: a biochemical-genetic perspective. *Annu Rev Microbiol.* 49: 335-66.

Peters, J.W., G.J. Schut, E.S. Boyd, D.W. Mulder, E.M. Shepard, J.B. Broderick, P.W. King, & M.W. Adams, (2015) [FeFe]- and [NiFe]-hydrogenase diversity, mechanism, and maturation. *Biochimica et biophysica acta.* 1853: 1350-69.

Ragsdale, S.W., (2000) Nickel containing CO dehydrogenases and hydrogenases. *Sub-cellular biochemistry.* 35: 487-518.

Rauch, B.J. & J.J. Perona, (2016) Efficient Sulfide Assimilation in Methanosarcina acetivorans Is Mediated by the MA1715 Protein. *J Bacteriol.* 198: 1974-83.

Roche, B., L. Aussel, B. Ezraty, P. Mandin, B. Py, & F. Barras, (2013) Iron/sulfur proteins biogenesis in prokaryotes: formation, regulation and diversity. *Biochimica et biophysica acta.* 1827: 455-69.

Sousa, F.L., T. Thiergart, G. Landan, S. Nelson-Sathi, I.A. Pereira, J.F. Allen, N. Lane, & W.F. Martin, (2013) Early bioenergetic evolution. *Philos Trans R Soc Lond B Biol Sci.* 368: 20130088.

Sowers, K.R., J.E. Boone, & R.P. Gunsalus, (1993) Disaggregation of Methanosarcina spp. and growth as single cells at elevated osmolarity. *Appl Environ Microbiol.* 59: 3832-9.

Tanaka, N., Kanazawa, M., Tonosaki, K., Yokoyama, N., Kuzuyama, T. & Takahashi, Y. (2016) Novel features of the ISC machinery revealed by characterization of Escherichia coli mutants that survive without iron-sulfur clusters, *Mol Microbiol.* 99, 835-48.

Thauer, R.K., (2012) The Wolfe cycle comes full circle. *Proc Natl Acad Sci U S A.* 109: 15084-5.

Thauer, R.K., A.K. Kaster, H. Seedorf, W. Buckel, & R. Hedderich, (2008) Methanogenic archaea: ecologically relevant differences in energy conservation. *Nat Rev Microbiol.* 6: 579-91.

Tian, T., H. He, & X.Q. Liu, (2014) The SufBCD protein complex is the scaffold for iron-sulfur cluster assembly in Thermus thermophiles HB8. *Biochemical and biophysical research communications.* 443: 376-81.

Unciuleac, M.C., K. Chandramouli, S. Naik, S. Mayer, B.H. Huynh, M.K. Johnson, & D.R. Dean, (2007) In vitro activation of apo-aconitase using a [4Fe-4S] cluster-loaded form of the IscU [Fe-S] cluster scaffolding protein. *Biochemistry.* 46: 6812-21.

Wagner, T., U. Ermler, & S. Shima, (2016) The methanogenic CO2 reducing-and-fixing enzyme is bifunctional and contains 46 [4Fe-4S] clusters. *Science.* 354: 114-117.

Welander, P.V. & W.W. Metcalf, (2008) Mutagenesis of the C1 oxidation pathway in Methanosarcina barkeri: new insights into the Mtr/Mer bypass pathway. *J Bacteriol.* 190: 1928-36.

Whitman, W.B., E. Ankwanda, & R.S. Wolfe, (1982) Nutrition and carbon metabolism of Methanococcus voltae. *J Bacteriol.* 149: 852-63.

Wolin, E.A., M.J. Wolin, & R.S. Wolfe, (1963) Formation of Methane by Bacterial Extracts. *J Biol Chem.* 238: 2882-6.

Wollers, S., G. Layer, R. Garcia-Serres, L. Signor, M. Clemancey, J.M. Latour, M. Fontecave, & S. Ollagnier de Choudens, (2010) Iron-sulfur (Fe-S) cluster assembly: the SufBCD complex is a new type of Fe-S scaffold with a flavin redox cofactor. *J Biol Chem.* 285: 23331-41.

Yamanaka, Y., L. Zeppieri, Y. Nicolet, E.N. Marinoni, J.S. de Oliveira, M. Odaka, D.R. Dean, & J.C. Fontecilla-Camps, (2013) Crystal structure and functional studies of an unusual L-cysteine desulfurase from Archaeoglobus fulgidus. *Dalton transactions.* 42: 3092-9.

Zheng, L., R.H. White, V.L. Cash, R.F. Jack, & D.R. Dean, (1993) Cysteine desulfurase activity indicates a role for NIFS in metallocluster biosynthesis. *Proc Natl Acad Sci U S A.* 90: 2754-8.

APPENDIX

Figures and Tables

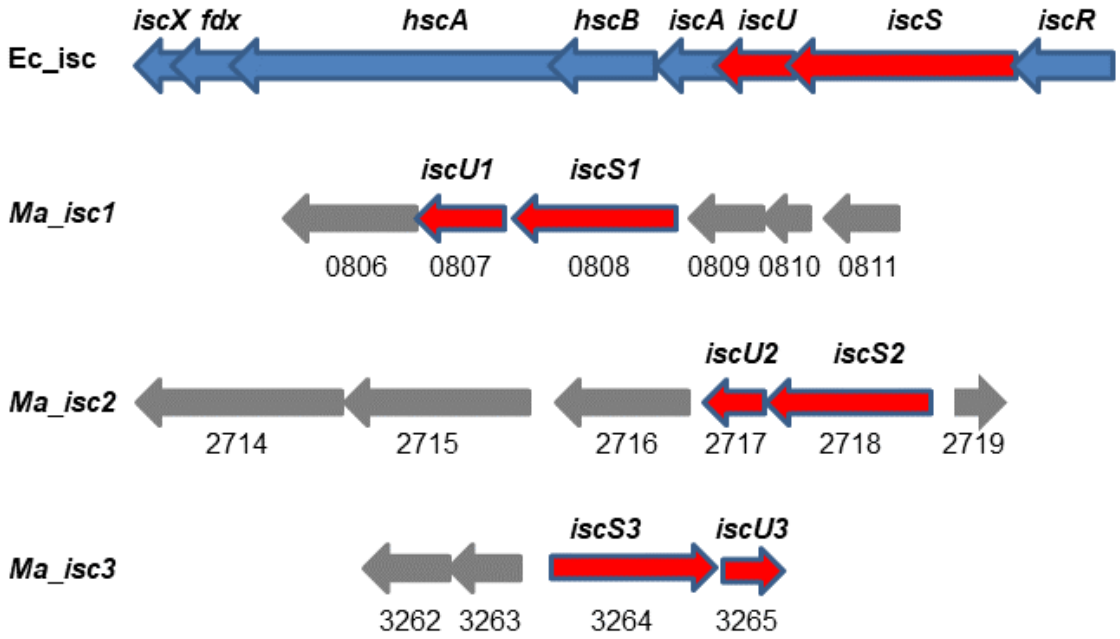

Figure 1. Arrangement of the gene clusters containing *iscS* and *iscU* in *E. coli* and *M. acetivorans* C2A. Other predicted gene functions: MA0806, conserved hypothetical protein; MA0809, DrsE superfamily protein; MA0810, SirA-like protein; MA0811, histidine triad protein; MA2714, homoserine O-acetyltransferase; MA2715, O-acetylhomoserine (thiol)-lyase; MA2716, quinolinate synthetase A; MA2719, helix-turn-helix XRE-family like protein; MA3262, LrgB superfamily protein; MA3263, LrgA superfamily protein.

Table 1. Comparison of predicted *M. acetivorans* IscS and IscU.

Canonical Protein (kDa)	Functional motif(s) or residues	*M. acetivorans* homolog	Gene ID:	Percent identity to *E. coli* IscS/U	Motif or residues in corresponding *M. acetivorans* protein
E. coli IscS (45.1 kDa)	323-SSGSACTS-330[a]	IscS1: MA0808[d] (42.2 kDa)	MA_RS04215	43	318-STGSACFS-325
		IscS2: MA2718[d] (43.3 kDa)	MA_RS14225	48	232-STGSACNS-330
		IscS3: MA3264 (43.6 kDa)	MA_RS17030	48	317-STGSACSS-324
E. coli IscU (13.8 kDa)	C37, D39, C63, C106[b] 99-LPPVK-103[c]	IscU1: MA0807 (24.2 kDa)	MA_RS04210	50	C45, D47, C72, C116 109-LPPIK-113
		IscU2: MA2717[d] (13.9 kDa)	MA_RS14220	54	C34, D36, C59, C103 96-LPPIK-100
		IscU3: MA3265 (14.0 kDa)	MA_RS17035	50	H32, D34, C57, C101 94-LPPGK-98

[a] Cysteine desulfurase active site motif
[b] Residues critical for Fe-S cluster binding and transfer
[c] Residues critical for interaction with the HscA chaperone
[d] Detected in *M. acetivorans* proteome (see text).

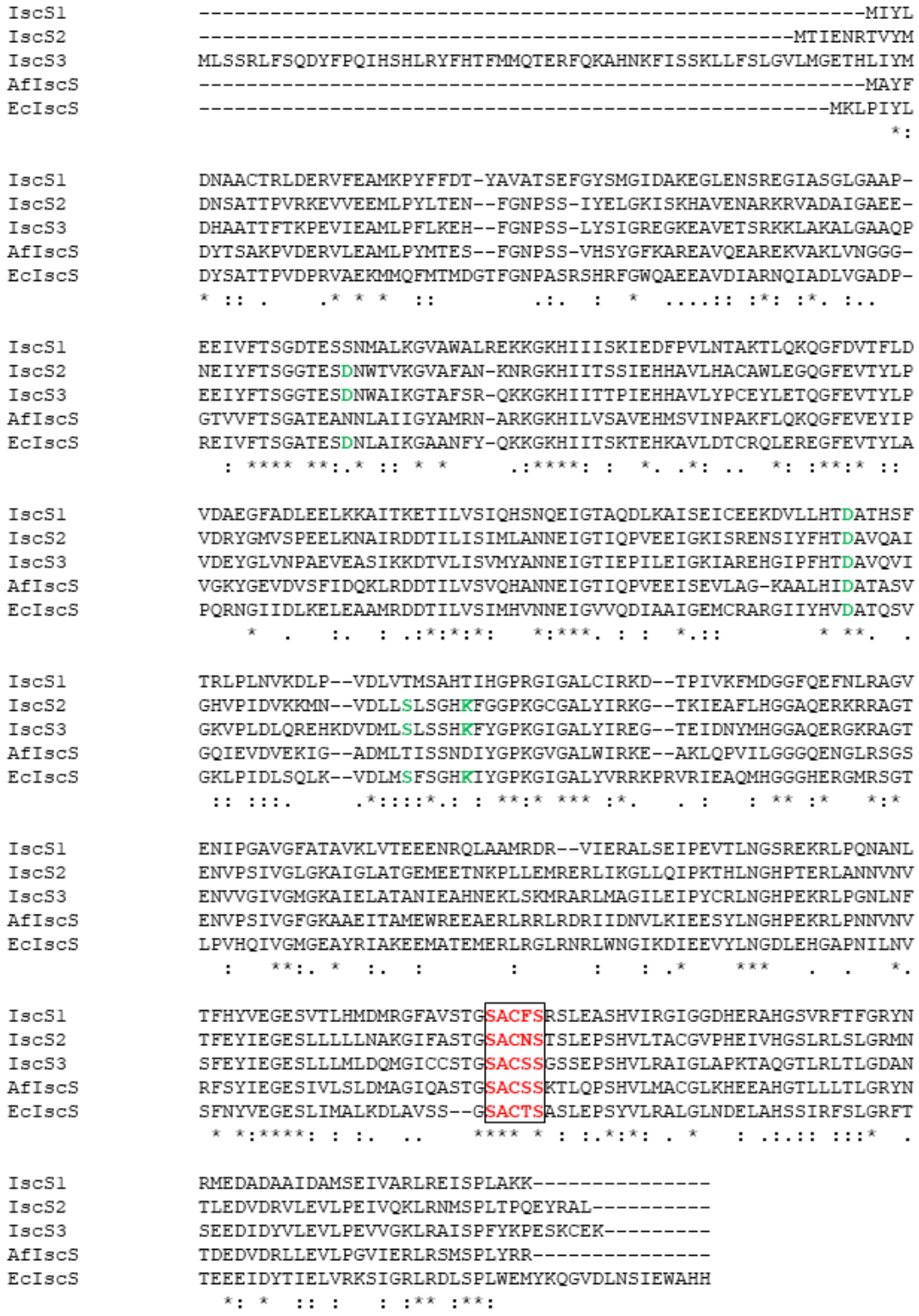

Figure 2. Amino acid sequence alignment of *M. acetivorans* IscS1-3 with IscS from *Escherichia coli* and *Archaeoglobus fulgidus*. The active site residues in *E. coli* IscS are red and boxed. The PLP binding residues in *E. coli* IscS are green. Ec: *E. coli*; Af: *A. fulgidus*.

Figure 3. Amino acid sequence alignment of *M. acetivorans* IscU1-3 with IscS from *Escherichia coli* and *Archaeoglobus fulgidus*. The Fe-S cluster binding residues in *E. coli* IscU are red, and the conserved as[artate and histidine are green. The HscA-interacting region is boxed. Ec: *E. coli*; Af: *A. fulgidus*.

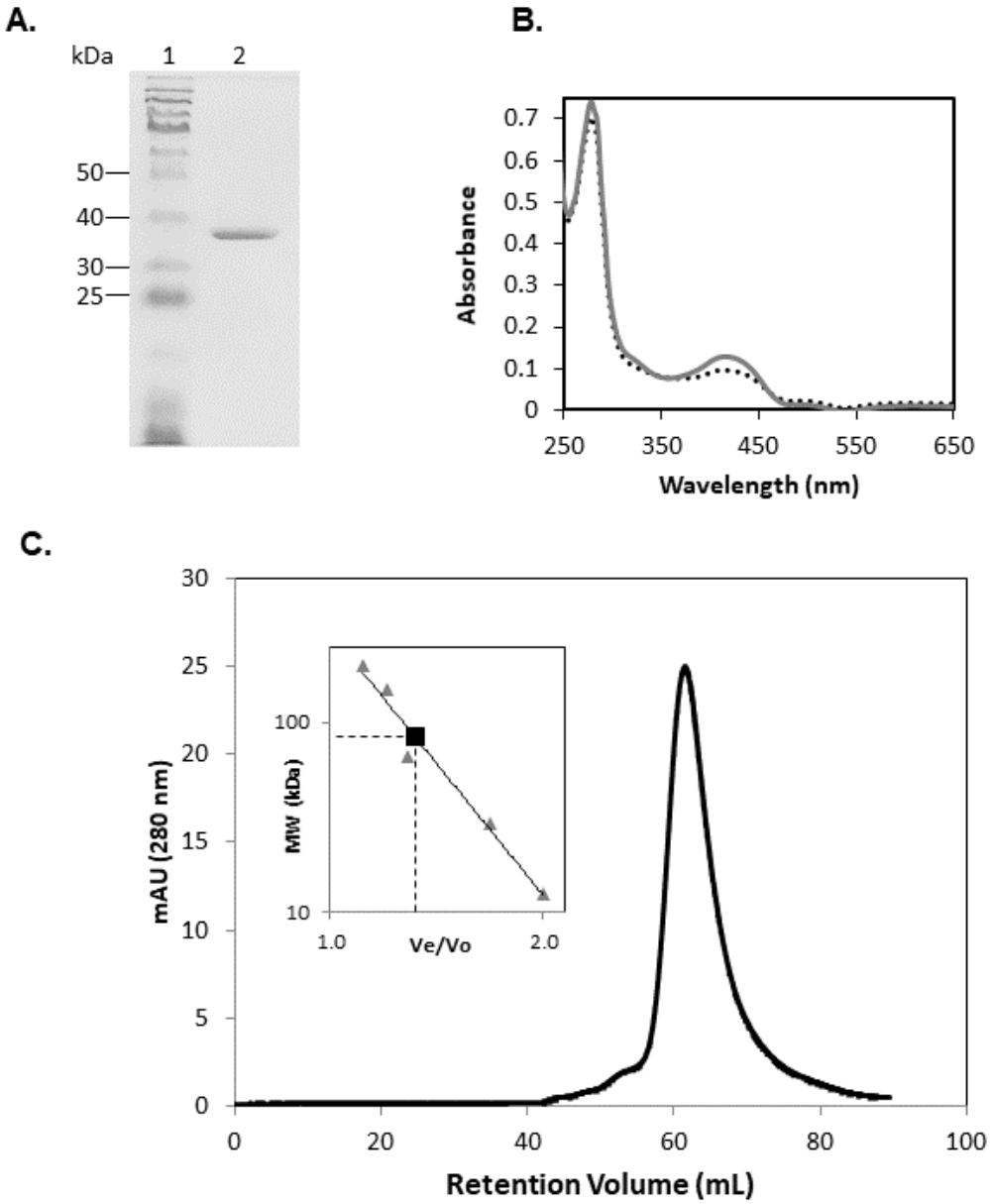

Figure 4. Purified IscS2 binds PLP and is a homodimer. A) SDS-PAGE analysis of purified IscS2 (cropped image of original). Lane 1, MW marker; lane 2, IscS2 (2.5 µg). B) UV-visible spectra of 20 µM IscS2 (dotted line) or IscS2^{PLP} (solid line) in 50 mM Tris pH 7.2, 150 mM NaCl. C) Size-exclusion chromatography of IscS2. IscS2 (3.3 mg loaded) was analyzed by size-exclusion chromatography with 50 mM Tris pH 8.0, 150 mM NaCl, 2 mM DTT, 10% glycerol. The molecular weight of IscS2 was calculated from a standard curve (inset). The square represents the V_e/V_o of IscS2 with a calculated molecular weight of 84 kDa, consistent with homodimer (87 kDa).

Table 2. Effect of PLP on cysteine desulfurase activity of purified IscS2.

Sample	Cysteine desulfurase activity[b]
IscS2	21.5 ± 1.2
IscS2 + PLP	33.8 ± 0.5
$IscS2^{PLP}$[a]	35.1 ± 2.1
$IscS2^{PLP}$ + PLP	33.4 ± 0.5

[a] IscS2 reconstituted with PLP

[b] Cysteine desulfurase activity (nmol sulfur min^{-1} mg^{-1} IscS2) of 5 µM IscS2 or $IscS2^{PLP}$ in the absence or presence of additional PLP (50 µM). Results are means from triplicates ± 1 standard deviation

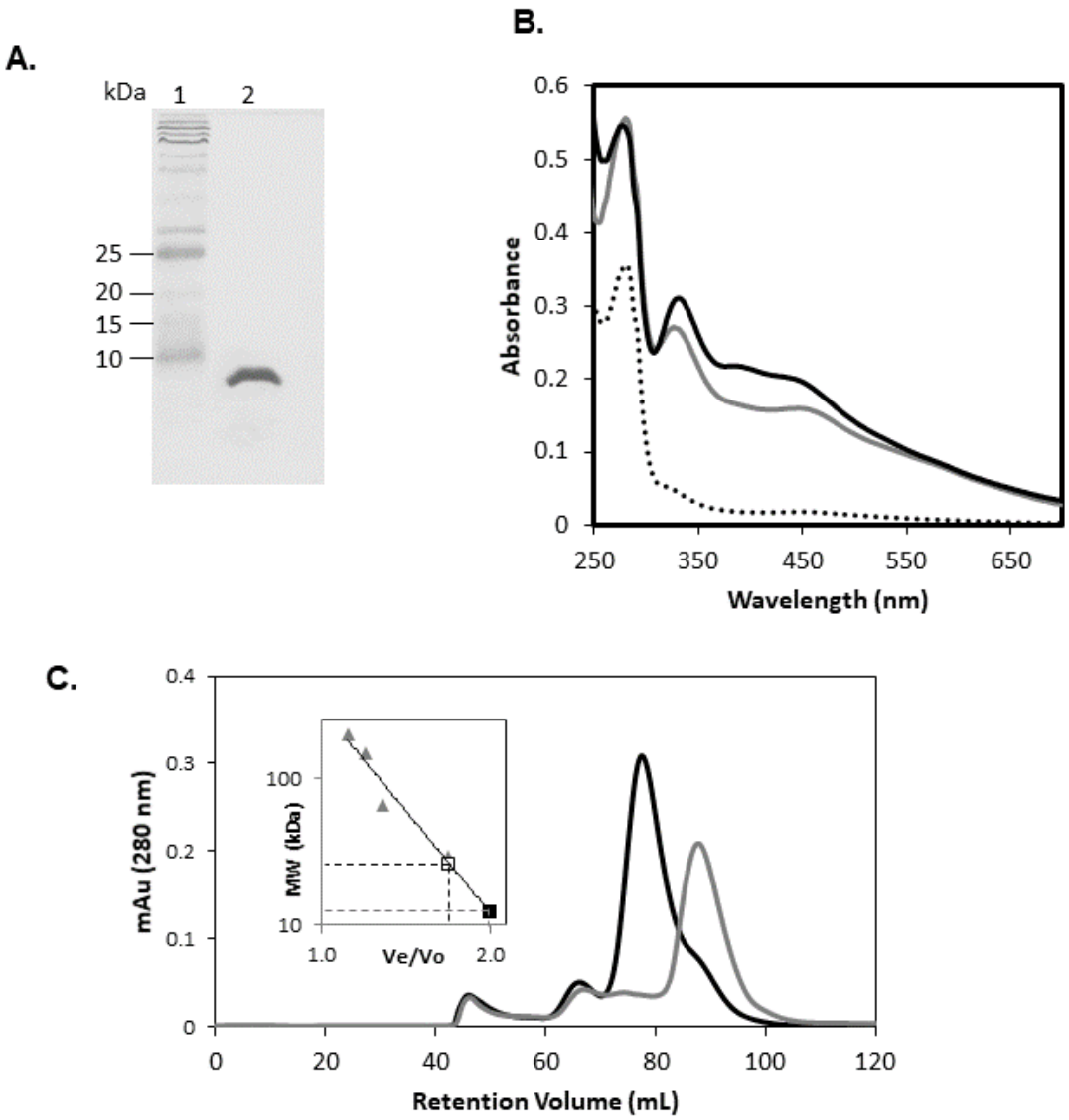

Figure 5. Fe-S cluster reconstitution of purified IscU2. A) SDS-PAGE analysis of purified IscU2 (cropped image of original). Lane 1, MW marker; lane 2, IscU2 (2.4 µg). B) Anaerobic UV-visible spectra of 20 µM IscU2 (dotted line), IscU2$^{S\text{-}FeS}$ (black line) and IscU2$^{C\text{-}FeS}$ (gray line) in 50 mM Tris pH 7.2, 150 mM NaCl. C) Anaerobic size exclusion chromatography of 14.8 mg of IscU2 (gray line) and 15.6 mg of IscU2$^{C\text{-}FeS}$ (black line) in 50 mM Tris pH 8.0, 150 mM NaCl, 2 mM DTT, 10% glycerol. The molecular weight of IscU2 and IscU2$^{C\text{-}FeS}$ were calculated with a standard curve (inset). The calculated MW of IscU2 (solid square symbol) was 12 kDa and the calculated MW of IscU2$^{C\text{-}FeS}$ (open square symbol) was 26 kDa.

Table 3. Comparison of the properties of purified *M. acetivorans* IscU2.

Protein	A_{438}/A_{280}	ε_{438} (mM^{-1} cm^{-1})	Iron[a]	Sulfide[b]
IscU2	0.10	0.90	0.57 ± 0.06	0.44 ± 0.04
$IscU2^{C\text{-}FeS}$	0.26	6.07	2.47 ± 0.11	1.99 ± 0.24
$IscU2^{S\text{-}FeS}$	0.27	5.91	3.15 ± 0.24	3.15 ± 0.39

[a] nmol iron/nmol of IscU2
[b] nmol acid-labile sulfide/nmol of IscU2

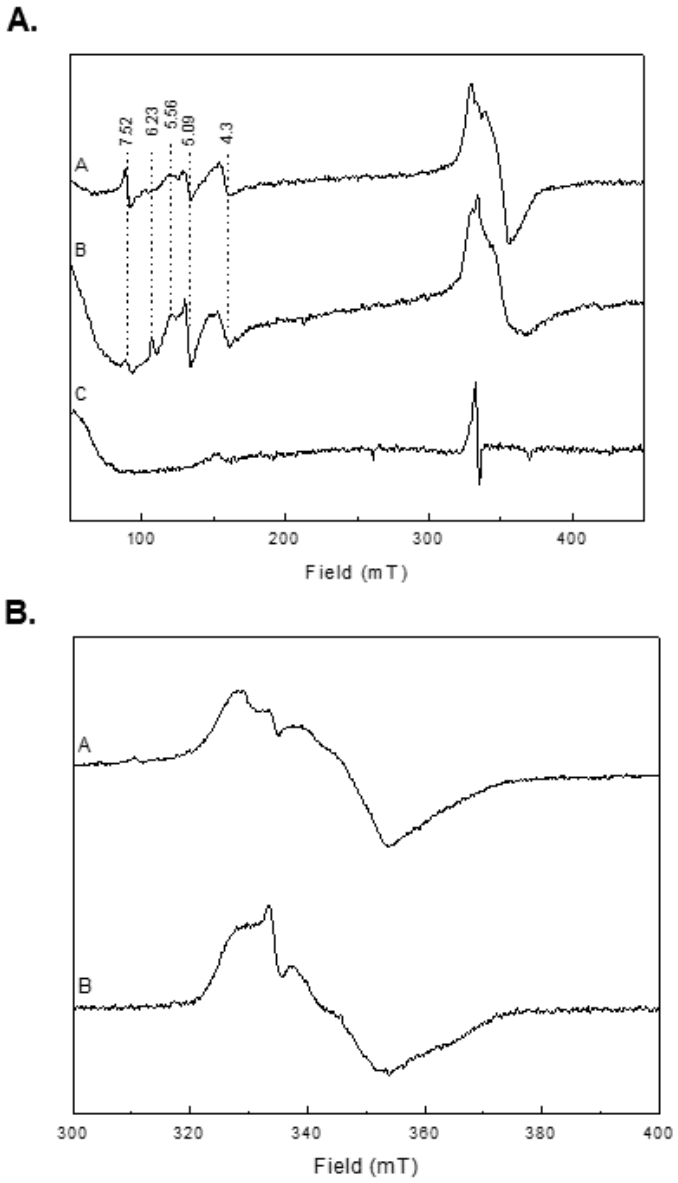

Figure 6. EPR spectra of IscU2. A) Expanded view, trace A: IscU2$^{C\text{-}FeS}$ (100 µM) reduced with dithionite, trace B: IscU2$^{S\text{-}FeS}$ (100 µM) reduced with dithionite, trace C: IscU2$^{S\text{-}FeS}$ (100 µM) as such. Numbers shown represent *g* values. B) Detailed view, trace A: IscU2$^{C\text{-}FeS}$ reduced with dithionite, trace B: IscU2$^{S\text{-}FeS}$ reduced with dithionite.

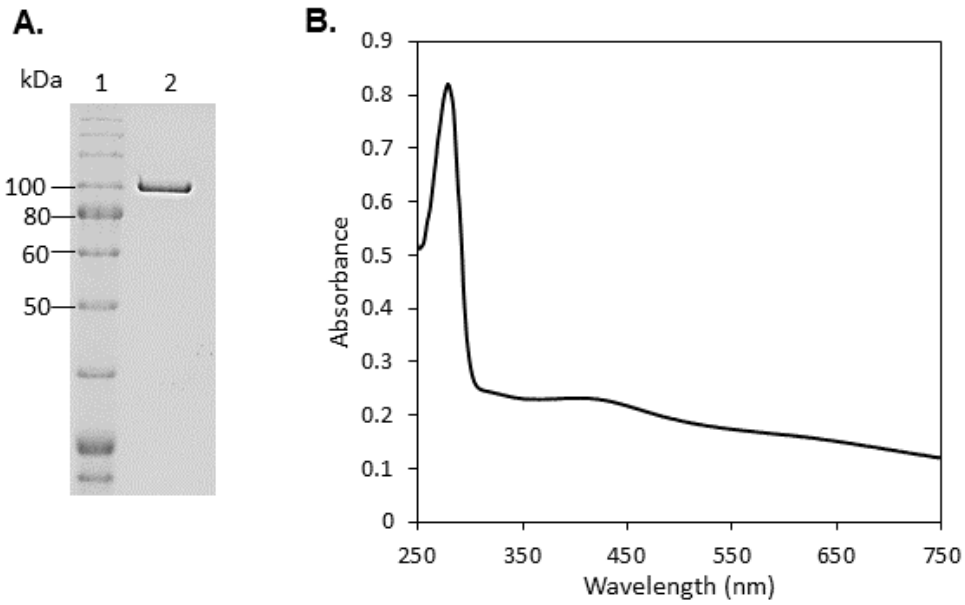

Figure 7. Characterization of recombinant *M. acetivorans* aconitase (AcnA). A) SDS-PAGE analysis of purified recombinant AcnA. B) UV-visible spectrum of purified AcnA after in vitro reconstitution with iron and sulfur.

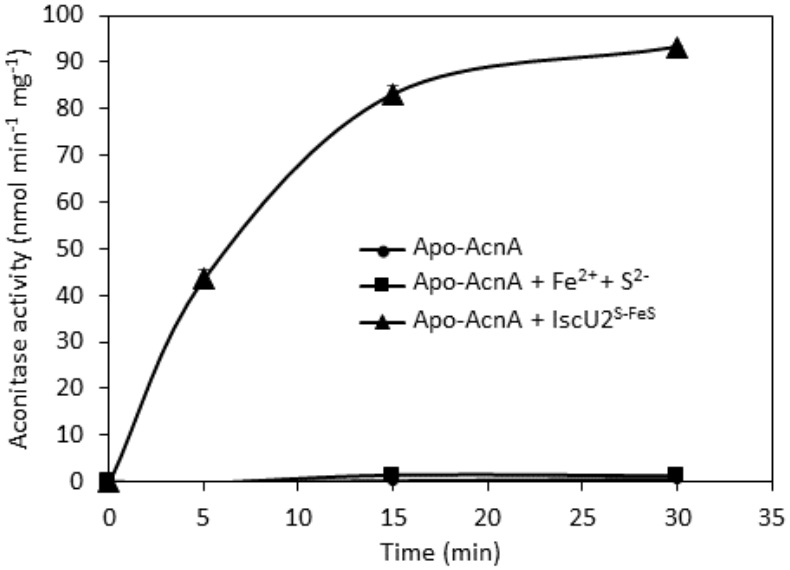

Figure 8. Reconstitution of apo-AcnA activity by [4Fe-4S]-IscU2. Apo-AcnA (4 μM) was incubated with IscU2$^{S\text{-}FeS}$ (40 μM) or iron (Fe^{2+}) and sulfide (S^{2-}) (80 μM each) and aconitase activity was measured over time.

Table 4. IscU2-dependent recovery of aconitase activity in air-exposed *M. acetivorans* cell lysates

Cell lysate treatment	Aconitase activity[a]
Anaerobic ⟶ anaerobic	5.2 ± 0.7
Aerobic ⟶ anaerobic	BDL[b]
Aerobic ⟶ anaerobic + IscU2	BDL[b]
Aerobic ⟶ anaerobic + IscU2$^{S\text{-}FeS}$	1.6 ± 0.3

[a] nmol NADPH $min^{-1}mg^{-1}$ protein; Results are means from triplicates ± 1 standard deviation
[b] Below Detection Limit (≥ 0.1 nmol NADPH $min^{-1}mg^{-1}$ protein)

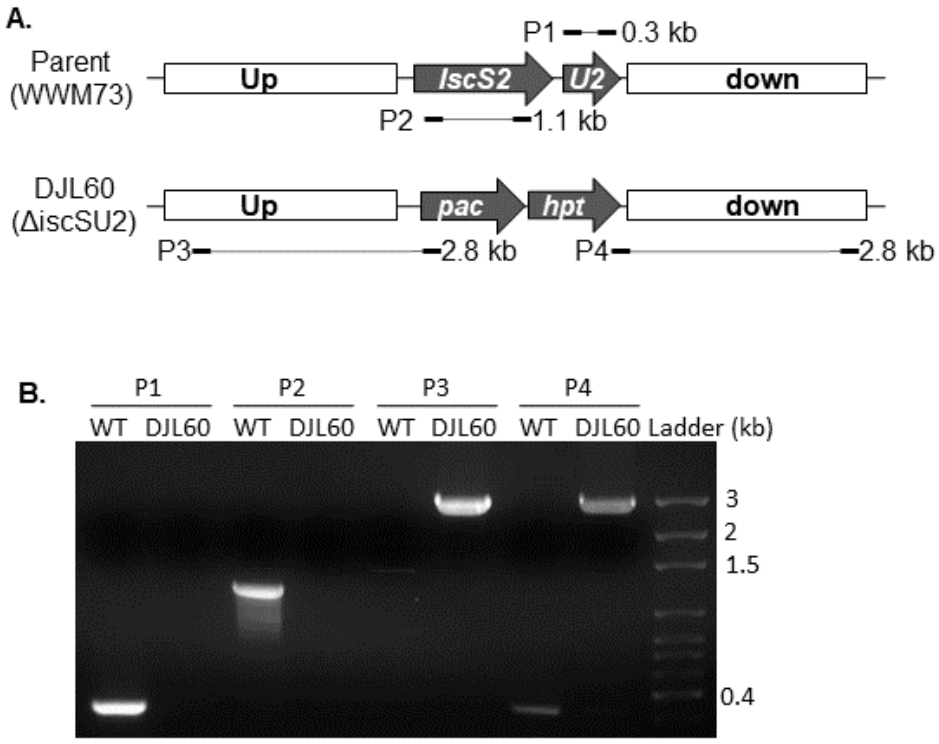

Figure 9. PCR confirmation of *iscSU2* deletion in *M. acetivorans* strain DJL60. **A.** Schematic showing replacement of *iscSU2* with *pac-hpt* in strain DJL60 and predicted PCR products are indicated by P1-4. **B.** Gel image of products of PCR reactions P1-4 with WWM73 and DJL60 genomic DNA.

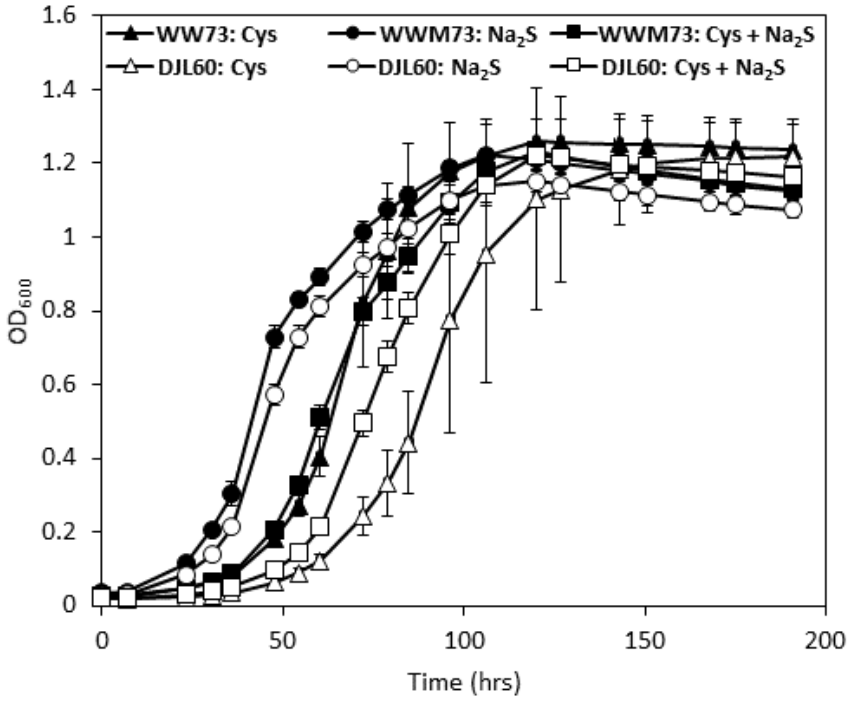

Figure 10. Growth of *M. acetivorans* strains WWM73 and DJL60 with different sulfur sources. Each strain was grown in HS_{DTT} medium containing 125 mM methanol supplemented with 3 mM cysteine (Cys) and/or 3 mM sodium sulfide (Na_2S). Growth was monitored by the optical density at 600 nm (OD_{600}). Data points are the mean of n = 3 with error bars ± STD.

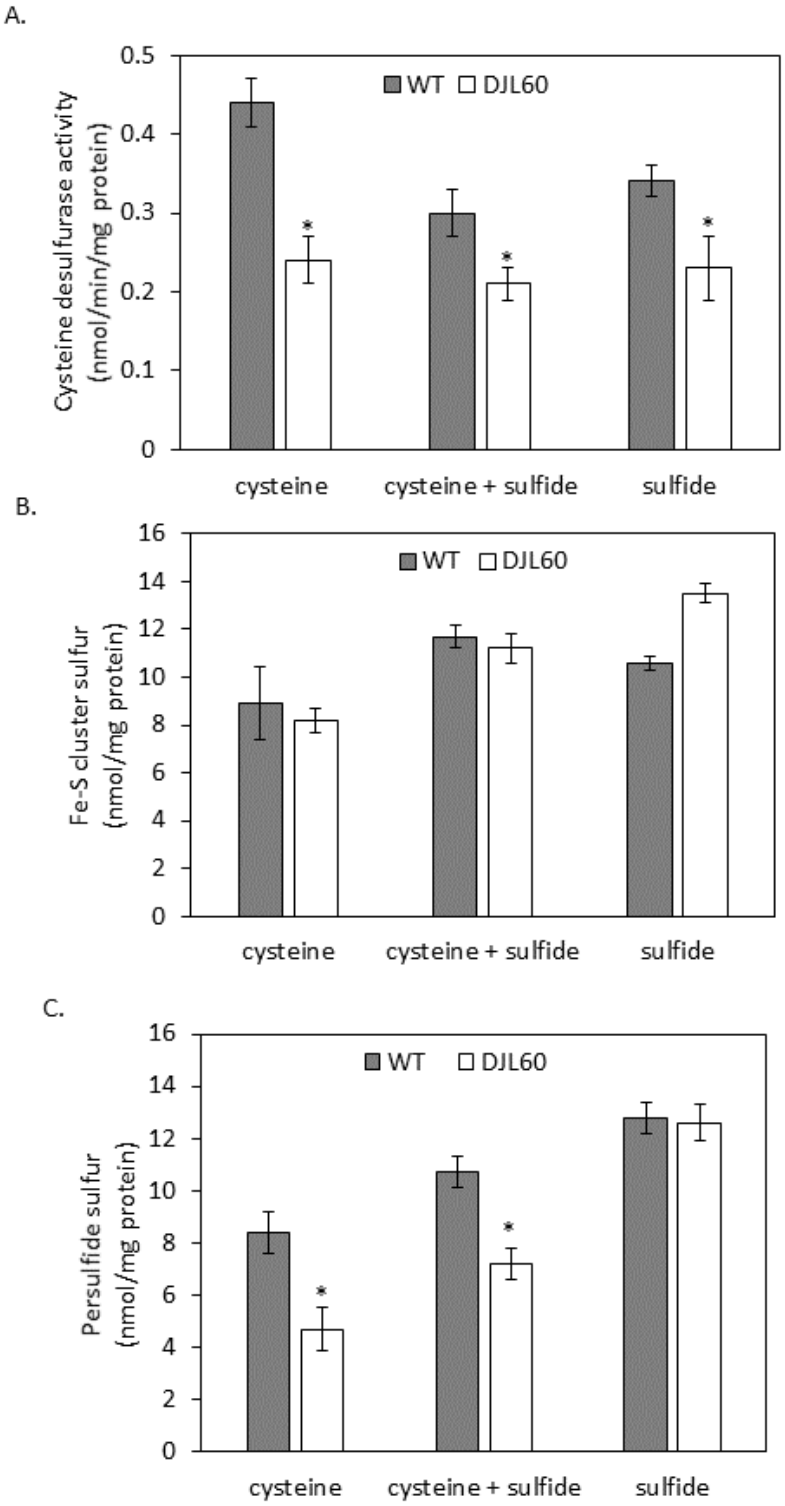

Figure 11. Cysteine desulfurase activity, Fe-S cluster, and persulfide levels in cell lysates of strains WWM73 and DJL60**.** Cysteine desulfurase activity (A), Fe-S cluster content (B) and persulfide content (C) were measured as described in methods. Asterisks indicate significant difference between WWM73 and DJL60 lysate, determined by t-test ($p < 0.02$ for A, $p < 0.01$ for C).

Table 5. Strains, plasmids, and primers used in this study

Name	Description	Source or reference
	Strains	
E. coli		
DH5α	Cloning strain	NEB
Rosetta (DE3) pLacI	Recombinant protein expression strain	NEB
M. acetivorans		
WWM73	Δ*hpt*::P*mcrB-tetR*-ϕC31-*int*-attP	(Guss Archaea 2008)
DJL60	WWM73 Δ*iscSU2*::*pac-hpt*	This study
	Plasmids	
pDL201	pET28a with *iscU2* cloned into *Nde*I & *Xho*I sites	This study
pDL202	pET28a with *iscS2* cloned into *Nde*I & *Xho*I sites	This study
pDL204	pET28a with *acnA* cloned into *Nhe*I & *Xho*I sites	This study
pJK301	Amp^R vector for making markerless deletions in *Methanosarcina* spp.; contains *pac-hpt* flanked by Flp recombinase FRT recognition sites	(Welander & Metcalf 2008)
pDL214	*iscSU2* knockout plasmid; pJK301 with regions upstream of iscS2 cloned into *Apa*I & *Hind*III sites, downstream of iscU2 cloned into *Bam*HI & *Spe*I sites	This study
	Primers	
IscSNdeF "P2 fwd"	ggtttgCATATGacaattgaaaacagaaccgtttac fwd primer with *Nde*I site to amplify *iscS2*	This study
IscSXhoR "P2 rev"	ggtggtCTCGAGtcaaagagctctgtattcctgaggg rev primer with *Xho*I site to amplify *iscS*2	This study
IscUNdeF "P1 fwd"	ggtggtCATATGgattacagcgctaaggtgttag fwd primer with *Nde*I site to amplify *iscU*2	This study
IscUXhoR "P1 rev"	ggtggtCTCGAGtcagtcccagggctcaagccc rev primer with *Xho*I site to amplify *iscU*2	This study
NheAconF	ggtggtGCTAGCatgagagaaggtctggacccc fwd primer with *Nhe*I site to amplify *acnA*	This study
AconXhoR	ggtggtCTCGAGttatttttttcttcaccgaatcccgc rev primer with *Xho*I site to amplify *acnA*	This study
ApausISCF	ggtggtGGGCCCccctgattcccatttgaatcttcc fwd primer with *Apa*I site to amplify *iscSU2* US region for insertion in pJK301	This study
HindusISCR	gttgttAAGCTTcgtagcagagttatccatgtaaacgg rev primer with *Hind*III site to amplify *iscSU2* US region for insertion in pJK301	This study
BamdsISCF	ggtggtGGATCCgggcttgagccctgggactgaatgagcc fwd primer with *Bam*HI site to amplify *iscSU2* DS region for insertion in pJK301	This study
SpedISCR	ggtggtACTAGTgctgttcatgggttgttgaagctggatg rev primer with *Spe*I site to amplify *iscSU2* DS region for insertion in pJK301	This study

Table 5 (cont.)

Name	Description	Source or reference
	Primers	
Isc2USKOseqF "P3 fwd"	gatgtcaaacgggcgagaaacaagagg fwd genomic primer to confirm *iscSU2* knockout	This study
JK301SupR(new) "P3 rev"	tagtatattacgaatagggcg rev plasmid primer to confirm *iscSU2* knockout	This study
JK301SdownF "P4 fwd"	gctgctggtgaaagagacc fwd plasmid primer to confirm *iscSU2* knockout	This study
Isc2DSKOseqR "P4 rev"	ggaagagttcacggaagaattcccgg rev genomic primer to confirm *iscSU2* knockout	This study

Chapter II

Synthesis and delivery of [Fe-S] in *Methanosarcina acetivorans*: ISC systems and beyond

Thomas M. Deere

Cell and Molecular Biology Program, University of Arkansas,

Fayetteville, AR 72701 USA

Introduction

Discussions of the importance of iron-sulfur clusters ([Fe-S]) often focus on electron transfer and regulatory roles, but Fe-S proteins are also implicated in the biosynthesis of critical cofactors including biotin, lipoic acid, and thiamine (Mashruwala *et al*., 2016, Cosper *et al*., 2004, Martinez-Gomez & Downs, 2008). Disruptions of specific Fe-S proteins involved in these pathways can produce conditional growth phenotypes, particularly when demand for the product cofactor is high. It is also noteworthy that several of these vitamins are sulfur-containing compounds, with the sulfur atom in question sometimes being donated directly by the [Fe-S] bound to the biosynthetic protein, as in the biotin synthase BioB (Gibson *et al*., 1999). A defect in [Fe-S] biogenesis that does not manifest in general growth disruption could potentially mask a deficiency in cofactor biosynthesis. Revealing a hidden phenotype of this form could require finding a growth condition that increases demand for the vitamin in question, most directly by simply withholding it from the culture medium.

Methanosarcina acetivorans is capable of growth using cysteine or sulfide as a sulfur source, as opposed to other methanogens such as *Methanococcus maripaludis* which are restricted to inorganic sulfur species (Whitman *et al*., 1982). The fact that the ISC system of [Fe-S] biogenesis is found in the genomes of methanogens capable of utilizing cysteine as a sole sulfur source but not in those that cannot has led to the hypothesis that the ISC system is specific to growth on cysteine while the more prevalent SUF system is used when growing on inorganic sulfide, as depicted in **Figure 1** (Deere *et al*., 2020, Rauch & Perona, 2016, Liu *et al*., 2010). Whereas the deletion of *iscS2* and *iscU2* did not result in a consistently measurable phenotype besides lower cysteine desulfurase activity and decreased intracellular persulfide when growing with cysteine, the possibility remains that disrupting one or more of the other putative Fe-S biogenesis system gene clusters will have more dramatic results (Deere *et al*, 2020). The

"auxiliary" SUF system might be expected to be responsible for "housekeeping" Fe-S cluster building, particularly given the broad co-conservation of putative SufB- and SufC-encoding genes in methanogenic orders and in archaea more generally (Liu *et al*., 2010).

In addition to putative ISC and SUF systems, *M. acetivorans* encodes predicted [Fe-S] carrier proteins, including ApbC which can be found in eukaryotes as well as bacteria (Lill *et al*., 2006). In fact, this gene's broad conservation across all domains of life, and apparent nearly universal prevalence within domain Archaea, has given rise to speculation that it or a precursor was present in the organisms referred to as Last Universal Common Ancestor(s) (LUCA) before the evolutionary divergence of the three Domains (Zhao *et al*., 2020). Given that the co-occurrence of ApbC and ISC systems in methanogens does not seem strongly correlated (Liu *et al*., 2012), our model is ambivalent as to whether ApbC is predicted to interact with ISC, SUF, or both. What client apo-proteins might be served by ApbC, and which sulfur-source pathways it might be implicated in, are unknown at this time. In addition to those already mentioned, organic sulfur compounds like cystine and thiosulfate are known to be used as sulfur sources in bacteria (Soutourina *et al*., 2009), as well as in other members of genus *Methanosarcina* (Mazumder *et al*, 1986). We hypothesize that the products of the other putative Suf and Isc gene clusters, as well as the predicted ApbC encoded by *M. acetivorans*, may be involved in the assembly or delivery of Fe-S clusters for proteins including those involved in central metabolism or in coenzyme synthesis. These activities may be sulfur-specific, potentially extending beyond the sulfur sources previously examined in this organism (Deere *et al*., 2020).

In addition to its demonstrated flexibility with respect to sulfur sources, *M. acetivorans* can use multiple pathways of methanogenesis with different carbon and energy sources. In the natural environment, acetate is believed to be the most abundant growth substrate (Thauer *et al.*,

2008). Switching between growth substrates requires extensive changes in protein expression, and in particular adapting from growth on methanol to acetate involves a steep increase in levels of Fe-S proteins such as the subunits of the carbon monoxide dehydrogenase/acetyl CoA synthase (ACDS) complex (Li *et al*., 2006). An overall increase in the share of Fe-S proteins in the proteome should boost demand for [Fe-S], and we hypothesize this would be reflected in higher activity of proteins like IscS and IscU. In the case of the former, this hypothesis could be tested using cysteine desulfurase assays.

Genetic manipulations to test hypotheses concerning Fe-S cluster biogenesis can be challenging in *Methanosarcina acetivorans*, given the high demand for [Fe-S] in methanogens (Major *et al.*, 2004), and the possible redundancy in biogenesis systems in members of genus *Methanosarcina*. In addition, puromycin resistance is the sole selectable marker available in this genetic system. Rigorous testing of hypotheses concerning the requirements and specificity of the three putative Isc gene clusters, for instance, calls for the generation of double or even triple mutants using a single selectable marker. Previous gene knockout experiments in *M. acetivorans* have frequently involved deleting genes by replacing them with a *pac-hpt* cassette designed to be removable by the action of Flp recombinase helped along by counterselection with 8-aza-2,6-diaminopurine, or 8ADP (Kohler & Metcalf, 2012). This process does not always work smoothly in practice, with counterselection most often generating only suppressor mutations While we have continued to use this system to knock out single genetic loci, new and better techniques for editing the genome of *M. acetivorans* have become available. A new system, modeled after the one created by Prof. Metcalf and others, was developed using smaller, high copy number plasmids derived from pNEB193 (Shea *et al*., 2016). These plasmids proved much easier to work with and purify. Unfortunately, after more than a year of work with these plasmids, we

determined that a crucial gene required for the system to finalize deleting a locus of interest is actually inserted backwards relative to its promoter in the plasmid provided to us (data not shown), and any constructs made with this plasmid would be all but useless. We have ceased using plasmids from this system.

An even newer and more improved system for editing the genome of *M. acetivorans* was recently created, namely a CRISPR/Cas9 genetic system based on the original suite of plasmids generated by Prof. William Metcalf's group supplemented with the *cas9* gene from *Streptococcus pyogenes* (Nayak & Metcalf, 2017). Constructs to generate truly markerless, scarless deletions rely on homology-directed repair (HDR), meaning the desired plasmid needs two regions of chromosomal homology inserted, along with at least one single guide RNA (sgRNA) sequence to guide Cas9 to the desired cut site. The plasmids generated for this system lack sufficient restriction endonuclease sites to accomplish all these insertions, so construction is achieved using the "Gibson Assembly" protocol (Gibson *et al*., 2009).

The questions we set out to answer in this chapter touch on multiple aspects of methanogen physiology. What is the total Fe-S cluster content of *M. acetivorans*, and how does the methanogen pathway in use affect it? We hypothesize that [Fe-S] content will be elevated in aceticlastic methanogenesis due to increased production of proteins like the ACDS subunits. Are Isc2 and ApbC required for vitamin biosynthesis? We propose that one or both of these (sets of) genes are required for optimal coenzyme synthesis, and possibly strictly required. Can *M. acetivorans* grow on sulfur sources other than cysteine and sulfide? We hypothesize that thiosulfate and cystine can serve as sulfur sources, though which sulfur source confers fastest relative growth remains to be seen. Are putative SUF systems active in Fe-S cluster biogenesis in *M. acetivorans*? We hypothesize that the Suf2 gene cluster is involved in building [Fe-S] for

proteins important for basic cellular processes. Herein we describe a series of growth studies, assays, and genetic manipulations, including using the new CRISPR/Cas9 editing system in *M. acetivorans*, to address the above questions and test the stated hypotheses.

Materials and Methods

***M. acetivorans* growth**. *M. acetivorans* strain WWM73 was obtained from Prof. Metcalf (Guss *et al.*, 2008) and was used as the parent strain for all experiments. All strains of *M. acetivorans* (**Table 1**) were grown in HS medium containing either 125 mM methanol or 100 mM sodium acetate as a carbon and energy source as previously described (Jennings *et al.*, 2016, Sowers *et al.*, 1993). Each liter of HS medium contains 23.4 g NaCl, 3.8 g $NaHCO_3$, 1.0 g KCl, 11.0 g $MgCl_2*6H_2O$, 0.3 g $CaCl_2*2H_2O$, 1.0 g NH_4Cl, 0.5 g L-cysteine, 5 mL of 1 M KH_2PO_4 at pH=7.4, 1 mL of 0.1% w/v resazurin, 10 mL of Wolfe's Mineral Solution (supplemented with 0.024 g/L $NiCl_2*H_2O$ in the stock), and 2 mL of a 5x concentrated Wolfe's Vitamin Solution (Wolin *et al.*, 1963). Vitamin-free HS medium was prepared by omitting only Wolfe's Vitamin Solution from this recipe, and nitrogen-free HS medium was prepared by omitting NH_4Cl. HS medium was made anoxic and dispensed into Balch tubes within an anaerobic chamber (Coy Laboratories) containing 75% N_2, 20% CO_2, and 5% H_2. Standard culture conditions include 0.025% w/v Na_2S*9H_2O added from a sterile, anoxic stock just prior to inoculation. To examine growth with different sulfur sources, 1.5 mM dithiothreitol (DTT) was added to HS medium (HS_{DTT} medium) in lieu of cysteine prior to autoclaving, with 1.5 mM sodium thiosulfate, 1.5 mM L-cystine, 3 mM L-cysteine and/or 1mM sodium sulfide added from sterile anoxic stock solutions prior to inoculation. Growth was monitored by measuring the optical density at 600 nm (OD_{600}) of the culture tubes using a spectrophotometer (Thermo Fisher, Genesys 10 Bio).

Deletion of *apbC* using traditional homologous recombination. The pseudo-wildtype parent strain, WWM73, and plasmid vectors for genetic manipulation, generously provided by Prof.

William Metcalf from the University of Illinois, are listed in **Table 1**. The *apbC* deletion mutant was generated using pJK301 with methods previously described (Deere *et al*., 2020, Welander & Metcalf, 2008). Briefly, homologous regions upstream (US) and downstream (DS) of MA4246 (*apbC*) were amplified by PCR from *M. acetivorans* C2A gDNA, using primers containing *Apa*I and *Hind*III recognition sites for the US region and *Bam*HI, and *Spe*I for the DS region. Each PCR product was double digested with the appropriate restriction enzymes and sequentially ligated into similarly digested pJK301. Restriction digestion, ligation, and transformation were all carried out as previously described (Deere *et al.*, 2020). The complete *apbC* knockout plasmid (pDL347) was confirmed by DNA sequencing (Eurofins). Unless otherwise noted, all procedures described below were performed in an anerobic chamber (Coy Laboratories). *M. acetivorans* strain WWM73 was transformed with approximately 2 µg of pDL347 linearized by digestion with *Not*I, using a liposomal transfection method as previously described (Metcalf *et al.*, 1997). Transformants were selected by spread plating on HS agar plates (0.8% w/v noble agar) containing 125 mM methanol and 2 µg/mL puromycin. The plates were placed in a canning jar along with a vial containing 2 ml of 2.5 % sodium sulfide. The jar was sealed and incubated at 35 °C in a standard incubator. Well-isolated colonies were inoculated into HS medium supplemented with 125 mM methanol and 2 µg/mL puromycin. Deletion of *apbC* and replacement with the *pac-hpt* cassette from pJK301 was confirmed in selected transformants by sequencing of PCR products amplified from genomic DNA isolated from transformants. Once confirmed, the *apbC* deletion strain was designated as *M. acetivorans* strain DJL61.

Deletion of *sufC2B2* using CRISPR-Cas9. This protocol was adapted from the approach previously described (Nayak & Metcalf, 2017). Approximately 1 kilobase regions of chromosomal DNA of *M. acetivorans* C2A located upstream of MA4406 (*sufC2*) and

downstream of MA4407 (*sufB2*) were amplified by PCR using primers with extra "Gibson overhangs" homologous to the adjacent regions in a *Bam*HI-digested pUC18 backbone for use in a Gibson Assembly reaction (Gibson *et al*., 2009). Two sgRNAs designed to target Cas9 machinery to the *suf2*-gene cluster, along with appropriate invariant CRISPR scaffold sequences and a *Methanosarcina*-specific P*mtaCB1* promotor to drive sgRNA expression, were designed into large DNA sequences ("gBlocks") and ordered from Integrated DNA Technologies, Inc. The pUC18 backbone was linearized by digestion at 37 ℃ for 1.5 hours with *Bam*HI-HF (New England Biolabs, Inc.), then cleaned up to re-isolate the cut plasmid. Assembly of the homology arms (present as a single fused 2,118 bp product), the 2,686 bp linearized pUC18, the 510 bp gBlock #1, and the 360 bp gBlock #2 was conducted using the Gibson Assembly Ultra Kit (Synthetic Genomics, Inc.) per the manufacturer's instructions. The backbone and fused homology arms were each present at 0.008 picomoles and the gBlocks each at 0.04 picomoles, all in 5 µL of ultrapure water. This was added to 5 µL of Master Mix A in a 0.2 mL PCR tube on ice. This mixture was incubated at 37 °C for 5 minutes for exonuclease digestion, heat-inactivated at 75 °C for 20 minutes, then cooled at a rate of 0.1 °C per second to a final temperature of 60 °C. The mixture then annealed at 60 °C for 30 minutes before cooling at a rate of 0.1 °C per second to a final temperature of 4 °C. The 10 µL reaction was combined with 10 µL of Master Mix B, mixed by pipetting on ice, then incubated for 15 minutes at 45 °C for repair and ligation. An aliquot of 7 µL of this mixture was then added to a 200 µL suspension of freshly thawed chemically competent DH5α cells and incubated on ice for 30 minutes. These transformed cells were heat-shocked at 42 °C for 1 minute, chilled on ice for 2 minutes, then supplemented with 500 µL of room-temperature SOC medium. The entire cell resuspension was transferred to a sterile glass 18 x 150 mm culture tube, which shook at 225 rpm for 1 hour at 37

°C. This transformation was spread equally over two agar plates of LB with ampicillin at 100 µg/mL and incubated overnight at 37 °C. Numerous colonies were observed the following day, and 25 were picked onto a screening agar plate of LB with 100 µg/mL ampicillin that had been spread with 40 µL of 20 mg/mL 5-Bromo-4-chloro-1*H*-indol-3-yl β-D-galactopyranoside (X-gal) and 6.72 µL of 0.5 M Isopropyl β-D-1-thiogalactopyranoside (IPTG). After incubating this patch plate at 37 °C overnight, 20 white colonies were observed alongside 5 blue colonies, suggesting an 80% rate of disruption in *lacZ* at the multicloning site in pUC18. Colony touch PCR screening with appropriate primers revealed successful assembly of the desired construct. Plasmid purified from one of these transformants was designated pDL248.

The primary plasmid backbone for the homology-directed repair (HDR) driven *M. acetivorans* CRISPR/Cas9 gene editing system, designated pDN203 (Nayak & Metcalf, 2017), was digested with *Asc*I, and religated with T4 DNA ligase, thereby removing the scaffold-sgRNA region between pDN203's two *Asc*I sites. The resulting derivative plasmid, designated pDL238 by its creator, Dr. Ahmed Dhamad, can be linearized with *Asc*I to serve as the backbone for Gibson Assembly to insert targeting sequences for CRISPR/Cas9. The homology/gBlock construct in pDL248, nearly 3 kbp in all, was amplified by PCR with primers bearing "Gibson overhangs" specific for *Asc*I-digested pDL238. A new Gibson Assembly reaction was set up with 0.008 picomoles of this digested vector and 0.04 picomoles of the PCR product in a total volume of 5 µL of ultrapure water. All steps in the Gibson Assembly reactions and transformation were identical to those taken in the pUC18-based assembly above, except a 50 µL aliquot of chemically competent WM4489 cells was used instead of 200 µL of DH5α cells, and the transformation reaction was plated on LB with chloramphenicol at 34 µg/mL instead of ampicillin. After growing up overnight at 37 °C, fewer than a dozen colonies grew on each plate

and were screened by touch PCR for insertion. Several colonies were grown in liquid LB, plasmids were isolated and rescreened by PCR, and one was chosen to sequence. After sequence confirmation, this pDL238-based plasmid was designated pDL249.

This pDL249 construct was cointegrated with the replicating plasmid pAMG40 to create a non-integrating plasmid (Guss *et al*., 2008). Plasmids pDL249 and pAMG40, each at a quantity of 150 ng, were combined and brought up to a volume of 8 µL by addition of TE buffer, pH = 8.0, then 2 µL of BP Clonase II mix (ThermoFisher Scientific) was added to this solution for a final volume of 10 µL in a 0.2 mL PCR tube. This mixture was incubated overnight at 25 °C in a thermocycler. The following day, 1 µL of Proteinase K was added, the solution was mixed briefly by vortexing, then the tube was incubated for 10 minutes 37 °C. Next, 2 µL of this solution was added to 50 µL of freshly thawed chemically competent WM4489 cells. The transformation conditions were identical to those of the pDL238-based Gibson Assembly above, and aliquots of the transformed cells (50 and 100 µL) were spread on agar plates of LB with kanamycin at 50 µg/mL and chloramphenicol at 17 µg/mL before incubating overnight at 37 °C. Five colonies grew up overnight, and colony touch PCR using primers specific to pDL238 and pAMG40 confirmed all five contained the cointegrated, replicating construct. Plasmid was purified from one colony, sequenced for confirmation, and designated pDL250.

Transformation of pseudo-wildtype *M. acetivorans* WWM73 with approximately 2 µg plasmid pDL250 following the same transfection protocol used to generate DJL60 and DJL61 yielded puromycin-resistant cells. Diagnostic PCR in which one primer of the pair anneals further upstream than the beginning of the upstream homology arm gave a product whose size (~1,5 kbp) was consistent with deletion of *sufC2B2* from the chromosome (**Figure 8**).

Sequencing confirmed markerless, scarless deletion of the *suf2* locus from the genome, and the resulting Δ*suf2* strain was designated DJL63.

Determination of cysteine desulfurase activity and Fe-S cluster content in lysate. Acid-labile ([Fe-S]) sulfur concentrations were determined in cell-free lysates from strain WWM73 grown with methanol or acetate as above. This was done using the methylene blue method as previously described (Deere *et al*., 2020, Beinert, 1983) Soluble protein (0.11 to 0.37 mg) in cell-free lysates was directly assayed by the methylene blue detection of free sulfide after incubating for 0 or 45 minutes at 37°C with 1 mM DTT in the presence or absence of 1 mM L-cysteine. Acid-labile sulfide content at 0 minutes yielded values for [Fe-S] content, while the change in sulfide content in the presence of cysteine after 45 minutes (minus the cysteine-free control) gave the value to calculate cysteine desulfurase activity. Control samples without lysate did not produce detectable sulfur over time.

Results

***M. acetivorans* contains more Fe-S clusters when growing on acetate than methanol.** The parent strain WWM73 exhibits significantly elevated [Fe-S] content, as measured by acid-labile sulfide in cell-free lysates, when growing on acetate versus when growing on methanol (**Figure 2**). Methanol-grown cells had 10.1 ± 0.04 nmol total sulfide per mg soluble protein, while acetate-grown cells contained 43.1 ± 0.02 nmol total sulfide per mg soluble protein. Cysteine desulfurase activity was also much higher in cells grown on acetate, at 0.82 ± 0.03 nmol sulfide evolved * min^{-1} * mg^{-1}, compared to cells grown on methanol, 0.24 ± 0.02 nmol sulfide evolved * min^{-1} * mg^{-1}.

ApbC is not essential for Fe-S cluster biogenesis. The *apbC* gene was successfully deleted by replacement with the *pac-hpt* cassette, which was confirmed by diagnostic PCR showing bands

consistent with cassette insertion and no band for the *apbC* gene in the pDL347-tranformed cells (**Figure 3**). This Δ*apbC* strain was designated DJL61. Generation of this mutant was achieved with extensive help from an undergraduate colleague, Chris Hill. Like the Δ*isc2* strain DJL60, DJL61 grew normally under standard conditions in HS media (methanol as carbon and energy source, cysteine and sulfide as sulfur sources), albeit with some initial delay entering exponential growth (**Figure 4**).

ApbC is involved in growth on acetate. Growth studies were conducted for both deletion mutants (*isc2* and *apbC*) growing with sulfide as a sulfur source and 100 mM sodium acetate as a carbon and energy source. WWM73 and DJL60 grew similarly, while DJL61 exhibited slower growth (**Figure 5**). While there was considerable variability between replicates, especially for the *apbC* mutant, the growth rate of DJL61 during exponential growth phase was lower than that of the parent strain WWM73 (p-value < 0.1 in t-test).

ApbC and IscS2/IscU2 are not essential for coenzyme biosynthesis. Media was prepared both with and without Wolfe's Vitamin Solution (Wolin *et al.*, 1963) and inoculated with WWM73, DJL60, and DJL61 supplied with a variety of sulfur sources, including L-cysteine, sodium sulfide, sodium thiosulfate, and L-cystine. Considerably increased variability between replicates was observed across a number of growth conditions, but the most drastic growth phenotype was seen in DJL61 as compared to WWM73 when growing on thiosulfate, particularly when the HS medium was prepared without the standard vitamin solution (**Figure 6**). Wolfe's Vitamin Solution (Wolin *et al.*, 1963) contains ten coenzymes and proto-coenzymes: biotin, folic acid, pyridoxine, riboflavin, thiamine, nicotinic acid, pantothenic acid, vitamin B12, p-aminobenzoic acid, and lipoic (thioctic) acid. Biotin, thiamine, and lipoic acid are all sulfur-containing compounds with biosynthetic pathways known to involve Fe-S proteins, though such proteins are

also involved in synthesizing non-sulfur coenzymes like vitamin B12 (Leech *et al*., 2003). All ten vitamins were withheld in the "no vitamin" condition. When generation times were calculated for WWM73, DJL60, and DJL61 growing on different sulfur sources, including cystine, the oxidized disulfide form of cysteine, the extent of growth deficiency on thiosulfate for DJL61 was particularly stark (**Figure 7)**. There were no conditions in which any strain failed to grow, though poorer growth in the absence of vitamins could reflect vitamin biosynthetic activity that is impaired but not abolished. The component(s) of the vitamin solution responsible for this phenotype is unknown at this time.

SufB2/SufC2 are not essential for Fe-S cluster biogenesis. Diagnostic PCR with a mixed primer pair, one annealing outside the 5' end of the *suf2* homology regions and the other inside the downstream homology region, gave a product whose size (~1,5 kbp) was consistent with deletion of *sufC2B2* from the chromosome of WWM73 transformed with pDL250 (**Figure 8**). Sequencing confirmed the markerless, scarless deletion of the *suf2* locus from the chromosome, and the strain was designated DJL63. Successfully deleting this locus suggests that neither *sufC2* nor *sufB2* is essential to growth in standard HS medium with methanol and sodium sulfide. Growth studies confirmed that there is no general growth phenotype associated with deletion of the *suf2* gene cluster, as depicted in **Figure 9** (unpublished data provided by Ms. Jasleen Saini).

Discussion

Growth on acetate calls for extensive changes in cofactor utilization and protein expression relative to growth on methanol in *M. acetivorans*. Especially important changes include switching from using the cofactor F_{420} as the primary electron carrier to using a [4Fe-4S] ferredoxin, and expressing high levels of the ACDS complex (Thauer *et al*., 2008, Li *et al*., 2006). In other methanogens of the genus *Methanosarcina*, the latter protein subunits have been

estimated to account for as much as 5-10% of the total protein in the cell (Krzycki & Zeikus, 1984, Terlesky *et al*., 1986). Here we have reported a roughly fourfold higher total soluble protein Fe-S cluster content in *M. acetivorans* growing on acetate compared to the same strain growing on methanol. The concomitant increase in cysteine desulfurization activity in cell-free lysates may implicate the putative ISC systems in meeting this higher [Fe-S] demand, though interestingly the *isc2* deletion strain DJL60 exhibits no difficulty in growing under these conditions when inorganic sulfide is present in the HS medium (**Figure 5**).

The activity and biosynthesis of coenzymes originally identified in methanogens and similar microorganisms have been extensively investigated, though the specifics of how more common coenzymes, such as those found in Wolfe's Vitamin Solution, are synthesized and used in methanogens is comparatively understudied (Abken *et al*., 1998, Grinter & Greening, 2021, Jin *et al*., 2020). Based on the assumption that biosynthesis of coenzyme molecules like biotin, thiamine, lipoic acid, and B12 in methanogens at least broadly resembles that described in bacteria, Fe-S proteins are expected to be involved. Neither of the mutants tested in the experiments described above (*isc2* and *apbC* deletions) exhibited an especially dramatic growth phenotype associated with the absence of vitamins. This might imply that the associated gene products are not involved in biosynthesis of these coenzymes, though it is quite possible that the growth conditions tested do not impose an especially great demand for these vitamins when they are not exogenously supplied.

The previously documented flexibility of members of the genus *Methanosarcina* with respect to sulfur sources for growth can be extended to include sodium thiosulfate and L-cystine for *M. acetivorans* (Mazumder *et al*., 1986, Rauch & Perona, 2016). Our results indicate that the thiosulfate ion may constitute the most preferable sulfur source tested, though the mechanism(s)

by which it is utilized are not yet known. That the Δ*apbC* strain DJL61 grew so much worse on this sulfur source indicates a potential role for ApbC in its utilization, whether in directly binding the ion or, more likely given the predicted function for this protein as an [Fe-S] carrier, in maturation of proteins involved in sulfur metabolism. This might also account for the longer generation times observed for DJL61 with several other sulfur sources. While thiosulfate is a reducing agent, it is not sufficiently powerful in this respect to serve as the primary reductant at a 1.5 mM concentration in making HS media for growing methanogens, though when this was attempted it did avoid the problem of metal precipitation observed when autoclaving HS media reduced with sodium sulfide alone (data not shown). The current practice of reducing HS media with DTT prior to autoclaving remains the best approach to examine different sulfur sources for growth. These results support the hypothesis that *apbC* in *M. acetivorans* encodes a protein involved in sulfur metabolism and are consistent with ApbC functioning in Fe-S trafficking. This conclusion is based on genetic manipulation and growth phenotypes that also potentially implicate it in growth on acetate.

In seeking to understand the consequences of mutations in putative [Fe-S] biogenesis systems, we again confront the difficulty in determining whether the lack of an obvious phenotype is due to gene products not being involved in important processes or rather that extensive functional overlap between potentially redundant systems is masking the involvement of individual gene clusters. For instance, the *suf2* deletion strain DJL63 presented here does not exhibit a growth phenotype under standard conditions. Since the demand for [Fe-S] is high in *M. acetivorans* we might conclude that the SufC2 and SufB2 gene products are not critically important in generating Fe-S clusters for basic cellular processes. For this mutant as well as for the *isc2* deletion strain and others, avenues for further study include further manipulating the

growth conditions in the search for a strong growth deficiency, and making multiple mutants. The ability to generate markerless mutations in a timely fashion, demonstrated here in the deletion of the *suf2* gene clusters, is a breakthrough that holds promise in addressing this complex problem by further editing the genome in a mutant background, or using established protocols for complementation *in trans* (Zhang *et al.*, 2002).

Our data support that there may not be a single "housekeeping" Fe-S cluster biogenesis system in *M. acetivorans* in the sense the term is used in this field (Outten *et al*., 2004). If there is a single critically important system, it's likely not the most highly-expressed Isc2 and Suf2 systems, nor does it likely rely upon ApbC for Fe-S cluster delivery to proteins involved in central pathways of methanogenesis. The prospect for extensive redundancy between the systems and lack of strong phenotypes makes it difficult to ascertain the function of these Fe-S biogenesis systems individually. Our model (**Figure 1**) entertains the possibility of individual specificities, such as an Fe-S apo-protein that cannot accept [Fe-S] directly from a SUF or ISC system, but must interact instead with a specific carrier like ApbC, but testing this hypothesis requires identifying the appropriate apo-protein target. While we have hypothesized that ISC and SUF could be engaged differentially based on the sulfur source input, it could also be the case that there is specificity at output, that is, there may be Fe-S cluster-binding apo-proteins that can interact only with ISC but not SUF or carriers. One prospective target protein known to exhibit [Fe-S] biogenesis specificity in other organisms would be nitrogenase (Dos Santos *et al*., 2007). Nitrogenase is a multi-subunit protein complex with an absolute requirement for Fe-S clusters to function, and microbes must have a functional nitrogenase to grow in minimal media not supplemented with fixed nitrogen (Kennedy & Dean, 1992). The absence of predicted NIF Fe-S

biogenesis genes in *M. acetivorans* make the nitrogenase enzyme an especially promising focus for further study of Fe-S cluster synthesis and delivery in this methanogen (Galagan *et al*., 2002).

References

Abken 1, H.J., M. Tietze, J. Brodersen, S. Bäumer, U. Beifuss, & U. Deppenmeier, (1998) Isolation and characterization of methanophenazine and function of phenazines in membrane-bound electron transport of Methanosarcina mazei Gö1. *J Bacteriol*. 180: 2027-32.

Beinert, H. (1983) Semi-micro methods for analysis of labile sulfide and of labile sulfide plus sulfane sulfur in unusually stable iron-sulfur proteins. *Analytical biochemistry.* 131: 373-8.

Cosper, M.M., G.N.L. Jameson, H.L. Hernández, C. Krebs, B.H. Huynh, & M.K. Johnson, (2004) Characterization of the cofactor composition of Escherichia coli biotin synthase. *Biochemistry*. 43: 2007-21.

Dean, D.R., J.T. Bolin, & L. Zheng, (1993) Nitrogenase metalloclusters: structures, organization, and synthesis. *J Bacteriol*. 175: 6737-44.

Deere, T.M., D. Prakash, F.H. Lessner, E.C. Duin, & D.J. Lessner, (2020) Methanosarcina acetivorans contains a functional ISC system for iron-sulfur cluster biogenesis. *BMC Microbiol*. 20: 323.

Dhamad, A.E. & D.J. Lessner, (2020) A CRISPRi-dCas9 System for Archaea and Its Use To Examine Gene Function during Nitrogen Fixation by Methanosarcina acetivorans. *Appl Environ Microbiol* 86(21):e01402-20.

Dilworth, M.J., (2004) Assay Methods for Products of Nitrogenase Action on Substrates. *Catalysts for Nitrogen Fixation*. 55-76.

Dos Santos, P.C., D.C. Johnson, B.E. Ragle, M.-C. Unciuleac, & D.R. Dean, (2007) Controlled expression of nif and isc iron-sulfur protein maturation components reveals target specificity and limited functional replacement between the two systems. *J Bacteriol*. 189: 2854-62.

Eliot, A.C., B.M. Griffin, P.M. Thomas, T.W. Johannes, N.L. Kelleher, H. Zhao, & W.W. Metcalf, (2008) Biosynthesis of the Potent Antimalarial Compound FR900098. *Chem Biol*. 15: 765–770.

Galagan, J.E., C. Nusbaum, A. Roy, M.G. Endrizzi, P. Macdonald, W. FitzHugh, S. Calvo, R. Engels, S. Smirnov, D. Atnoor, A. Brown, N. Allen, J. Naylor, N. Stange-Thomann, K. DeArellano, R. Johnson, L. Linton, P. McEwan, K. McKernan, J. Talamas, A. Tirrell, W. Ye, A. Zimmer, R.D. Barber, I. Cann, D.E. Graham, D.A. Grahame, A.M. Guss, R. Hedderich, C. Ingram-Smith, H.C. Kuettner, J.A. Krzycki, J.A. Leigh, W. Li, J Liu, B. Mukhopadhyay, J.N. Reeve, K. Smith, T.A. Springer, L.A. Umayam, O. White, R.H. White, E. Conway de Macario, J.G. Ferry, K.F. Jarrell, H. Jing, A.J. Macario, I. Paulsen, M. Pritchett, K.R. Sowers, R.V. Swanson, S.H. Zinder, E. Lander, W.W. Metcalf, & B. Birren, (2002) The genome of Methanosarcina acetivorans reveals extensive metabolic and physiological diversity. *Genome Res.* 12: 532-42.

Gibson, D.G., L. Young, R.-Y. Chuang, J.C. Venter, C.A. Hutchison 3rd, H.O. Smith, (2009) Enzymatic assembly of DNA molecules up to several hundred kilobases. *Nat Methods*. 6(5):343-5.

Gibson, K.J., D.A. Pelletier, & I.M. Turner Sr, (1999) Transfer of sulfur to biotin from biotin synthase (BioB protein). *Biochem Biophys Res Commun*. 254: 632-5.

Grinter, R., & C. Greening, (2021) Cofactor F420: an expanded view of its distribution, biosynthesis, and roles in bacteria and archaea. *FEMS Microbiol Rev*. 14;fuab021.

Guss, A.M., M. Rother, J.K. Zhang, G. Kulkarni, W.W. Metcalf, (2008) New methods for tightly regulated gene expression and highly efficient chromosomal integration of cloned genes for Methanosarcina species. *Archaea*. 2(3):193-203.

Jennings, M.E., F.H. Lessner, E.A. Karr, & D.J. Lessner, (2016) The [4Fe-4S] clusters of Rpo3 are key determinants in the post Rpo3/Rpo11 heterodimer formation of RNA polymerase in Methanosarcina acetivorans. *MicrobiologyOpen*. 6: e00399.

Jimenez-Vicente, E., Z.-Y. Yang, W.K. Ray, C. Echavarri-Erasun, V.L. Cash, L.M. Rubio, L.C. Seefeldt, & D.R. Dean, (2018) Sequential and differential interaction of assembly factors during nitrogenase MoFe protein maturation. *J Biol Chem*. 293: 9812-9823.

Jin, J.-Q., S.-I. Hachisuka, T. Sato, T. Fujiwara, & H. Atomi, (2020) A Structurally Novel Lipoyl Synthase in the Hyperthermophilic Archaeon Thermococcus kodakarensis. *Appl Environ Microbiol*. 86: e01359-20.

Kennedy, C. & D. Dean, (1992) The nifU, nifS and nifV gene products are required for activity of all three nitrogenases of Azotobacter vinelandii. *Mol Gen Genet*. 231: 494-8.

Kohler, P.R.A. & W.W. Metcalf, (2012) Genetic manipulation of Methanosarcina spp. *Front Microbiol*. 3:259.

Krzycki, J.A. & J.G. Zeikus, (1984) Characterization and purification of carbon monoxide dehydrogenase from Methanosarcina barkeri. *J Bacteriol*. 158: 231-7.

Leech, H.K., E. Raux, K.J. McLean, A.W. Munro, N.J. Robinson, G.P. Borrelly, M. Malten, D. Jahn, S.E. Rigby, P. Heathcote, & M.J. Warren, (2003) Characterization of the cobaltochelatase CbiXL: evidence for a 4Fe-4S center housed within an MXCXXC motif. *J Biol Chem*. 278: 41900-7.

Lessner, D.J., L. Li, Q. Li, T. Rejtar, V.P. Andreev, M. Reichlen, K. Hill, J.J. Moran, B.L. Karger, J.G. Ferry, (2006) An unconventional pathway for reduction of CO2 to methane in CO-grown Methanosarcina acetivorans revealed by proteomics. *Proc Natl Acad Sci U S A*. 103(47):17921-6.

Li, Q., L. Li, T. Rejtar, B.L. Karger, J.G. Ferry, (2005) Proteome of Methanosarcina acetivorans Part II: comparison of protein levels in acetate- and methanol-grown cells. *J Proteome Res*. 4(1):129-35.

Li, Q., L. Li, T. Rejtar, D.J. Lessner, B.L. Karger, & J.G. Ferry, (2006) Electron transport in the pathway of acetate conversion to methane in the marine archaeon Methanosarcina acetivorans. *J Bacteriol*. 188: 702-10.

Lill, R., R. Dutkiewicz, H.-P. Elsässer, A. Hausmann, D.J.A. Netz, A.J. Pierik, O. Stehling, E. Urzica, U. Mühlenhoff, (2006) Mechanisms of iron-sulfur protein maturation in mitochondria, cytosol and nucleus of eukaryotes. *Biochim Biophys Acta*. 1763(7):652-67.

Liu, Y., M. Sieprawska-Lupa, W.B. Whitman, R.H. White (2010) Cysteine is not the sulfur source for iron-sulfur cluster and methionine biosynthesis in the methanogenic archaeon Methanococcus maripaludis. *J Biol Chem*. 285(42):31923-9.

Liu, Y., L.L. Beer, & W.B. Whitman, (2012) Sulfur metabolism in archaea reveals novel processes. *Environ Microbiol.* 14: 2632-44.

Major, T.A., H. Burd, & W.B. Whitman, (2004) Abundance of 4Fe-4S motifs in the genomes of methanogens and other prokaryotes. *FEMS Microbiol Lett.* 239: 117-23.

Martinez-Gomez, N.C. & D.M. Downs (2008) ThiC is an [Fe-S] cluster protein that requires AdoMet to generate the 4-amino-5-hydroxymethyl-2-methylpyrimidine moiety in thiamin synthesis. *Biochemistry*. 47: 9054-6.

Mashruwala, A.A., C.A. Roberts, S. Bhatt, K.L. May, R.K. Carroll, L.N. Shaw, & J.M. Boyd, (2016) Staphylococcus aureus SufT: an essential iron-sulphur cluster assembly factor in cells experiencing a high-demand for lipoic acid. *Mol Microbiol*. 102: 1099-1119.

Mazumder, T.K., N. Nishio, S. Fukuzaki, & S. Nagai, (1986) Effect of Sulfur-Containing Compounds on Growth of Methanosarcina barkeri in Defined Medium. *Appl Environ Microbiol*. 52: 617-22.

Metcalf, W.W., J.K. Zhang, E. Apolinario, K.R. Sowers, & R.S. Wolfe, (1997) A genetic system for Archaea of the genus Methanosarcina: liposome-mediated transformation and construction of shuttle vectors. *Proc Natl Acad Sci USA.* 94: 2626-31.

Nayak, D.D., W.W. Metcalf, (2017) Cas9-mediated genome editing in the methanogenic archaeon Methanosarcina acetivorans. *Proc Natl Acad Sci U S A.* 114(11):2976-2981.

Norrander, J., T. Kempe, & J. Messinga, (1983) Construction of improved M13 vectors using oligodeoxynucleotide-directed mutagenesis. *Gene*. 26: 101-106.

Outten, F.W., O. Djaman, & G. Storz, (2004) A suf operon requirement for Fe-S cluster assembly during iron starvation in Escherichia coli. *Mol Microbiol*. 52: 861-72.

Peters, J.W., K. Fisher, & D.R. Dean, (1995) Nitrogenase structure and function: a biochemical-genetic perspective. *Annu Rev Microbiol.* 49: 335-66.

Rauch, B.J. & J.J. Perona, (2016) Efficient Sulfide Assimilation in Methanosarcina acetivorans Is Mediated by the MA1715 Protein. *J Bacteriol.* 198: 1974-83.

Shea, M.T., M.E. Walter, N. Duszenko, A.-L. Ducluzeau, J. Aldridge, S.K. King, & N.R. Buan, (2016) pNEB193-derived suicide plasmids for gene deletion and protein expression in the methane-producing archaeon, Methanosarcina acetivorans. *Plasmid*. 84-85: 27-35.

Soutourina, O., O. Poupel, J.-Y. Coppée, A. Danchin, T. Msadek, & I. Martin-Verstraete, (2009) CymR, the master regulator of cysteine metabolism in Staphylococcus aureus, controls host sulphur source utilization and plays a role in biofilm formation. *Mol Microbiol*. 73: 194-211.

Sowers, K.R., J.E. Boone, & R.P. Gunsalus, (1993) Disaggregation of Methanosarcina spp. and growth as single cells at elevated osmolarity. *Appl Environ Microbiol.* 59: 3832-9.

Terlesky, K.C., M.J. Nelson, & J.G. Ferry, (1986) Isolation of an enzyme complex with carbon monoxide dehydrogenase activity containing corrinoid and nickel from acetate-grown Methanosarcina thermophila. *J Bacteriol*. 168: 1053-8.

Thauer, R.K., A.K. Kaster, H. Seedorf, W. Buckel, & R. Hedderich, (2008) Methanogenic archaea: ecologically relevant differences in energy conservation. *Nat Rev Microbiol.* 6: 579-91.

Welander, P.V., W.W. Metcalf, (2008) Mutagenesis of the C1 oxidation pathway in Methanosarcina barkeri: new insights into the Mtr/Mer bypass pathway. *J Bacteriol*. 190(6):1928-36.

Whitman, W.B., E. Ankwanda, & R.S. Wolfe, (1982) Nutrition and carbon metabolism of Methanococcus voltae. *J Bacteriol*. 149: 852-63.

Wild, J., Z, Hradecna, W, Szybalski, (2002) Conditionally amplifiable BACs: switching from single-copy to high-copy vectors and genomic clones. *Genome Res*. 12(9):1434-44.

Wolin, E.A., M.J. Wolin, & R.S. Wolfe, (1963) Formation of Methane by Bacterial Extracts. *J Biol Chem.* 238: 2882-6.

Zhang, J.K., A.K. White, H.C. Kuettner, P. Boccazzi, & W.W. Metcalf, (2002) Directed mutagenesis and plasmid-based complementation in the methanogenic archaeon Methanosarcina acetivorans C2A demonstrated by genetic analysis of proline biosynthesis. *J Bacteriol*. 184: 1449-54.

Zheng, L. & D.R. Dean, (1994) Catalytic formation of a nitrogenase iron-sulfur cluster. *J Biol Chem*. 269: 18723-6.

Zhao, C., Z. Lyu, F. Long, T. Akinyemi, K. Manakongtreecheep, D. Söll, W.B. Whitman, D.J. Vinyard, Y. Liu, (2020) The Nbp35/ApbC homolog acts as a nonessential [4Fe-4S] transfer protein in methanogenic archaea. *FEBS Lett*. 594(5):924-932.

APPENDIX

Figures and Tables

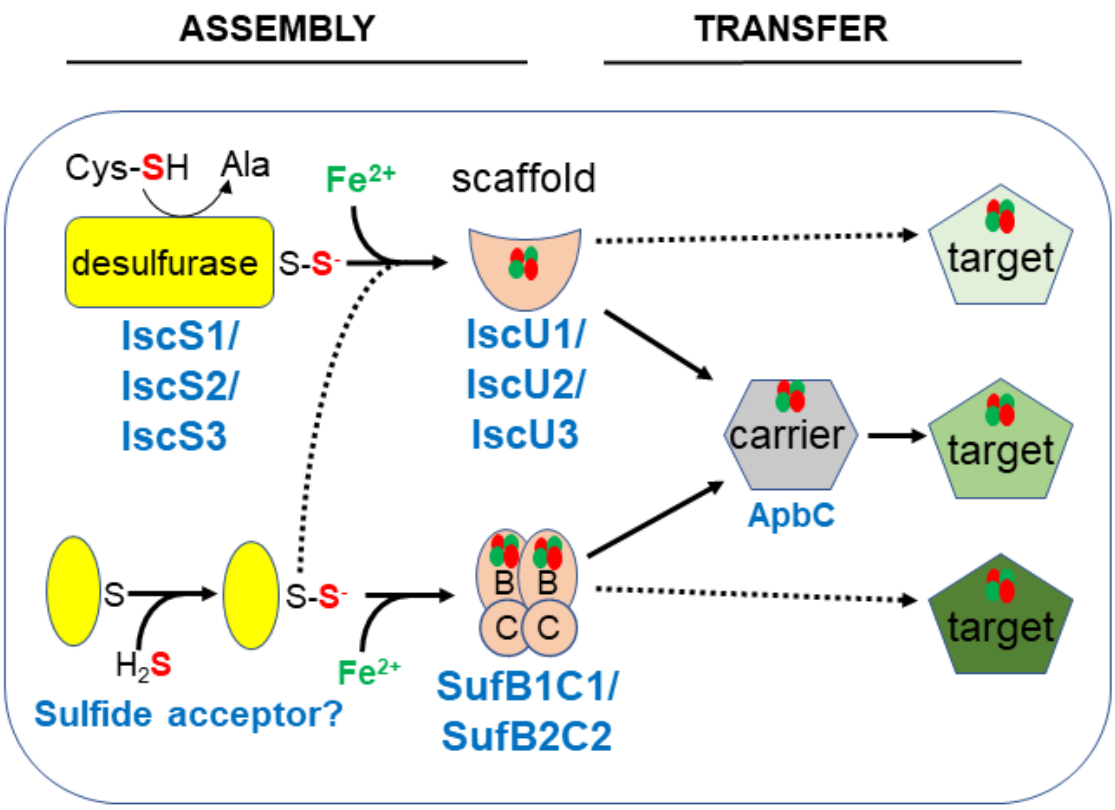

Figure 1. Proposed model of Fe-S cluster biogenesis and delivery in *Methanosarcina acetivorans*. ISC is used when cysteine is the sulfur source, SUF when growing on inorganic sulfide. The potential for interaction between the systems exists, but has not been demonstrated. ApbC may serve as an intermediate [Fe-S] carrier and delivery protein.

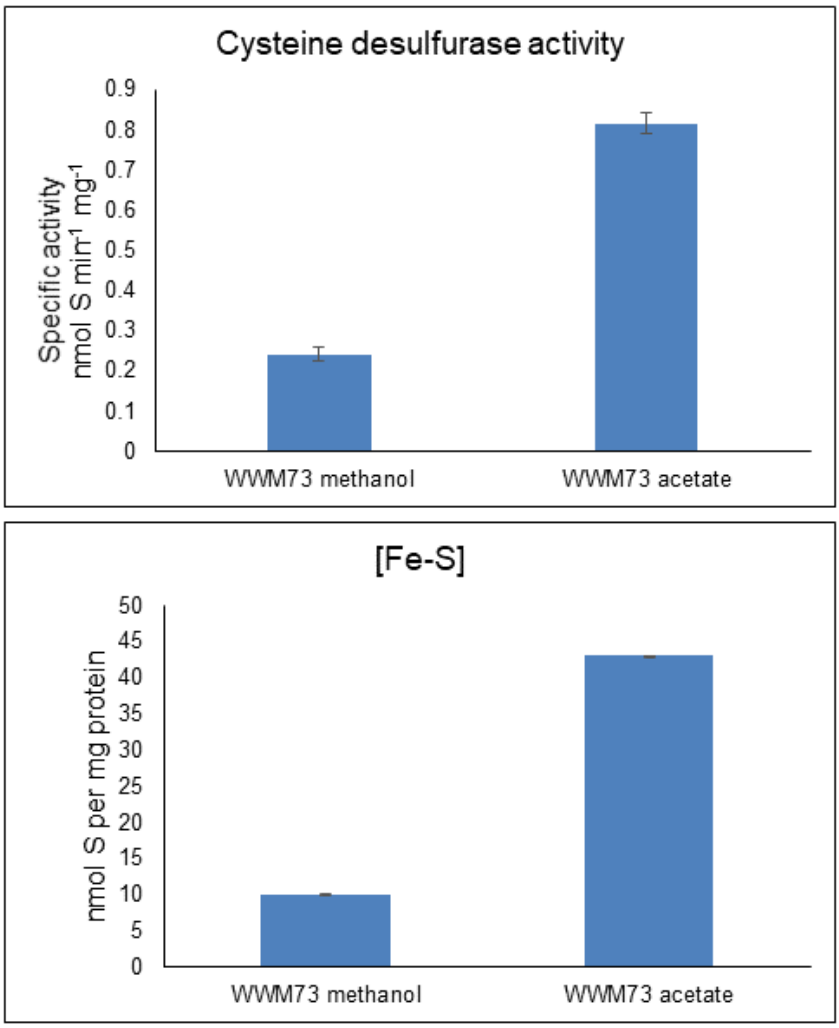

Figure 2. Cysteine desulfurase activity and [Fe-S] content changes with carbon source. **Top)** Cysteine desulfurase activity measured in cell-free lysates from WWM73 growing on methanol or acetate. **Bottom)** Acid-labile sulfide content in cell-free lysates from WWM73 growing on methanol or acetate. All cultures were grown in standard HS media with cysteine and sulfide + 125 mM methanol or 100 mM sodium acetate. Data are the mean ± SD of three technical replicates.

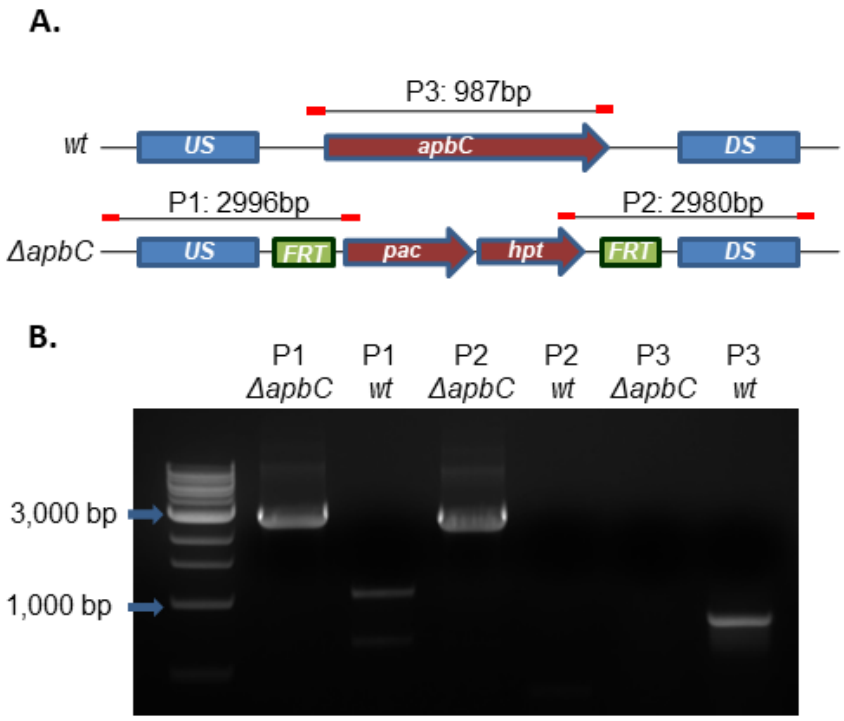

Figure 3. PCR confirmation of *apbC* deletion in *M. acetivorans* strain DJL61. **A.** Schematic showing replacement of *apbC* with *pac-hpt* in strain DJL61 and predicted PCR products are indicated by P1-3. **B.** Gel image of products of PCR reactions P1-3 with WWM73 and DJL61 genomic DNA.

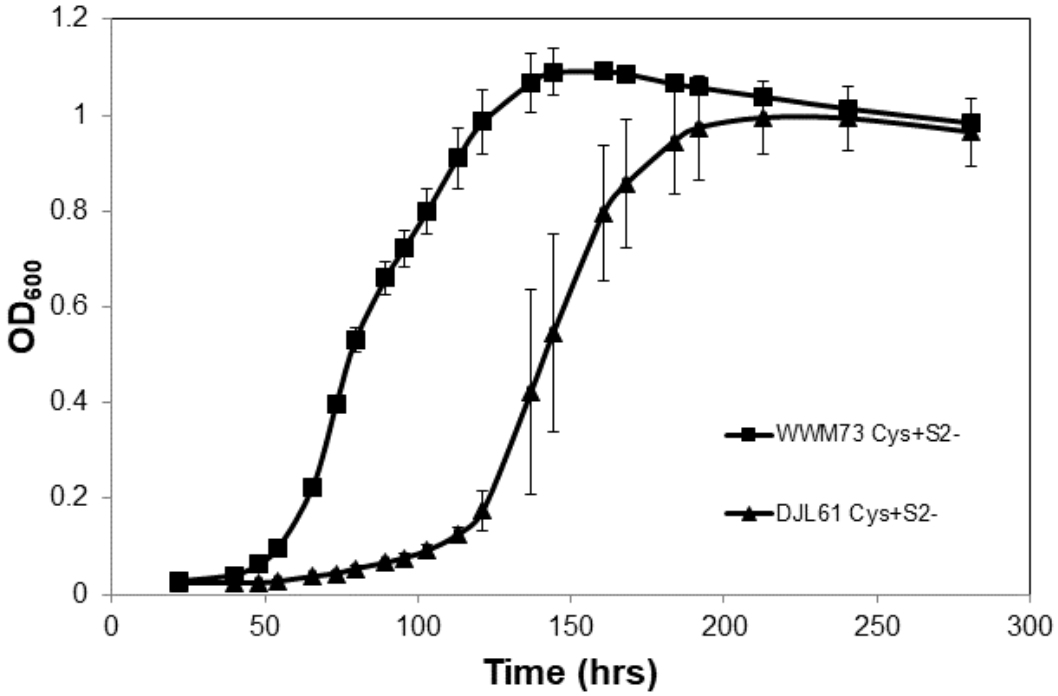

Figure 4. Strains WWM73 and DJL61 grown with cysteine and sulfide. WWM73 (wt, squares) and DJL61 (Δ*apbC*, triangles) were inoculated into DTT-reduced HS media and grown with 125 mM methanol, 3 mM cysteine, and 1 mM sodium sulfide. Data plotted are the mean ± SD of three replicates.

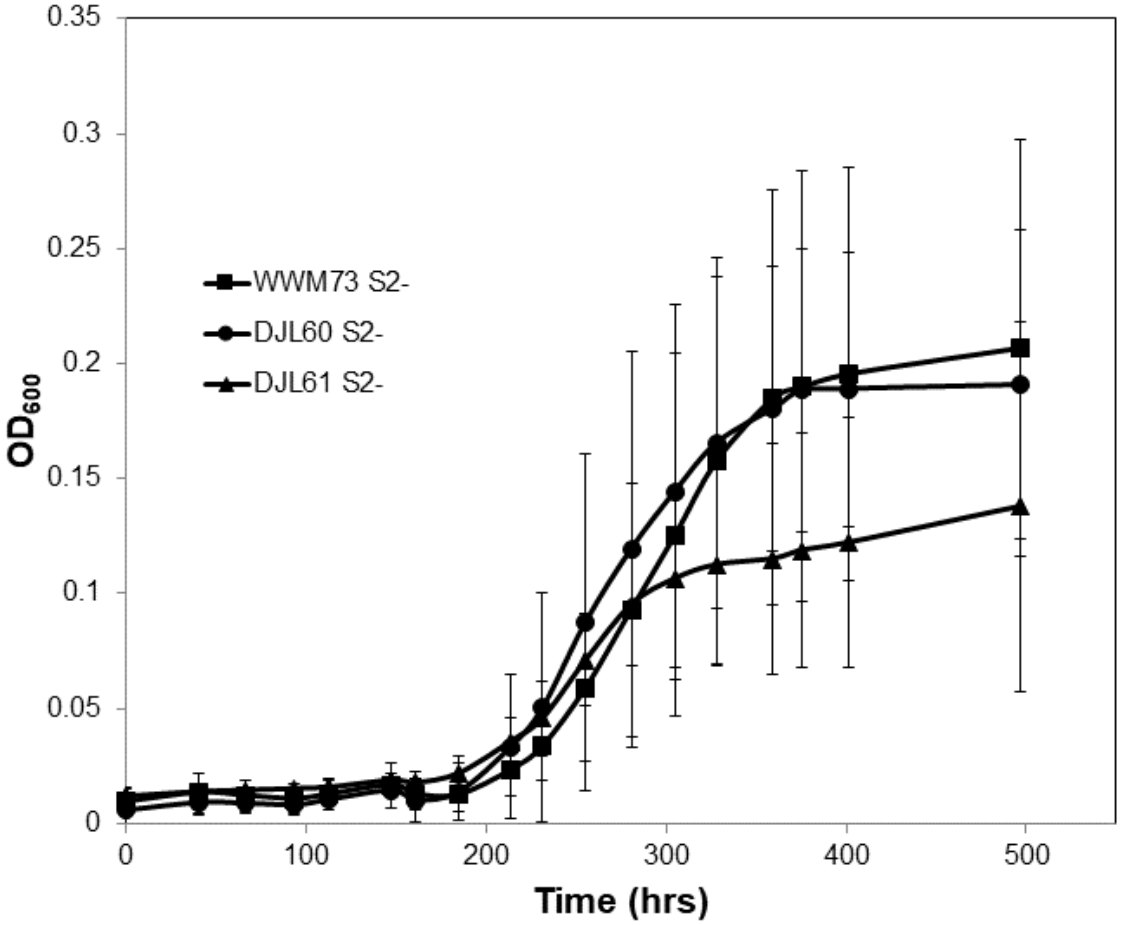

Figure 5. Strains WWM73, DJL60 (Δ*isc2*), and DJL61 (Δ*apbC*) growing on acetate. WWM73 (squares), DJL60 (circles), and DJL61 (triangles) were grown in DTT-reduced HS medium on 0.1 M sodium acetate with 0.025% sodium sulfide. Data plotted are the mean ± SD of three replicates.

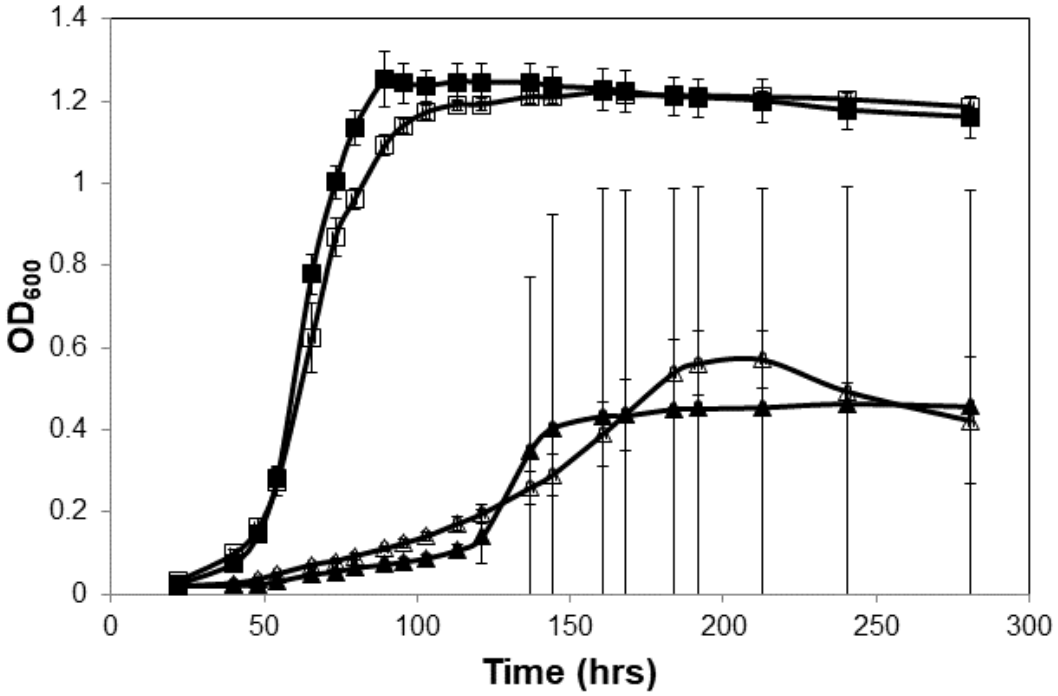

Figure 6. Strains WWM73 and DJL61 growing on methanol with thiosulfate. WWM73 (squares) was grown with (solid) or without (hollow) vitamin solution added. DJL61 (triangles) was also grown with (solid) and without (hollow) vitamins. All cultures were grown on 125 mM methanol in DTT-reduced HS medium supplemented with 1.5 mM sodium thiosulfate. Data plotted are the mean ± SD of three replicates.

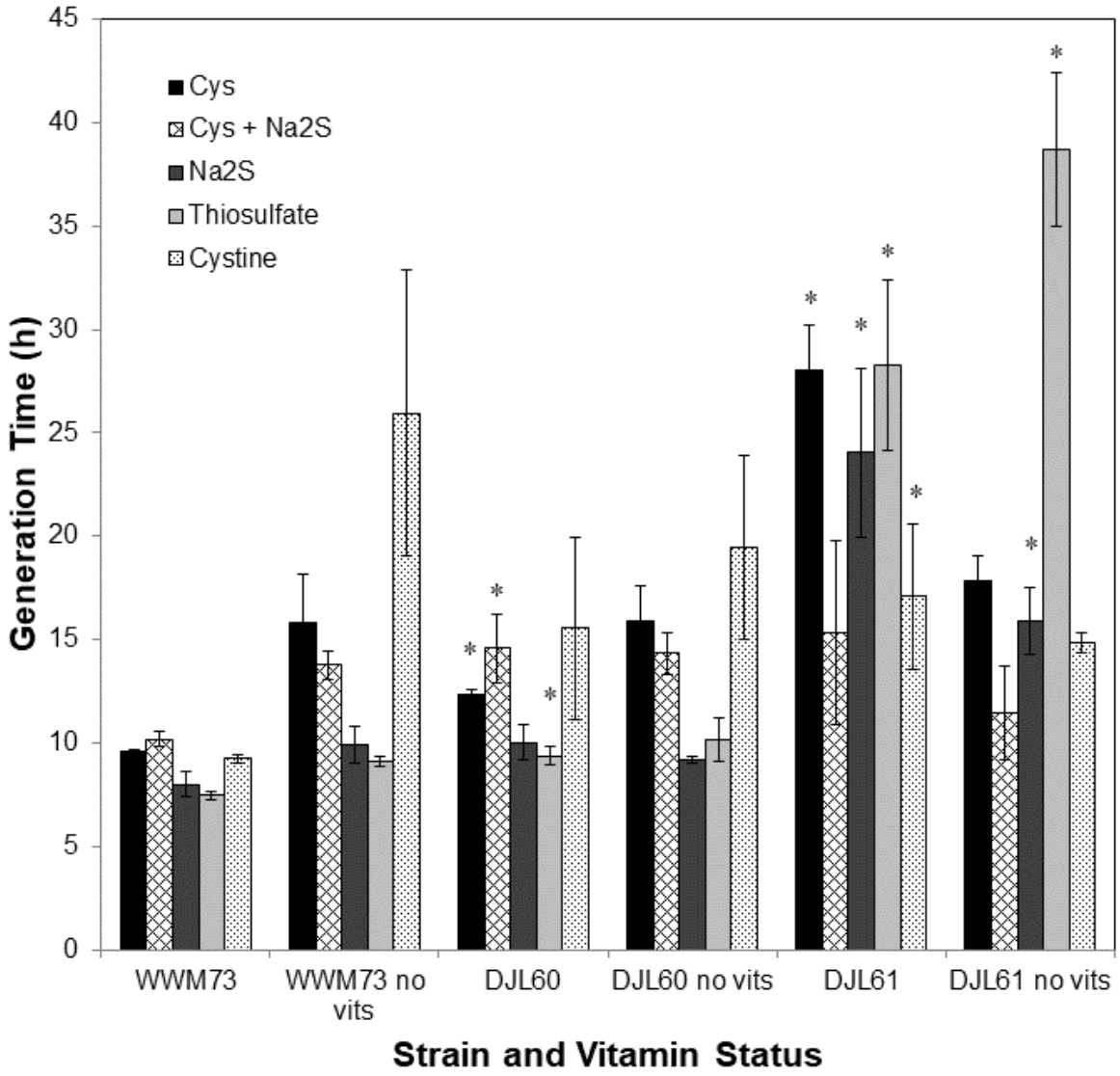

Figure 7. Generation times of strains WWM73, DJL60, and DJL61 growing on methanol with different sulfur sources. All were grown in DTT-reduced HS medium with 3 mM cysteine (black), 3 mM cysteine + 1 mM sulfide (hatched), 1 mM sulfide (dark gray), 1.5 mM thiosulfate (light gray), or 1.5 mM cystine (spotted), with or without Wolfe's vitamins as indicated. Data plotted are the mean ± SD of three replicates. *denotes significant difference from WWM73 parent strain ($p < 0.02$ in Student's t-test).

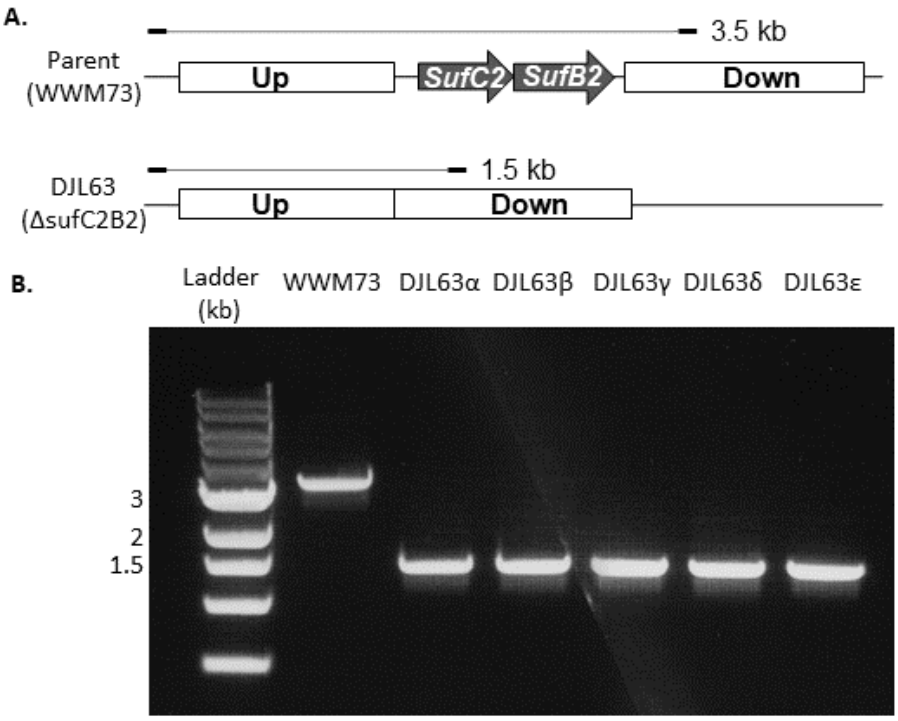

Figure 8. PCR confirmation of *sufC2B2* deletion in *M. acetivorans* strain DJL63. **A.** Schematic showing markerless deletion of *sufC2B2* in strain DJL63 and predicted PCR products from the same primer pair are indicated. **B.** Gel image of products of PCR reaction with primers indicated in the schematic, using actively growing cultures of WWM73 and DJL63 ("α" through "ε" isolates) as template. The "α" PCR product was sequenced, confirmed, and the strain saved and designated simply DJL63.

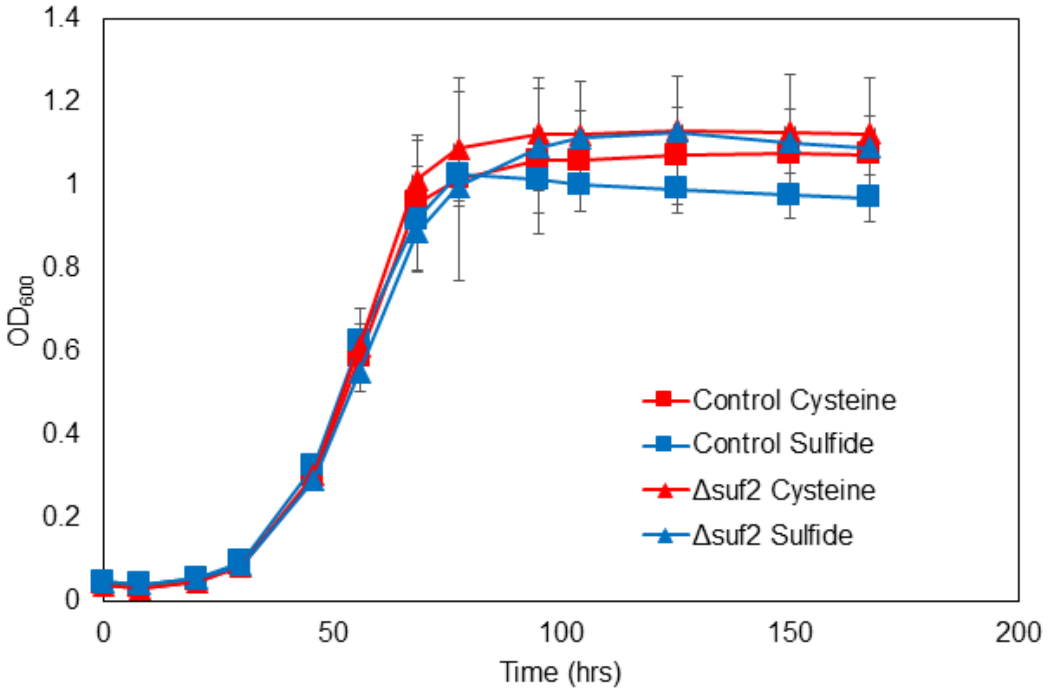

Figure 9. Parent strain versus DJL63 (Δ*suf2*) growing on methanol with different sulfur sources. WWM73 (squares) and DJL63 (triangles) were grown in DTT-reduced HS medium on 125 mM methanol with 3 mM cysteine (red) or 1 mM sodium sulfide (blue). Data plotted are the mean ± SD of three replicates.

Table 1. Strains and plasmids used in this study

Name	Description	Source or reference
	Strains	
E. coli		
DH5α	Cloning strain	NEB
WM4489	DH10β-derived host to boost copy number of pJK- and pDN-derived plasmids containing *oriV*	(Eliot *et al.*, 2008)
M. acetivorans		
WWM73	Δ*hpt*::P*mcrB-tetR*-ϕC31-*int*-attP	(Guss *et al.*, 2008)
DJL60	WWM73 Δ*iscSU2*::*pac-hpt*	(Deere *et al.*, 2020)
DJL61	WWM73 Δ*apbC*::*pac-hpt*	This study
DJL63	WWM73 Δ*sufCB2*	This study
	Plasmids	
pAMG40	*E. coli-Methanosarcina* shuttle vector for fosmid retrofitting encoding ampicillin resistance and λattB	(Guss *et al.*, 2008)
pDL238	Empty vector for HDR CRISPR/Cas9 system; pDN203 with region between *Asc*I sites deleted	This study
pDL243	pDL734 with sgRNA to target *isc1* for CRISPRi	This study
pDL244	pDL734 with sgRNA to target *isc2* for CRISPRi	This study
pDL245	pDL734 with faulty sgRNA meant to target *isc3* for CRISPRi	This study
pDL248	*suf2* proto-knockout plasmid with upstream and downstream regions, sgRNA complexes Gibson Assembled in *Bam*HI-cut pUC18	This study
pDL249	*suf2* knockout plasmid with upstream and downstream regions, sgRNA complexes Gibson Assembled in *Asc*I-cut pDL238	This study
pDL250	pDL249 cointegrated with pAMG40 to create replicating plasmid	This study
pDL347	*apbC* knockout plasmid; pJK301 with regions upstream of *apbC* cloned into *Apa*I & *Hind*III sites, downstream of *apbC* cloned into *Bam*HI & *Spe*I sites	This study
pDN203	Vector for HDR CRISPR/Cas9 editing, contains sgRNA for *ssuC* gene	(Nayak & Metcalf, 2017)
pJK301	Amp^R vector for making markerless deletions in *Methanosarcina* spp.; contains *pac-hpt* flanked by Flp recombinase FRT recognition sites	(Welander & Metcalf 2008)
pUC18	Cloning plasmid with Amp^R	(Norrander *et al.*, 1983)

Chapter III

Towards an understanding of the assembly and activity of nitrogenase and hydrogenase in *Methanosarcina acetivorans?*

Thomas M. Deere

Cell and Molecular Biology Program, University of Arkansas,

Fayetteville, AR 72701 USA

Introduction

Nitrogenase research has, over several decades, developed along both genetic and biochemical avenues of inquiry. As briefly described in the introductory chapter, painstaking work in deleting genes suspected to be involved in the production, maturation, maintenance, and function of the nitrogenase protein complex has led to the elucidation of the core components required for dinitrogen fixation (Peters *et al.*, 1995, Dean *et al*., 1993, Jimenez-Vicente *et al.*, 2018, Zheng & Dean, 1994). The free-living aerobic diazotrophic bacterium *Azotobacter vinelandii* emerged as a favored model species for nitrogenase researchers, with the full set of genes and an apparent minimal core system being described (Dos Santos *et al.*, 2012). Sequence homology searches of the genome of *Methanosarcina acetivorans* suggest a system more complex than the minimal set of core genes but considerably simpler than bacterial systems like that of *A. vinelandii* (**Figure 1**). The core gene products in bacteria have established functions, pictured in the top half of **Figure 2**. NifD and NifK are subunits that form an $\alpha_2\beta_2$ heterotetramer binding the catalytic iron-molybdenum cofactor (FeMoCo, or "M" cluster) and functioning as the dinitrogen reductase. NifDK binds a second Fe-S cluster, an [8Fe-7S] known as the "P" cluster, which receives incoming electrons to convey them to the M cluster. NifH forms a [4Fe-4S]-binding homodimer that associates with $NifD_2K_2$, serving as a conduit for reducing equivalents as well as playing roles in maturation and maintenance of the P and M clusters (Harris *et al*., 2018). NifB is a [4Fe-4S]-binding protein responsible for assembling the precursor of the P cluster, which is further matured by a NifEN complex before transfer to apo-$NifD_2K_2$ (Jimenez-Vicente *et al*., 2018). As depicted in **Figure 2**, the NIF system of Fe-S cluster biogenesis is responsible for producing the multiple [Fe-S] required to build and maintain the components of the nitrogenase system in bacteria, principally by the action of the specialized

cysteine desulfurase NifS and scaffold NifU. The genes for these two proteins in bacteria do not have clear homologs in Domain Archaea, and the question of how the assembly and activation of the NifHDK complex is achieved in their absence is one without an obvious *a priori* answer. As detailed above, canonical cysteine desulfurases for instance are far from universal among methanogens, and homologs are entirely missing in some known diazotrophs (Liu *et al*., 2012, Kessler *et al*., 1998). While this mechanism almost certainly cannot be universal among diazotrophic methanogens, we hypothesize that the ISC system(s) assembles Fe-S clusters for nitrogenase proteins when *M. acetivorans* is growing with cysteine as the sole sulfur source, and that the SUF system(s) serve this function when inorganic sulfide is the sulfur source, as depicted in **Figure 3**. Testing this hypothesis requires assaying *M. acetivorans* nitrogenase activity, ideally both in cultures or cell-free lysates, and with purified proteins.

Studies of *in vitro* nitrogenase activity have long demonstrated that the enzyme complex is relatively promiscuous, with substrate and product gases shown to include dinitrogen, acetylene, ethylene, ethane, carbon monoxide, and dihydrogen (Shah *et al*., 1972, Dilworth *et al*., 1987, Yang *et al*., 2011). Assays for *in vitro* activity of purified nitrogenase complexes are conducted anaerobically with an excess of reducing equivalents and an ATP-regenerating system (Dilworth, 2004). Measurements of enzyme activity focused on the products from these different reactions take a few forms. The "natural" product of nitrogenase, ammonium produced from dinitrogen reduction, can be detected using high-performance liquid chromatography (HPLC) or using a colorimetric assay based on the color change associated with formation of indophenol from phenol (Fawcett & Scott, 1960). There are serious limitations to ammonia detection assays (Dilworth &Thorneley, 1981), that can be overcome by partially purifying ammonia from terminated reaction mixtures using microdistillation or cation exchange resins (Dilworth &

Fisher, 1998). Measuring hydrogen produced from proton reduction is simpler in most ways, but requires gas chromatography with a column capable of separating hydrogen from other permanent gases and a detector such as a thermal conductivity detector (TCD) or discharge ionization detector (DID/BID) suitable for hydrogen detection (Devi *et al*., 2018).

The most widely employed assay of nitrogenase activity is the acetylene reduction assay, in which the carbon-carbon triple bond in acetylene (ethyne) is enzymatically reduced to a double bond, yielding ethylene (ethene). Some nitrogenases, especially the "alternative" V-nitrogenases and Fe-nitrogenases, have been observed to further reduce the carbon bond to ethane, though this activity appears not to be universally observed across bacteria and archaea (Dilworth *et al*., 1987, Lobo & Zinder, 1990, Eady, 1996). This experimental approach requires that dinitrogen be purged from a sealed anaerobic vial's headspace prior to adding the substrate acetylene. Measuring acetylene reduction activity presents special challenges in methanogens. Standard assay protocols include acetylene in the headspace at 10% to drive the reaction forward, but acetylene concentrations above 0.3% are inhibitory to methanogenesis, so metabolically active whole-cell assays must be conducted at this lower mole fraction (Lobo & Zinder, 1988). In addition, purified nitrogenases from *Methanococcus maripaludis* and *Methanosarcina barkeri* have exhibited lower acetylene reduction activity than complexes from *Azotobacter vinelandii* and *Klebsiella pneumoniae*, with acetylene proving to be a poorer substrate than dinitrogen in *M. barkeri* whereas the two substrates are generally reduced equally well by bacterial nitrogenases (Dodsworth & Leigh, 2006, Lobo & Zinder, 1990).

Functional nitrogenase is known to produce hydrogen while reducing nitrogen, and while side-reactions are not uncommon in enzymology, hydrogen evolution is an obligate process for the active site metallocluster, FeMoCo (Harris *et al*., 2018[b]). This presents a potentially

significant bioenergetic cost to diazotrophic cells, given the electrons consumed and ATP hydrolysis required to move them through the complex. Diazotrophs have been observed to conserve some of this energy by way of "uptake hydrogenases," membrane-bound complexes that interact with electron acceptors of midpoint potential sufficiently higher than the H_2/H^+ to drive oxidation of H_2 (Vignais & Billoud, 2007). Transcription of these hydrogenase genes has been observed to be regulated by Nif proteins or coregulated by factors acting on nitrogenase genes (Brito *et al*., 1997, Elsen *et al.*, 2000). In facultative and obligate aerobes, in which most nitrogenase research has been conducted, these hydrogenases also help exert a protective effect on the nitrogenase complex, preventing exposure to oxygen and ROS (Zhang *et al*., 2014).

The primary hydrogenases in methanogens are of the [NiFe] type, which require numerous Fe-S proteins for their maturation (Mand & Metcalf, 2019, Pinske & Sawers, 2012). The protein complexes are broadly categorized into a few separate systems: Ech, Frh, Vho/Vht, and Vhx (Mand *et al*., 2018). The membrane-bound energy-converting Ech hydrogenase oxidizes H_2 and reduces the Fe-S protein electron carrier ferredoxin, though it can also be run "in reverse" as a proton pump to build the H^+ membrane gradient used by ATP synthase, in which case it oxidizes ferredoxin (Kulkarni *et al*., 2018). The cytoplasmic Frh hydrogenases, also known as coenzyme F_{420}-reducing hydrogenases, are important enzymes for linking hydrogen oxidation to broader metabolism in methanogens through the flavin derivative coenzyme F_{420} (Baron & Ferry, 1989, Greening *et al*., 2016). The cytochrome-containing Vho/Vht hydrogenases, initially named "viologen-reducing hydrogenases one/two" because they do not reduce F_{420} but are active when measured with the redox-sensitive viologen dyes, are also located in the cell membrane where they use hydrogen to reduce the cofactor methanophenazine (Deppenmeier *et al.*, 1995, Mand & Metcalf, 2019). Vhx hydrogenases perform essentially the same functions as the Vho/Vht types,

and are broadly similar in amino acid sequence, but a few key substitutions and some differences in their promoters have led some methanogen researchers to consider them a separate type (Guss *et al*., 2009). What influence these various hydrogenases exert on nitrogen fixation in *M. acetivorans* is difficult to predict, especially given the relatively low abundance of functional energy-conserving hydrogenases documented in this marine methanogen and the fact that Ech is entirely absent in this species (Guss *et al.*, 2009). Understanding the interactions would be greatly aided by the ability to detect hydrogenase activity in *M. acetivorans*.

The simplest and most widely used assay of hydrogenase activity measures the oxidation or reduction of an organic dye like 1,1′-dimethyl-4,4′-bipyridinium dichloride (commonly known as methyl viologen) or 1,1′-dibenzyl-4,4′-bipyridinium dichloride (benzyl viologen). Since reduced methyl viologen (but not the oxidized form) has a characteristic absorption peak at 578 nm, the appearance of the reduced form over time can be monitored as a marker for the oxidation of dihydrogen by hydrogenase (Yu & Wolin, 1969, Gitlitz & Krasna, 1975). Like nitrogenases, hydrogenases are extremely oxygen-sensitive, so these assays must be conducted under strictly anoxic conditions such as an atmosphere of pure nitrogen or argon. While hydrogenase activity has been measured in methanogens, including the freshwater species *Methanosarcina barkeri*, previously published work documents little to no hydrogenase activity measured in *M. acetivorans* (Guss *et al*., 2005, Nelson & Ferry, 1984).

Previous genetic manipulations of predicted Fe-S cluster biogenesis systems in *M. acetivorans* have relied upon homologous recombination to replace genes with a selectable marker (Deere *et al*, 2020), or have employed a CRISPR/Cas9 system for genome editing (Nayak & Metcalf, 2017). While the latter approach is a clear improvement in many ways, Cas9-based deletions are still time-intensive, sometimes requiring months to generate and confirm

mutants. Recently, an alternative strategy involving knocking down genes in *M. acetivorans*, instead of deleting them entirely, was pioneered by a researcher in our laboratory, Dr. Ahmed Dhamad. The system he created is designed for targeted interference in transcription based on the previously described CRISPR/Cas9 system (Nayak & Metcalf, 2017, Dhamad & Lessner, 2020). A handful of point mutations to the *cas9* gene gives rise to a protein product that is "dead" with respect to its activity in generating double-stranded DNA breaks, hence the name dCas9. The target-recognition and DNA-binding activity of the protein are unaffected by these changes, but upon binding the sgRNA-designated PAM sequence the dCas9 is difficult to dislodge by the RNA polymerase complex (Jinek *et al*., 2012). The result is a powerful sequence-specific CRISPR-based interference ("CRISPRi") that, given the relative simplicity of the plasmid construct required, can generate knockdown strains in a fraction of the time needed to make deletion mutants (Dhamad & Lessner, 2020). This approach to genetic analysis is particularly attractive for studying [Fe-S] biogenesis in *M. acetivorans* given the potential for redundancy across the five putative Fe-S cluster synthesis systems. This CRISPRi system was chosen to target the three putative *isc* gene clusters.

Outstanding questions regarding nitrogen fixation and [Fe-S] biogenesis in *M. acetivorans* include: Can we measure nitrogenase activity in this methanogen as a tool to study [Fe-S] biogenesis? Do IscS2 and IscU2 function in nitrogenase maturation in methanogens as NIF does in bacteria? Are the other putative ISC systems required for general growth? What impact does the sulfur source for methanogenic growth have on nitrogen fixation? What influence does hydrogen exert in nitrogen fixation? Does hydrogenase activity change under diazotrophic growth conditions? Herein we attempt to answer these questions.

Materials and Methods

Growth of microbes and preparation of extracts. *M. acetivorans* strains, including WWM73, DJL60, DJL91, and DJL92, as well as *Methanosarcina barkeri* WWM85 (**Table 1**), were grown in standard HS medium reduced with DTT as previously described (Deere *et al*., 2020). The bacterium *Azotobacter vinelandii* DJ (generously provided by Dennis Dean and Valerie Cash at Virginia Polytechnic institute) was grown in nitrogen-free Burk's medium at 30 °C shaking at 300 rpm (Navarro-Rodríguez *et al*., 2019, Strandberg & Wilson, 1968). When necessary, gas additions were made through butyl stoppers into culture tube headspaces using gas-purged syringes. *M. acetivorans* and *M. barkeri* cells were harvested at an optical density at 600 nm of 0.3 - 0.7, as described previously (Sowers *et al*., 1984). Pelleted cells were harvested and resuspended in anaerobic storage buffer (50 mM Tris pH 8.0, 150 mM NaCl) with dithiothreitol (DTT), benzamidine chloride, and phenylmethylsulfonyl fluoride (PMSF) all at 1 mM concentrations. Methanogen cell pellets were stored under nitrogen in sealed vials at -80 °C until use. Cultures of diazotrophically growing *A. vinelandii* were harvested at an optical density at 600 nm of 0.8 – 1.5, by centrifugation at 5,000 rpm for 10 minutes at 4 °C. Pellets were stored in argon-purged 50 mL conical tubes at -80 °C until use. Subsequent procedures were all performed anaerobically in a Coy Laboratories glovebag with an atmosphere of 95% nitrogen, 5% hydrogen, including for heretofore aerobically handled *A. vinelandii.* Methanogens and bacteria were lysed by sonication on ice with a QSonica model Q55 equipped with a model CL-188 probe. Methanogen resuspensions were sonicated three times at an amplitude of "40" for 10 seconds at a time, while bacterial resuspensions were sonicated five times at an amplitude of "80" for 10 seconds at a time. All lysates were cleared by centrifugation at 16,000 x *g* for 10

minutes and removal of the supernatant. Total soluble protein in this cell-free lysate was determined by the Bradford method, using bovine serum albumin as a standard (Bradford, 1976).

CRISPRi constructs for *isc1-3*. Gene-specific sgRNA sequences were designed into gBlocks that also carry a promoter and CRISPR scaffold. Sequences of DNA were ordered from Integrated DNA Technologies, Inc., comprising 3 gBlocks, each with one sgRNA to target *iscS1*, *iscS2*, and *iscS3* respectively. Previous work in our laboratory has demonstrated that targeting the first gene in an operon with dCas9 results in genes immediately downstream being repressed as well, so no constructs targeting the "U" genes were deemed necessary (Dhamad & Lessner, 2020). The vector pDL734, present at 1 µg in a 20 µL reaction with 1 µL of *Asc*I, was digested overnight at 37 °C before heat-inactivation by incubating at 80 °C at 20 minutes. Gibson Assemblies were set up, with 0.008 picomoles of cut vector (1.36 µL of the inactivated 50 ng/µL digest) placed into each of three 0.2 mL PCR tubes with 0.04 picomoles (1.69 µL of the 10 ng/µL gBlock solution) of the appropriate *iscS* gBlock and ultrapure water to reach volumes of 5 µL. The master mix additions and reaction conditions were identical to those used in generating the CRISPR/Cas9 *suf2* deletion construct, as were the transformation conditions with aliquots of competent WM4489 cells. Transformants that grew on LB + 34 µg/mL chloramphenicol plates were screened by PCR to confirm gBlock insertion. Plasmids purified from these colonies were designated pDL243 (targeting *iscS1*), pDL244 (targeting *iscS2*), and pDL245 (targeting *iscS3*). These constructs did not need to be able to replicate in *M. acetivorans*, and the plasmid is designed for site-specific integration into the chromosome via the λ integrase system. All three plasmids (approximately 5 µg each) were transfected into *M. acetivorans* WWM73 cells by the same protocol described previously. Puromycin-resistant colonies were selected from HS agar and inoculated to liquid HS medium. PCR amplification with primers specific to the gBlock-

derived region was performed, with template provided by genomic DNA isolated from these cultures. Sequencing of these PCR products confirmed that the *isc1* and *isc2* dCas9 knockdown strains (*isc1*-KD and *isc2*-KD) were correct, but the strains generated to knock down expression of *isc3* all had an insertion mutation in the sgRNA sequence (not present in plasmid pDL245, which was confirmed by sequencing) that likely prevent this construct from recognizing and repressing *iscS3*. The *isc1*-KD and *isc2*-KD strains were saved and designated DJL91 and DJL92, respectively. Work to obtain the correct *isc3*-KD mutant is ongoing.

Acetylene reduction assays. Cell-free lysates, or purified proteins provided by colleagues, were assayed in a method broadly similar to the traditional acetylene reduction experiment (Dilworth, 2004). Sodium dithionite (dissolved in 13 mM sodium hydroxide) was added to all cell lysates to a concentration of 2 mM. The assay buffer was 50 mM HEPES pH 8.0, with 20 mM sodium dithionite, 5 mM ATP, 5 mM $MgCl_2$, 25 mM creatine phosphate (or phosphocreatine), 0.2 mg/mL creatine kinase (or creatine phosphokinase), and lysate at total quantities ranging from 0.24 mg to 1.34 mg soluble protein. A master mix of all components except lysate was aliquoted to 2 mL serum vials, leaving just enough room for the later lysate addition to bring the total volumes to 500 µL. Lysates were transferred to similar vials. All vials were stoppered with red rubber septa and crimped with 13 mm aluminum seals inside the anaerobic chamber. Reaction vials were purged for 2 minutes each with ultra-high purity argon passing through a tube attached to an oxygen scrubber (Restek #20601) and ending in a 22G needle. Lysates were purged similarly, but for 5 minutes on ice. All were then cycled into the anaerobic chamber without vacuum cycles. Acetylene (atomic absorption grade, Airgas, Inc.) was purged into a sealed, argon-purged serum bottle sealed with a butyl rubber stopper and capped with a 20 mm aluminum crimp that was brought into the anaerobic chamber. A gas-tight Hamilton syringe was

purged with argon and acetylene, then used to transfer 200 µL into the headspace of each reaction vial. Reactions were started by adding the appropriate volume of protein using an argon-purged Hamilton syringe, and incubated in a heating block at 30 °C until termination by adding trichloroacetic acid to a final concentration of 6% w/v. Ethylene production was measured by gas chromatography using a Shimadzu GC-2030 gas chromatograph running ultrahigh purity helium as a carrier gas, with a Varian CP-PoraPLOT Q column installed (27.5 m, 0.32 mm, 10 µm) and a Barrier Ionization Detector (BID-2030) attached. A headspace sample of 50 µL was injected into the port with an inlet pressure of 132.4 kPa, linear velocity at a constant 59.0 cm/s, purge flow 3.0 mL/min, and a split ratio of 10.0. The runs were isocratic, with the column set to a constant 27 °C, and a runtime of 6 minutes. Ethylene was quantified by comparison to a standard curve prepared from dilutions of pure ethylene (Airgas, Inc.).

Resting cell assays. Cultures of *M. acetivorans* were grown to mid-logarithmic phase, anaerobically harvested at an optical density at 600 nm of 0.3 - 0.7, pelleted, then resuspended in fresh DTT-reduced, NH_4Cl-free HS medium to a normalized OD_{600} of 2.0. Aliquots of 1 mL normalized resuspensions were transferred to 2 mL serum vials, which were stoppered and crimped in an anaerobic chamber with an atmosphere of 75% nitrogen, 20% carbon dioxide, and 5% hydrogen. Methanol was added to 125 mM, along with cysteine or sulfide to some vials, acetylene was added to 0.3% using a Hamilton syringe, and the vials were incubated at 35 °C, with 50 µL headspace samples being periodically run on the gas chromatograph as described above.

Hydrogenase assays. Reaction mixtures were made up in 50 mM Tris pH 8.0, with 20 mM methyl viologen and 0.1 mM DTT. A master mix for the reactions, excluding enough volume for lysate to bring final volumes up to 250 µL, was made up and aliquoted into Micro-UV cuvettes

(BrandTech Scientific, Inc.). Cell-free lysates were pre-reacted to ensure hydrogenases were in the reduced, active state by ambient incubation for 5 minutes with 1 mM DTT while exposed to the anaerobic chamber atmosphere of 5% hydrogen. These were then transferred to 2 mL serum vials, stoppered, crimped, and purged for 3 minutes with 100% nitrogen from a dedicated line in the anaerobic chamber showing a resting pressure of 10 pounds per square inch. Red rubber sleeve stoppers were wrapped in PTFE tape and used to close the cuvettes containing the master mix aliquots. These were also purged with 100% nitrogen for 3 minutes, using a hemostat to maintain pressure on the stoppers to keep them from rising out of the cuvettes. Cuvette headspaces received either 1 mL 100% N_2 or 1 mL 100% H_2 using appropriately purged syringes, and the cuvettes were briefly shaken to evenly distribute the inject gas. Reactions were initiated by addition of cell-free lysates using purged glass syringes, and the absorbance at 578 nm was continuously monitored by a Cary 60 spectrophotometer. Specific activity was calculated as nmol methyl viologen reduced per minute per mg protein, using an extinction coefficient at 578 nm of 9.78 x 10^3 M^{-1} cm^{-1}.

Identification of hydrogenases in fully sequenced Methanosarcinales. The order Methanosarcinales was surveyed to ascertain the distribution of putative Ech, Frh, Vho/Vht, and Vhx type hydrogenases in fully sequenced genomes. The *M. barkeri str. Fusaro* EchA protein sequence (WP_011305192.1) was used in a BLASTP search of order Methanosarcinales sequences in the non-redundant NCBI database. The *M. barkeri str. Fusaro* FrhA sequence (WP_011305486.1), the *Methanosarcina Mazei Go1* VhoA sequence (WP_011034101.1), and the *Methanosarcina Mazei Go1* VhxA sequence (WP_011034107.1) were also used in BLASTP searches in the exact same conditions. The returned sequences were screened, discarding all that did not come from a genome of either “Complete” or “Chromosome” assembly status in the

NCBI Genome Browser as of November 18, 2020, as well as duplicates and sequences from environmental samples and metagenomes. The cutoff for matches was an E-value of less than 1E-20. Any sequences that fell within the defined cutoff for more than one protein query sequence were assigned to the query sequence yielding the lowest E-value. Sequences that fell within the cutoff criteria but which show greater similarity to some protein other than the four hydrogenase types under investigation, e.g. a membrane-bound Na^+/H^+ antiporter, were flagged. A spreadsheet containing results from all four searches is attached as **Appendix 1**.

Results

CRISPRi indicates Isc1 and Isc2 are likely not essential. In growth studies with cysteine or sulfide as the sulfur source in standard HS media, strains DJL91 and DJL92 exhibit no obvious growth phenotype (**Figure 4**). This suggests that these gene clusters are likely not essential, which in the latter case is in good agreement with the lack of general growth phenotype previously demonstrated for DJL60, the Δ*isc2* strain. That the attempted Isc3 CRISPRi strain generated a mutation in the sgRNA sequence could be indicative of selective pressure against this knockdown strain, since sequencing confirmed that the plasmid transformed into WWM73 was carrying the correct plasmid.

Strain DJL60 grows poorly without fixed nitrogen when cysteine is the sulfur source. *M. acetivorans* is known to be able to fix nitrogen with a typical molybdenum-binding nitrogenase (Dhamad & Lessner, 2020). Strains WWM73 and DJL60 grew significantly differently in the absence of ammonium chloride, but only when cysteine was the sulfur source (**Figure 5**). Even strain WWM73 grew significantly worse on cysteine in the absence of fixed nitrogen. This pattern may indicate a larger shift in Fe-S cluster trafficking during growth on different sulfur

sources when fixing nitrogen, or possibly that cysteine desulfurization becomes a metabolic bottleneck under these growth conditions.

Repression of the *isc2* genes also impairs diazotrophic growth. *M. acetivorans* strain DJL60 has had *iscS2* and *iscU2* deleted from its genome. Strain DJL92 has these genes repressed by the dCas9 system described in the previous chapter. Both exhibit no growth phenotype when growing nondiazotrophically, whether using cysteine or sulfide as a sulfur source (**Figure 6**). Both are deficient in growth without fixed nitrogen, but only when cysteine is the sulfur source (**Figure 7**). This phenotype is less severe in the knockdown strain, DJL92, than in the knockout strain, DJL60. These culture tubes also displayed greater variation between replicates within a given condition than did any of the cultures of the parent strain, WWM73, or the nondiazotrophic or sulfide-grown mutant tubes.

Excess hydrogen inhibits diazotrophic growth of *M. acetivorans*. When culture tubes of the parent strain WWM73 growing under N_2-fixing conditions had 10 mL of gas added to their headspace upon inoculation, cultures with extra hydrogen exhibited deficient growth as compared to those that received argon instead (**Figure 8**). Standard headspace contains 75% nitrogen, 20% carbon dioxide, and ~5% hydrogen, so adding 10 mL pure H_2 raises the hydrogen mole fraction in the headspace to around 40%. A 10 mL Ar addition gives a final hydrogen mole fraction of just ~3%, with argon constituting 37% of the gas fraction. For both sulfur sources, 3 mM cysteine and 1 mM sodium sulfide, elevated H_2 levels exhibited a clear negative effect in diazotrophic growth, whereas elevated hydrogen levels did not seem to affect the growth of a control cysteine culture that was supplemented with NH_4Cl to the standard concentration of 1 mg/mL.

Acetylene reduction activity in whole cells. Ethylene was produced by whole WWM73 cells resuspended in fresh NH_4-Cl-free HS medium with 125 mM methanol and acetylene added to the headspace to 0.3% (**Figure 9a**). This assay was only semi-quantitative, but useful for comparative purposes. Cysteine-grown cells not supplied with a sulfur source in the resuspension buffer failed to reduce any acetylene, while cells grown on sulfide or both cysteine and sulfide initially produced some ethylene but stopped after 4 hours. Sulfide-grown cells that were supplied with either cysteine or sulfide in the resuspension medium continued to produce additional ethylene all the way out to 20 hours. One potential confounding factor is methanogenesis, which is required to generate ATP consumed by the nitrogenase complex during catalysis. Methane production (**Figure 9b**) closely mirrored ethylene production for most cultures, indicating that the undetectable acetylene reduction observed in the cysteine-only samples may reflect some failure to restart methanogenesis rather than genuinely lower nitrogenase activity. The highest rate of methane production was observed in a control sample with no acetylene in the headspace, consistent with acetylene's reported inhibition of methanogenesis. Along with the difficulty in synchronizing logarithmic growth in diazotrophic cultures to generate the cells to be normalized by resuspension, these drawbacks favor *in vitro* measurements of cell-free lysate activity in *M. acetivorans*.

Sulfur source exerts a modest influence on bulk nitrogenase activity in *M. acetivorans*. Cell-free lysates of diazotrophically grown strain WWM73 were assayed for acetylene reduction activity, and specific activities were calculated separately for cells grown with 3 mM cysteine and with 1 mM sodium sulfide (**Table 2**). There was a modest difference between the two results, with cysteine-grown WWM73 exhibiting a specific activity of 0.41 nmol * min^{-1} * mg^{-1} soluble protein, compared to 1.06 for sulfide-grown cells. Both values were far lower than the

specific activity for *A. vinelandii* DJ cell-free lysate included in the same assay, found to be 14.23. This is in fairly good agreement with reported values from previous publications, where *A. vinelandii* extracts have exhibited acetylene reduction activities in the range of 45 to 91 nmol*min^{-1}*mg^{-1} protein when grown in a chemostat (Klugkist *et al*., 1985). Presumably the nitrogenase complex of *M. acetivorans* may share some of the limitations previously identified in *M. barkeri*, some combination of high lability and a lower intrinsic activity with acetylene as a substrate, relative to activity in reducing dinitrogen (Lobo & Zinder, 1990).

Purified NifDK activity. *M. acetivorans* NifDK complex was purified to homogeneity directly from *M. acetivorans* using a Strep tag by a laboratory colleague, Dr. Ahmed Dhamad, and graciously provided for activity assays. *M. acetivorans* NifH was heterologously expressed with a His_6 tag in *E. coli* and isolated to high purity by another colleague, Dr. Carly Engel, and generously provided for activity assays. SDS-PAGE imaging confirmed the high purity of both components (**Figure 10**). The calculated specific activity for MaNifHDK, 50.7 nmol*min^{-1}*mg^{-1} (**Table 2**), is considerably higher than a figure previously reported for *M. barkeri* NifDK, 8.6 nmol * min^{-1} * mg^{-1} (Lobo & Zinder, 1990). Both these reported activities pale in comparison with the 1,638 nmol * min^{-1} * mg^{-1} exhibited by *A. vinelandii* (Shah & Brill, 1973).

Hydrogenase activity in *M. acetivorans*. Assays measuring hydrogenase activity by monitoring reduction of the dye methyl viologen reveal very modest activity regardless of growth conditions in *M. acetivorans* compared to *M. barkeri* (**Figure 11**). When growing with a fixed nitrogen source, *M. acetivorans* WWM73 exhibited higher hydrogenase activity on cysteine (263 ± 20) rather than sulfide (61 ± 5) as the sulfur source. When growing diazotrophically, this pattern reversed, with cysteine (142 ± 16) showing lower activity than sulfide (233 ± 8). Diazotrophic *M. barkeri* cells displayed a specific activity of 3,784 ± 84. These results are consistent with

published work showing much higher hydrogenase expression in the freshwater *Methanosarcina* species (*M. barkeri, M. mazei*) than in the marine *Methanosarcina*, as well as genes for the energy-converting hydrogenase EchA being entirely absent from the genome of *M. acetivorans*.

Discussion

Both nitrogenase and hydrogenase complexes implicate numerous Fe-S proteins either in the subunits themselves or in their biosynthesis, maturation, and catalysis. There is intense interest in the prospect of genes for nitrogen fixation, naturally found only among bacteria and archaea, being heterologously expressed in agricultural plants, alleviating the need for nitrogen-based fertilizers. Attempts to achieve this goal have proven unsuccessful, despite the expression of as many as 16 bacterial nitrogenase genes in plant tissues (Allen *et al*., 2017). The more minimal *nif* gene clusters found in methanogens, along with the lack of dedicated NifS/NifU machinery in archaeal diazotrophs, might indicate an Fe-S protein-utilizing nitrogenase system better suited to the toolkit available to eukaryotes. Plants generally possess both ISC and SUF systems for [Fe-S] biogenesis, located in the mitochondria and chloroplasts, respectively (Schwenkert *et al*., 2009). Though there are important differences, this pattern broadly reflects the putative Fe-S cluster biosynthetic machinery in *M. acetivorans* and closely related methanogens. A deeper understanding of nitrogenase and the cellular machinery required to generate it in this model organism might open the door to expression of functional nitrogenase in plant cells.

The *isc2* gene cluster appears to be involved in diazotrophic growth, especially with cysteine, which mirrors the canonical ISC systems described in bacteria and eukaryotes. This supports our model of Fe-S cluster assembly for nitrogenase in *M. acetivorans* (**Figure 3**). Exactly how disrupting *isc2* inhibits diazotrophic growth is not clear from the results generated

thus far. The results from knocking down the *isc2* genes in strain DJL92 (**Figures 6, 7**) are consistent with strong repression from the CRISPR/dCas9 system that nevertheless is allowing some amount of mRNA transcript to be produced, presumably leading to low levels of IscS2 and IscU2 production rather than outright elimination from the translated proteome. This is reflected in phenotypes that are similar to those observed in the *isc2* deletion strain DJL60, but less severe. Importantly, there are two gene products missing in the mutant DJL60, and whether the diazotrophic phenotype observed is a result of missing *iscS2*, *iscU2*, or both cannot be directly determined with the strains currently in hand. The sulfur specificity of the phenotype does offer some clues, given that we know from the results discussed in Chapter I that DJL60 has no bulk defect in [Fe-S] biogenesis. Markerless mutations allow for complementation *in trans* using plasmids, so if the *pac-hpt* cassette can be eliminated, a derivative or analog of DJL60 could be combinatorically provided with *iscS2*, *iscU2*, and *iscS2U2* to determine what specific component is responsible for the cysteine-specific diazotrophic growth defect. Whatever the outcome of such a future study, the model presented in **Figure 3** predicts that an ISC system is responsible for nitrogenase maturation when cysteine is the sulfur source. A similar experiment studying nitrogen fixation in a SUF mutant might be expected to show difficulty growing on sulfide.

Whether the nitrogenase complex itself is somehow less active in DJL60 can potentially be determined using the *in vitro* lysate acetylene reduction assay, but there is considerable difficulty involved in generating enough cell material under the relevant growth conditions; strain DJL60 grows to quite a low final OD_{600} on cysteine, and the range of absorbances associated with mid-exponential growth is correspondingly narrow. Nevertheless, developing a working protocol for acetylene reduction assays required a great deal of trial and error, and devising a successful approach allows us to test the activity of a complex [Fe-S] reliant process

that is entirely conditional on growing without fixed nitrogen. Mutations that disrupt nitrogenase maturation and function but not methanogenesis or other central metabolic pathways can be made and then tested under relevant growth conditions.

Hydrogen inhibits growth of *M. acetivorans* specifically when fixed nitrogen is absent from the media, but not when ammonium chloride is present. There are two possible explanations for this effect, not necessarily mutually exclusive. First, it is well documented that hydrogen can exert an inhibitory pressure on the nitrogenase complex itself (Harris *et al*., 2018[a]). The NifDK complex evolves hydrogen at the active site FeMoCo in the late stages of its mechanism, and elevated hydrogen levels are believed to exert a back pressure through mass action that inhibits activity. A second, less defined possibility exists wherein elevated levels of hydrogen inhibit some other enzyme activity necessary for optimal nitrogenase function. This is harder to articulate a case for, since aside from its direct effect upon nitrogenase hydrogen generally has effects via uptake hydrogenase(s) that would be considered salutary, such as generating reducing equivalents through electron carriers such as ferredoxins and also contributing to the membrane proton gradient used for ATP generation in diazotrophic microbes (Vignais & Billoud, 2007). Still, given the lacunae in our understanding of hydrogenase expression and importance in *M. acetivorans* we should not dismiss a more circuitous mechanism of hydrogen inhibition in diazotrophic growth out of hand.

The rationale for maintaining membrane-bound hydrogenases in a methanogen incapable of hydrogenotrophic carbon dioxide reduction has been a puzzle for some time (Guss *et al*., 2009). The obligate generation of hydrogen by nitrogenases, along with the potential for hydrogen inhibition of the catalytic NifDK subunits, offers a potential explanation. Our lysate hydrogenase results support a modest activation of hydrogenase expression during diazotrophic

growth, but only when inorganic sulfide is the sulfur source. With cysteine as the sulfur source, hydrogenase expression actually seems to fall when switching from growth with fixed nitrogen to diazotrophic growth. What mechanism drives this counterintuitive result remains unclear, but the overall level of activity under all conditions is roughly two orders of magnitude lower than in non-diazotrophically grown *M. barkeri*, which unlike *M. acetivorans* encodes and expresses an Ech hydrogenase (Guss *et al*., 2009).

The distribution of the Ech, Frh, Vho/t, and Vhx-type hydrogenases in the order Methanosarcinales appears extremely uneven (**Appendix 1**). The typical membrane-bound energy-converting Ech hydrogenase seems confined to the genus *Methanosarcina*, though several species including *M. acetivorans* C2A (the type strain), *M. horonobensis*, and *M. siciliae* are not predicted to code for it. The cytoplasmic Frh hydrogenases, is predicted to be present in most members of genus *Methanosarcina*, including *M. acetivorans* C2A, though in a few species including *M. lacustris* it is not. Outside the genus, no other members of the order appear to possess an *frhA* gene. At least one and often two putative membrane-bound VhoA/VhtA homologs are encoded by every member of genus *Methanosarcina*, but only two other members of order Methanosarcinales, *Methanococcoides methylutens* and *Methanosalsum zhilinae*, appear to possess them, with one copy in each. The closely related Vhx hydrogenases turned up only within the genus *Methanosarcina*, including *M. acetivorans* C2A, though six species lack a putative VhxA. Interestingly, all six are predicted to encode at least two VhoA/VhtA homologs. Put another way, every member of the genus *Methanosarcina* encodes between 2 and 3 putative homologs of the methanophenazine-reducing hydrogenases.

The evidence laid out in this chapter supports a conclusion that the [Fe-S] biogenesis machinery in *Methanosarcina acetivorans*, in particular the *isc2* gene cluster and its

products, is tied in to nitrogenase function. There is sulfur specificity in these effects, and it is unclear at this time whether the mechanism responsible implicates Fe-S cluster building, or whether perhaps the lost cysteine desulfurase activity of IscS2 described in Chapter I might be the cause. The CRISPRi tools developed in our lab (Dhamad & Lessner, 2020) have been applied to the study of Fe-S biogenesis in *M. acetivorans*, with the results for Isc2-KD in good agreement with previous observations for Isc2 deletion (**Figures 6-7**). In addition, knockdown of Isc1 seems to have no general growth phenotype. Future directions of research for these individual strains include qPCR measurement of the extent of gene repression and generation of the correct Isc3-KD strain. Alternatively, if transformations with the Isc3 knockdown plasmid pDL245 continue to exhibit mutations in the sgRNA sequence, this might reflect selective pressure and indicate an important role for the products of *iscS3U3*. Additionally, my colleague, PhD student Jalseen Saini, has begun combining the CRISPR/Cas9 and CRISPRi systems, transforming plasmids prepared for the latter system into cells already mutated by the former to knock down genes in a background of another gene having been knocked out. Ms. Saini has generated several multiple mutants using the strains and plasmids described in this chapter and Chapter II. The markerless Suf2 deletion mutant DJL63, having been cured of the plasmid pDL250 by Ms. Saini via counterselection with 8ADP, has been transfected multiple times using our standard protocol. WWM73-derived strains with genotypes including Δ*suf2 isc1*-KD, Δ*suf2 isc2*-KD, and Δ*suf2 isc3*-KD have been generated, as well as *suf2*-KD and Δ*suf2 suf1*-KD strains for which Ms. Saini created the plasmids. None of these *M. acetivorans* strains has exhibited an obvious growth phenotype under standard conditions, casting further doubt on the hypothesis that any one of these gene clusters is uniquely important in providing [Fe-S] to essential proteins (data not shown).

Hydrogen appears to exert an important effect on this methanogen specifically when it is growing diazotrophically, notwithstanding that it is incapable of consuming hydrogen for ordinary growth in the CO_2-reduction pathway of methanogenesis, and that its membrane-bound hydrogenases are ordinarily not expressed at appreciable levels. Herein we have established protocols for measuring nitrogenase and hydrogenase activity in *M. acetivorans* cell-free lysate, as well as the ability to measure the activity of purified MaNifHDK protein complexes. These will serve as an important resource for researchers studying Fe-S cluster biogenesis and nitrogen fixation in *M. acetivorans*.

References

Allen, R.S., K. Tilbrook, A.C. Warden, P.C. Campbell, V. Rolland, S.P. Singh, & C.C. Wood, (2017) Expression of 16 Nitrogenase Proteins within the Plant Mitochondrial Matrix. *Front Plant Sci*. 8: 287.

Baron, S.F. & J.G. Ferry, (1989) Purification and properties of the membrane-associated coenzyme F420-reducing hydrogenase from Methanobacterium formicicum. *J Bacteriol*. 171: 3846-53.

Bradford, M.M., (1976) A rapid and sensitive method for the quantitation of microgram quantities of protein utilizing the principle of protein-dye binding. *Anal. Biochem.* 72: 248-254.

Brito, B., M. Martínez, D. Fernández, L. Rey, E. Cabrera, J.M. Palacios, J. Imperial, & T. Ruiz-Argüeso, (1997) Hydrogenase genes from Rhizobium leguminosarum bv. viciae are controlled by the nitrogen fixation regulatory protein nifA. *Proc Natl Acad Sci U S A*. 94: 6019-24.

Dean, D.R., J.T. Bolin, & L. Zheng, (1993) Nitrogenase metalloclusters: structures, organization, and synthesis. *J Bacteriol*. 175: 6737-44.

Deere, T.M., D. Prakash, F.H. Lessner, E.C. Duin, & D.J. Lessner, (2020) Methanosarcina acetivorans contains a functional ISC system for iron-sulfur cluster biogenesis. *BMC Microbiol*. 20: 323.

Deppenmeier, U., M. Blaut, S. Lentes, C. Herzberg, & G. Gottschalk, (1995) Analysis of the vhoGAC and vhtGAC operons from Methanosarcina mazei strain Gö1, both encoding a membrane-bound hydrogenase and a cytochrome b. *Eur J Biochem*. 227: 261-9.

Devi, V.G., A. Sircar, D. Yadav, & J. Parmar, (2018) Analysis of trace levels of impurities and hydrogen isotopes in helium purge gas using gas chromatography for tritium extraction system of an Indian lead lithium ceramic breeder test blanket module. *J Sep Sci*. 41: 1798-1804.

Dhamad, A.E. & D.J. Lessner, (2020) A CRISPRi-dCas9 System for Archaea and Its Use To Examine Gene Function during Nitrogen Fixation by Methanosarcina acetivorans. *Appl Environ Microbiol* 86: e01402-20.

Dilworth, M.J., (2004) Assay Methods for Products of Nitrogenase Action on Substrates. *Catalysts for Nitrogen Fixation*. 55-76.

Dilworth, M.J. & K. Fisher, (1998) Elimination of creatine interference with the indophenol measurement of NH3 produced during nitrogenase assays. *Anal Biochem*. 256: 242-4.

Dilworth, M.J. & R.N. Thorneley, (1981) Nitrogenase of Klebsiella pneumoniae. Hydrazine is a product of azide reduction. *Biochem J*. 193: 971-83.

Dilworth, M.J., R.R. Eady, R.L. Robson, & R.W. Miller, (1987) Ethane formation from acetylene as a potential test for vanadium nitrogenase in vivo. *Nature*. 327: 167-168.

Dodsworth, J.A. & J.A. Leigh, (2006) Regulation of nitrogenase by 2-oxoglutarate-reversible, direct binding of a PII-like nitrogen sensor protein to dinitrogenase. *Proc Natl Acad Sci U S A*. 103: 9779-84.

Dos Santos, P.C., Z. Fang, S.W. Mason, J.C. Setubal, & R. Dixon, (2012) Distribution of nitrogen fixation and nitrogenase-like sequences amongst microbial genomes. *BMC Genomics*. 13: 162.

Eady, R.R., (1996) Structure-Function Relationships of Alternative Nitrogenases. *Chem Rev*. 96: 3013-3030.

Elsen, S., W. Dischert, A. Colbeau, & C.E. Bauer, (2000) Expression of uptake hydrogenase and molybdenum nitrogenase in Rhodobacter capsulatus is coregulated by the RegB-RegA two-component regulatory system. *J Bacteriol*. 182: 2831-7.

Fawcett, J.K. & J.E. Scott, (1960) A rapid and precise method for the determination of urea. *J Clin Pathol*. 13: 156-9.

Gitlitz, P.H. & A.I. Krasna, (1975) Structural and catalytic properties of hydrogenase from Chromatium. *Biochemistry*. 14: 2561-8.

Greening, C., F.H. Ahmed, A.E. Mohamed, B.M. Lee, G. Pandey, A.C. Warden, C. Scott, J.G. Oakeshott, M.C. Taylor, & C.J. Jackson, (2016) Physiology, Biochemistry, and Applications of F420- and Fo-Dependent Redox Reactions. *Microbiol Mol Biol Rev*. 80: 451-93.

Guss, A.M., B. Mukhopadhyay, J.K. Zhang, & W.W. Metcalf, (2005) Genetic analysis of mch mutants in two Methanosarcina species demonstrates multiple roles for the methanopterin-dependent C-1 oxidation/reduction pathway and differences in H(2) metabolism between closely related species. *Mol Microbiol*. 55: 1671-80.

Guss, A.M., G. Kulkarni, & W.W. Metcalf, (2009) Differences in hydrogenase gene expression between Methanosarcina acetivorans and Methanosarcina barkeri. *J Bacteriol*. 191: 2826-33.

Harris, D.F., D.A. Lukoyanov, S. Shaw, P. Compton, M. Tokmina-Lukaszewska, B. Bothner, N. Kelleher, D.R. Dean, B.M. Hoffman, & L.C. Seefeldt, (2018) Mechanism of N 2 Reduction Catalyzed by Fe-Nitrogenase Involves Reductive Elimination of H 2. *Biochemistry*. 57: 701-710.

Harris, D.F., Z.-Y. Yang, D.R. Dean, L.C. Seefeldt, & B.M. Hoffman, (2018) Kinetic Understanding of N 2 Reduction versus H 2 Evolution at the E 4(4H) Janus State in the Three Nitrogenases. *Biochemistry*. 57: 5706-5714.

Jimenez-Vicente, E., Z.-Y. Yang, W.K. Ray, C. Echavarri-Erasun, V.L. Cash, L.M. Rubio, L.C. Seefeldt, & D.R. Dean, (2018) Sequential and differential interaction of assembly factors during nitrogenase MoFe protein maturation. *J Biol Chem*. 293: 9812-9823.

Jinek, M., K. Chylinski, I. Fonfara, M. Hauer, J.A. Doudna, & E. Charpentier, (2012) A programmable dual-RNA-guided DNA endonuclease in adaptive bacterial immunity. *Science*. 337: 816-21.

Kessler, P.S., C. Blank, & J.A. Leigh, (1998) The nif gene operon of the methanogenic archaeon Methanococcus maripaludis. *J Bacteriol*. 180: 1504-11.

Klugkist, J., H. Haaker, H. Wassink, & C. Veeger, (1985) The catalytic activity of nitrogenase in intact Azotobacter vinelandii cells. *Eur J Biochem*. 146: 509-15.

Kulkarni, G., T.D. Mand, & W.W. Metcalf, (2018) Energy Conservation via Hydrogen Cycling in the Methanogenic Archaeon Methanosarcina barkeri. *mBio*. 9: e01256-18.

Liu, Y., L.L. Beer, & W.B. Whitman, (2012) Sulfur metabolism in archaea reveals novel processes. *Environ Microbiol.* 14: 2632-44.

Lobo, A.L. & S.H. Zinder, (1988) Diazotrophy and Nitrogenase Activity in the Archaebacterium Methanosarcina barkeri 227. *Appl Environ Microbiol*. 54: 1656-61.

Lobo, A.L. & S.H. Zinder, (1990) Nitrogenase in the archaebacterium Methanosarcina barkeri 227. *J Bacteriol*. 172: 6789-96.

Mand, T.D., G. Kulkarni, & W.W. Metcalf, (2018) Genetic, Biochemical, and Molecular Characterization of Methanosarcina barkeri Mutants Lacking Three Distinct Classes of Hydrogenase. *J Bacteriol*. 200: e00342-18.

Mand, T.D. & W.W. Metcalf, (2019) Energy Conservation and Hydrogenase Function in Methanogenic Archaea, in Particular the Genus Methanosarcina. *Microbiol Mol Biol Rev*. 83: e00020-19.

Navarro-Rodríguez, M., J.M. Buesa, & L.M. Rubio, (2019) Genetic and Biochemical Analysis of the Azotobacter vinelandii Molybdenum Storage Protein. *Front Microbiol*. 10: 579.

Nelson, M.J. & J.G. Ferry, (1984) Carbon monoxide-dependent methyl coenzyme M methylreductase in acetotrophic Methosarcina spp. *J Bacteriol*. 160: 526-32.

Peters, J.W., K. Fisher, & D.R. Dean, (1995) Nitrogenase structure and function: a biochemical-genetic perspective. *Annu Rev Microbiol.* 49: 335-66.

Pinske, C. & R.G. Sawers, (2012) Delivery of iron-sulfur clusters to the hydrogen-oxidizing [NiFe]-hydrogenases in Escherichia coli requires the A-type carrier proteins ErpA and IscA. *PLoS One*. 7: e31755.

Schwenkert, S., D.J.A. Netz, J. Frazzon, A.J. Pierik, E. Bill, J. Gross, R. Lill, & J. Meurer, (2009) Chloroplast HCF101 is a scaffold protein for [4Fe-4S] cluster assembly. *Biochem J*. 425: 207-14.

Shah, V.K. & W.J. Brill, (1973) Nitrogenase. IV. Simple method of purification to homogeneity of nitrogenase components from Azotobacter vinelandii. *Biochim Biophys Acta*. 305: 445-54.

Shah, V.K., L.C. Davis, & W.J. Brill, (1972) Nitrogenase. I. Repression and derepression of the iron-molybdenum and iron proteins of nitrogenase in Azotobacter vinelandii. *Biochim Biophys Acta*. 256: 498-511.

Sowers, K.R., S.F. Baron, & J.G. Ferry, (1984) Methanosarcina acetivorans sp. nov., an Acetotrophic Methane-Producing Bacterium Isolated from Marine Sediments. *Appl Environ Microbiol*. 47: 971-8.

Strandberg, G.W. & P.W. Wilson, (1968) Formation of the nitrogen-fixing enzyme system in Azotobacter vinelandii. *Can J Microbiol*. 14: 25-31.

Vignais, P.M. & B. Billoud, (2007) Occurrence, classification, and biological function of hydrogenases: an overview. *Chem Rev*. 107: 4206-72.

Yang, Z.-Y., D.R. Dean, & L.C. Seefeldt, (2011) Molybdenum nitrogenase catalyzes the reduction and coupling of CO to form hydrocarbons. *J Biol Chem*. 286: 19417-21.

Yu, L. & M.J. Wolin, (1969) Hydrogenase measurement with photochemically reduced methyl viologen. *J Bacteriol*. 98: 51-5.

Zhang, X., D.M. Sherman, & L.A. Sherman, (2014) The uptake hydrogenase in the unicellular diazotrophic cyanobacterium Cyanothece sp. strain PCC 7822 protects nitrogenase from oxygen toxicity. *J Bacteriol*. 196: 840-9.

Zheng, L. & D.R. Dean, (1994) Catalytic formation of a nitrogenase iron-sulfur cluster. *J Biol Chem*. 269: 18723-6.

APPENDIX

Figures and Tables

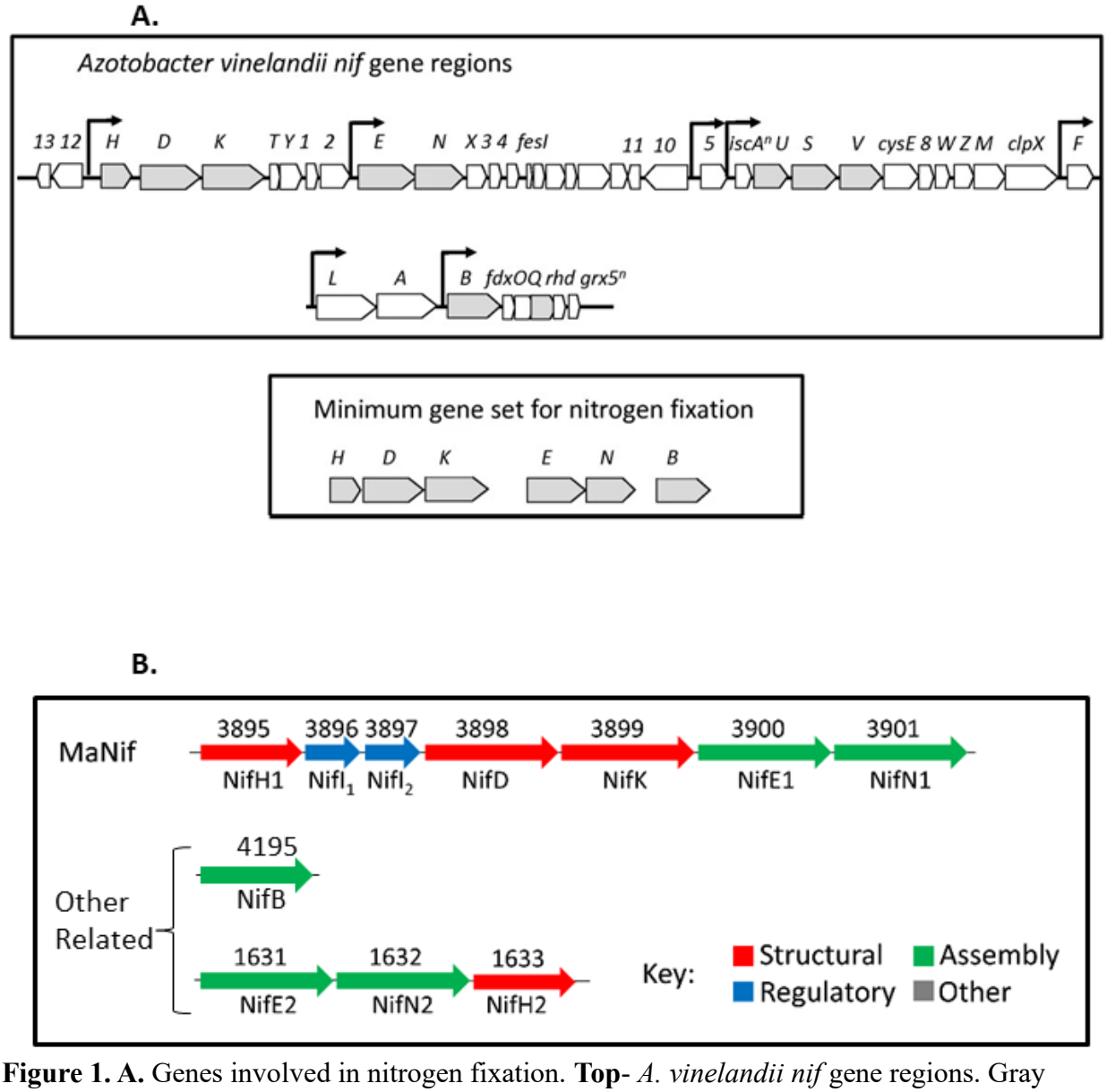

Figure 1. A. Genes involved in nitrogen fixation. **Top**- *A. vinelandii nif* gene regions. Gray arrows are essential genes in nitrogen fixation by Mo nitrogenase **Bottom**- A proposed minimum set of genes required for nitrogen fixation. Sequence homology searches of known diazotrophs confirm all contain at least the minimum gene set. Adapted from Dos Santos et al., *BMC Genomics* 2012.
B. The putative Nif gene cluster in *M. acetivorans* (MaNif) along with core components in other loci. Numbers above arrows (genes) are the locus tags and below is the predicted protein.

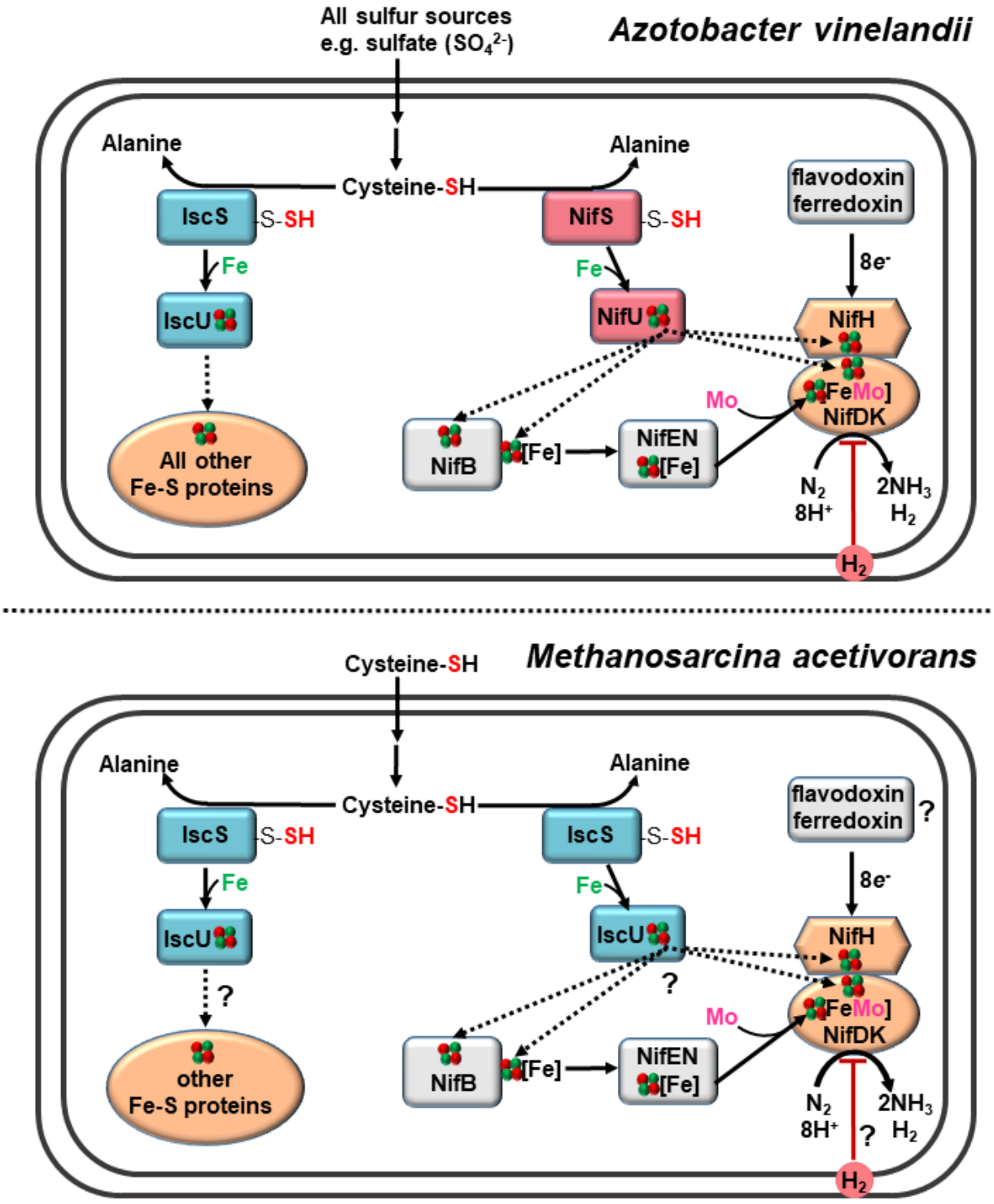

Figure 2. Models depicting the roles of IscSU and NifSU in assembling Fe-S clusters in apo-proteins in *A. vinelandii* (top) and the proposed role of IscSU in assembling Fe-S clusters in apo-proteins in *M. acetivorans* (bottom). Fe-S clusters are represented as indicated. NifH & NifDK are shown non-stoichiometrically as part of the nitrogenase complex, while NifB, NifE, and NifN are shown assembling FeMoCo and delivering it to NifDK.

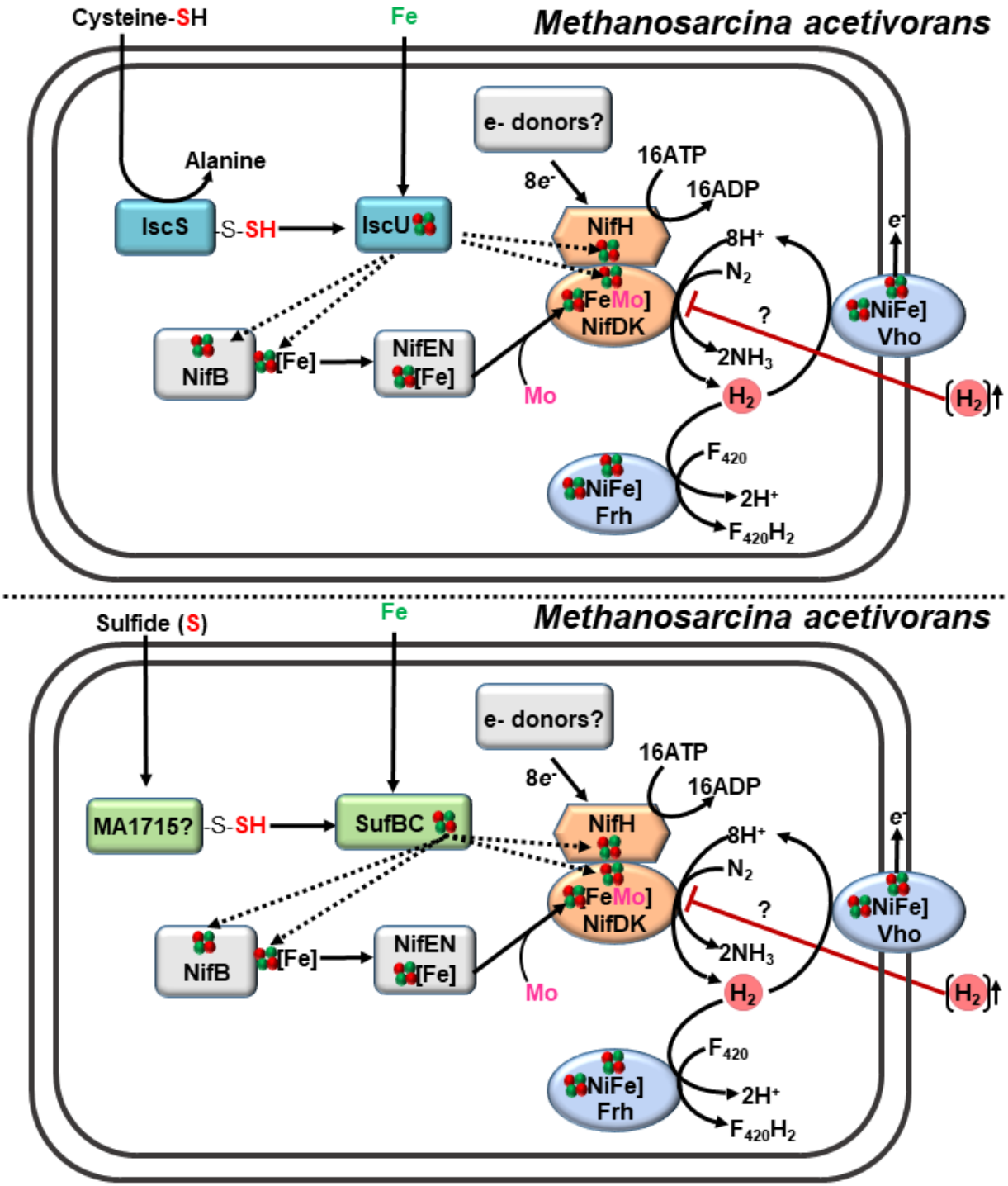

Figure 3. Models depicting the proposed roles in *Methanosarcina acetivorans* of the ISC and SUF systems in assembling Fe-S clusters in nitrogenase proteins. ISC is proposed to be responsible for [Fe-S] biogenesis during growth with cysteine as the sulfur source (top), while SUF is proposed to be responsible for [Fe-S] biogenesis during growth with inorganic sulfide as the sulfur source (bottom). The extent of hydrogen inhibition and its alleviation by the hydrogenases Frh and Vho is unknown.

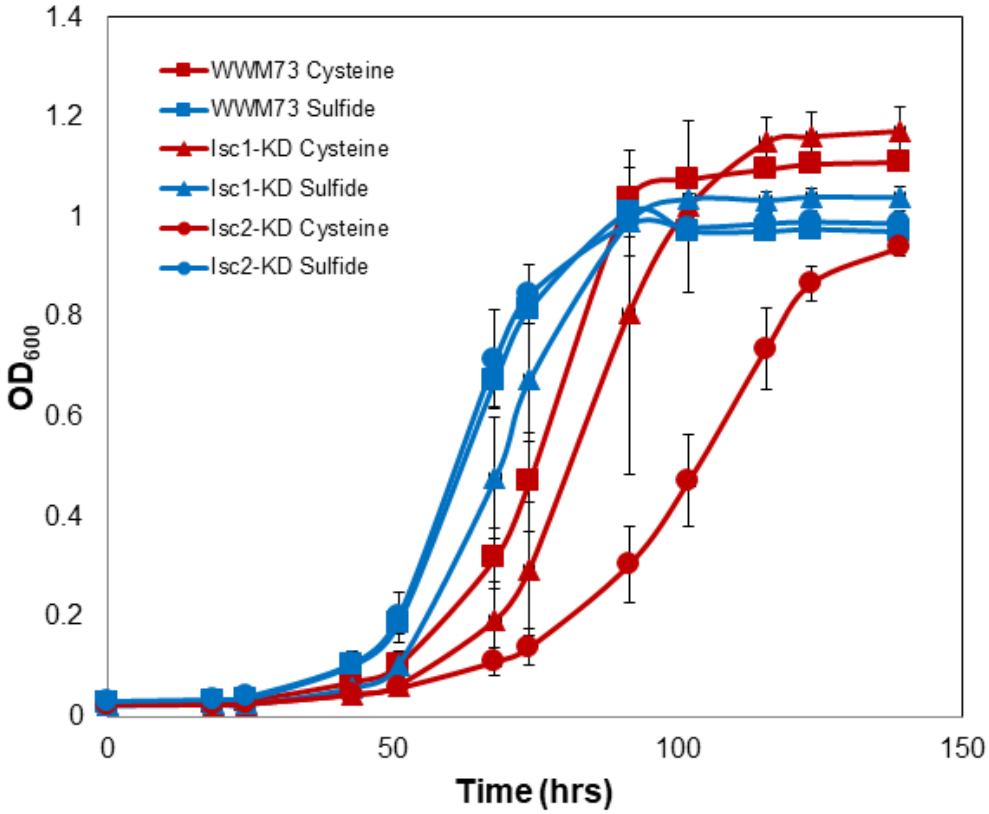

Figure 4. Strains WWM73, DJL91 (Isc1-KD), and DJL92 (Isc2-KD) growing on different sulfur sources. WWM73 (squares), DJL91 (triangles), and DJL92 (circles) were grown in DTT-reduced HS medium on 125 mM methanol with 3 mM cysteine (red) or 1 mM sodium sulfide (blue). Data plotted are the mean ± SD of three replicates.

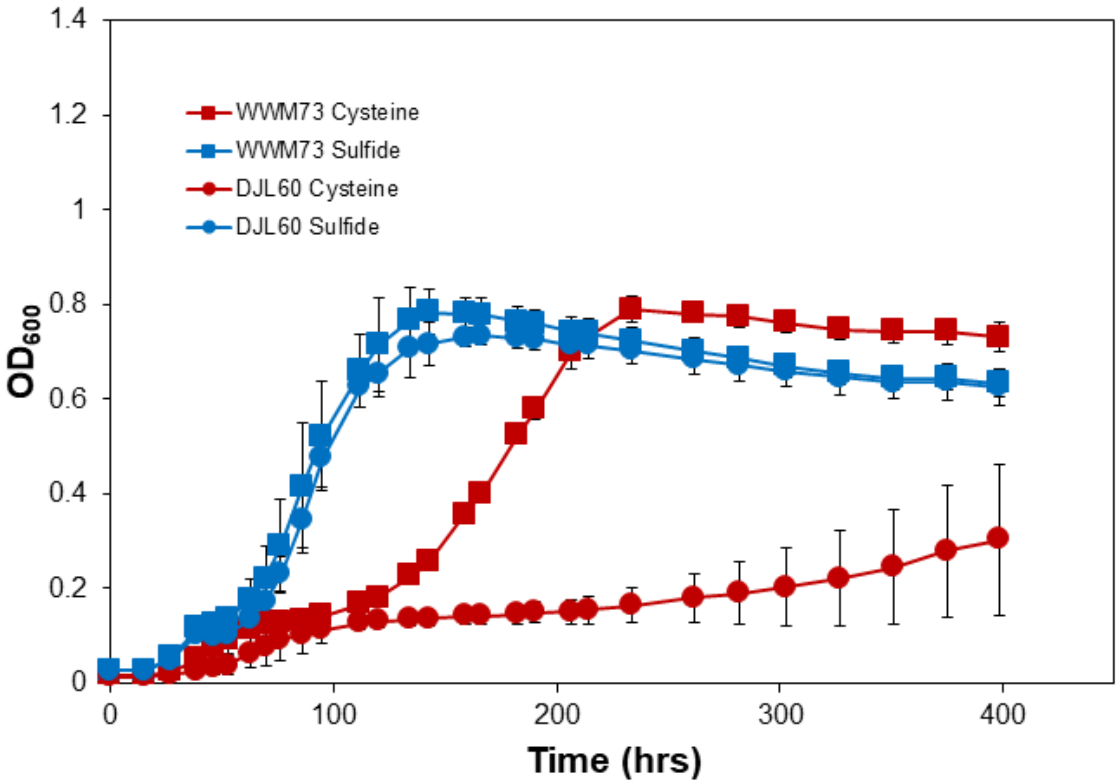

Figure 5. Strains WWM73 (wt) and DJL60 (Δ*isc2*) growing without fixed nitrogen. WWM73 (squares) and DJL60 (circles) were grown in DTT-reduced HS medium without NH_4Cl on 125 mM methanol with 3 mM cysteine (red) or 1 mM sodium sulfide (blue). Data plotted are the mean ± SD of three replicates.

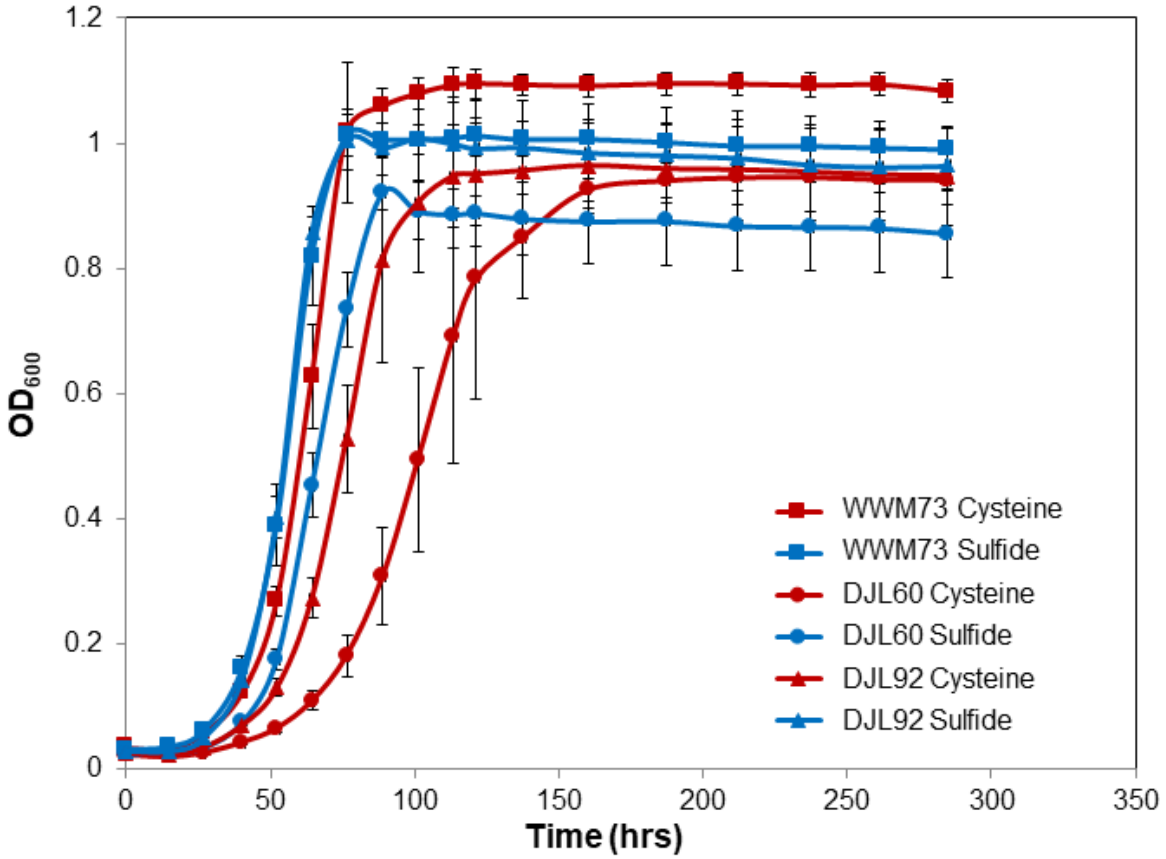

Figure 6. *Methanosarcina acetivorans* parent and mutant strains growing non-diazotrophically in different sulfur conditions. WWM73 (wt, squares), DJL60 (Δ*isc2*, circles), and DJL92 (*isc2*-KD, triangles) growing in DTT-reduced HS medium on 125 mM methanol. Sulfur conditions are 3 mM cysteine (red) or 1 mM sulfide (blue). OD at 600 nm is mean ± SD.

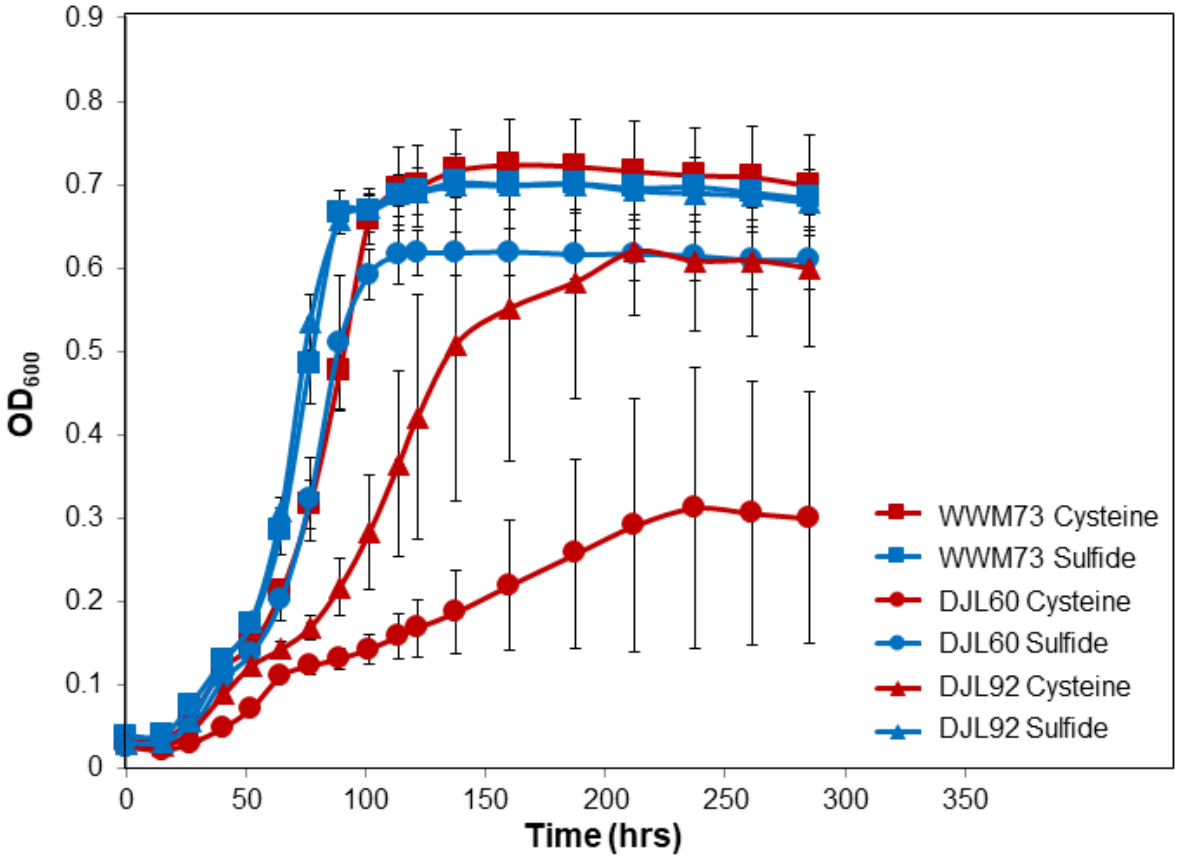

Figure 7. *Methanosarcina acetivorans* parent and mutant strains growing diazotrophically in different sulfur conditions. WWM73 (wt, squares), DJL60 (Δ*isc2*, circles), and DJL92 (*isc2*-KD, triangles) growing in NH_4Cl-free DTT-reduced HS medium on 125 mM methanol. Sulfur conditions are 3 mM cysteine (red) or 1 mM sulfide (blue). OD at 600 nm is mean ± SD.

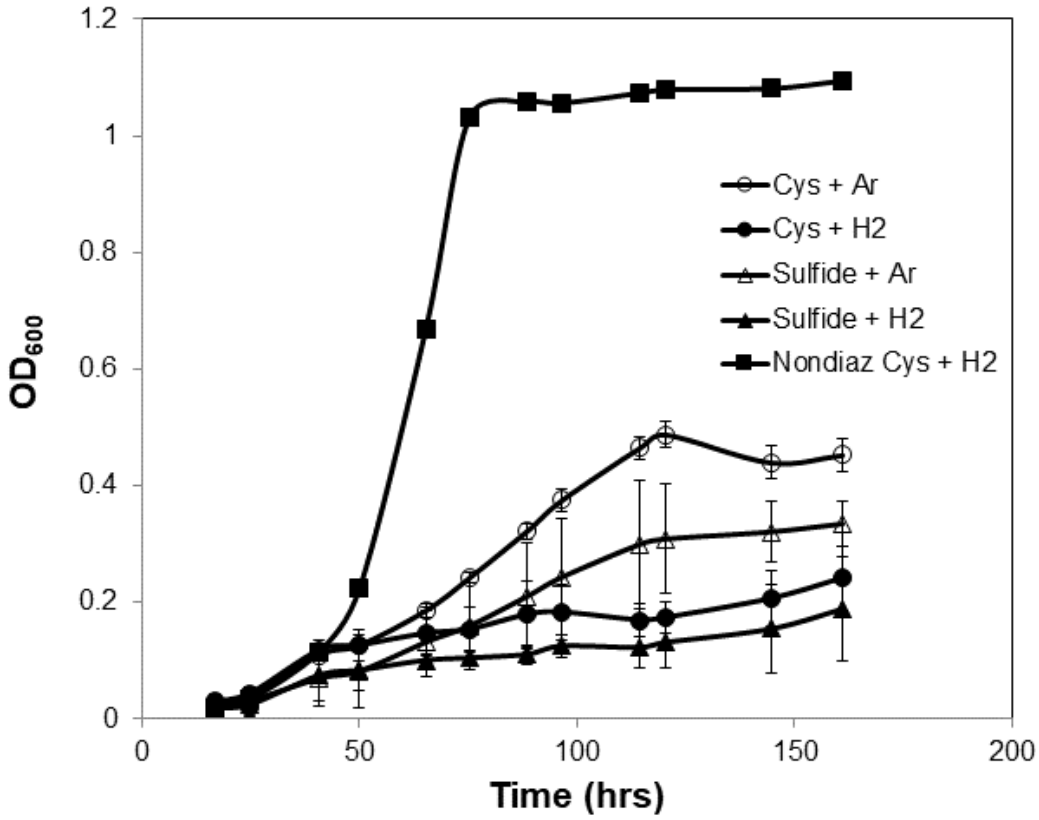

Figure 8. *Methanosarcina acetivorans* WWM73 grown in NH_4Cl-free DTT-reduced HS medium on 125 mM methanol with 3 mM cysteine (circles) or 1 mM sodium sulfide (triangles). Cultures received either 10 mL H_2 (solid) or 10 mL Ar (hollow). One control culture of cysteine-grown, H_2-added, NH_4Cl-supplemented WWM73 (solid squares) was included.

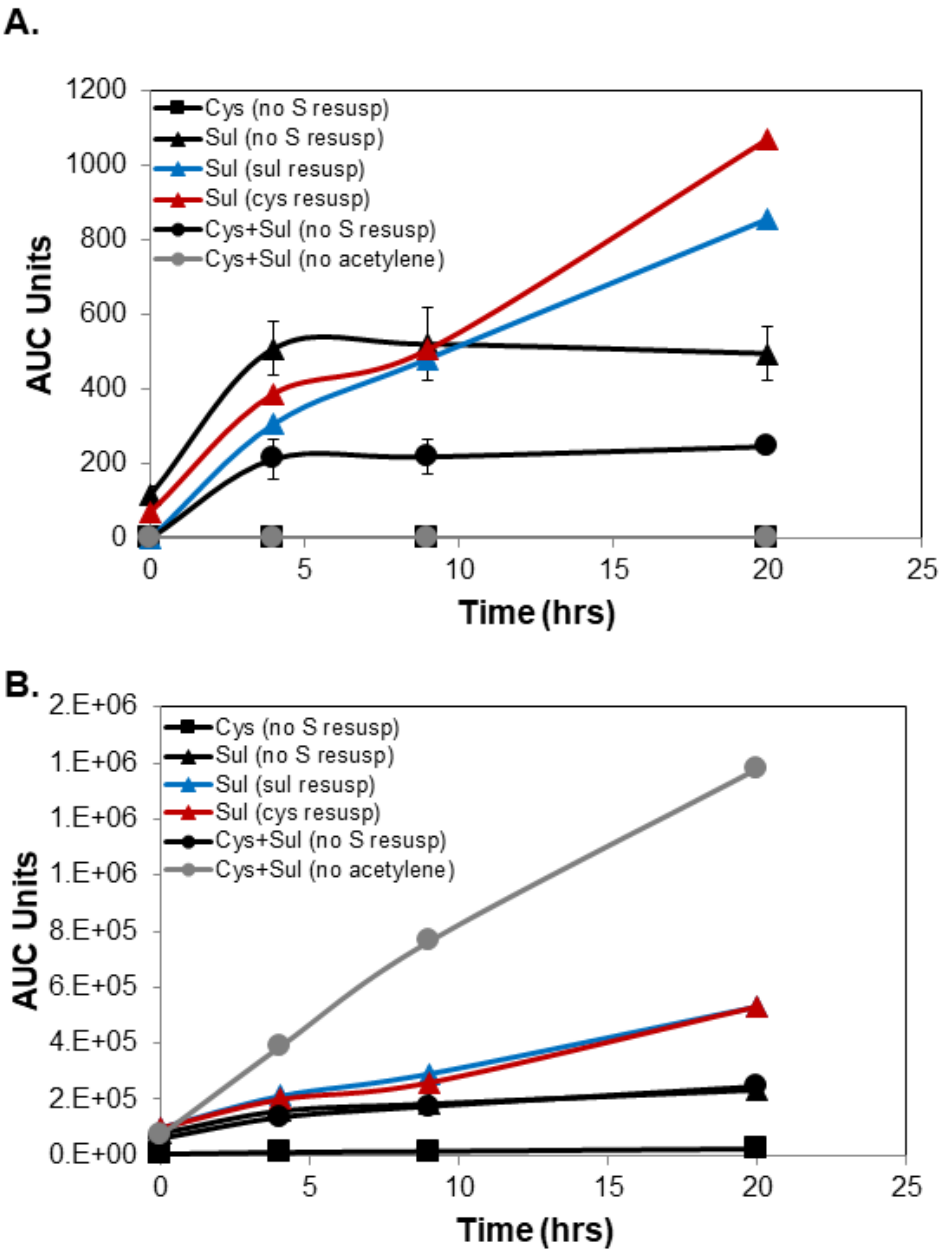

Figure 9. A. Ethylene produced by diazotrophic *M. acetivorans* growing with acetylene present. Cysteine-grown cells (squares), sulfide-grown cells (triangles), and cells grown on cysteine and sulfide (circles) are plotted over time with dimensionless units of ethylene detected by gas chromatography. Cells were resuspended with no sulfur (black), sulfide (blue), or cysteine (red) added to the resuspension buffer. A no-acetylene control reaction of cysteine + sulfide cells (gray) is also shown. **B.** Methane evolved over time with dimensionless units from same samples plotted above. Column was replaced on GC before standards could be run.

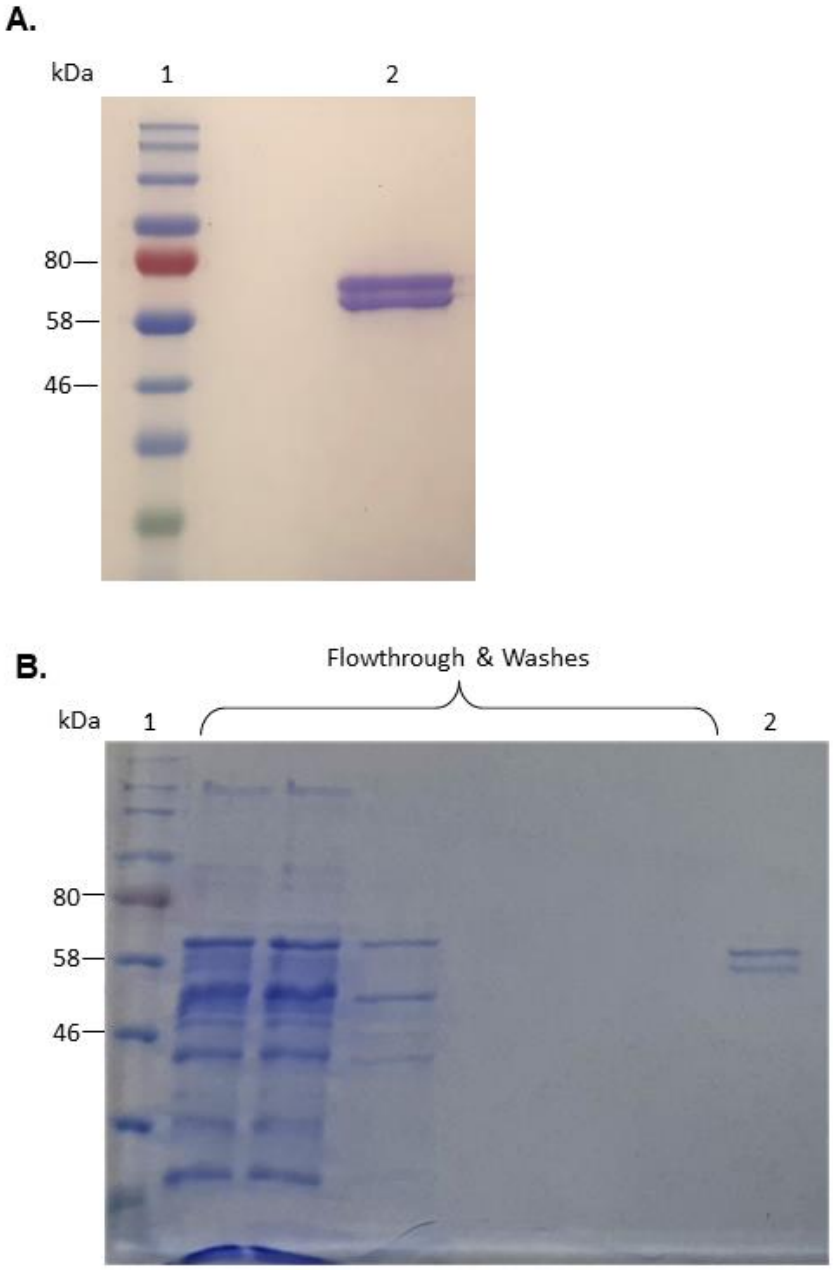

Figure 10. SDS-PAGE images of *M. acetivorans* Nif proteins purified in our laboratory. **A.** SDS-PAGE of purified MaNifH (cropped image of original). Lane 1, MW marker; lane 2, MaNifH. **B.** SDS-PAGE of purified Strep-NifD (cropped image of original). Mass spectrometry has previously confirmed that NifK copurifies with Strep-NifD from *M. acetivorans*. Lane 1, MW marker; lane 2, Strep column eluate (NifDK). NifH was heterologously purified from *E. coli*, NifDK directly from *M. acetivorans*.

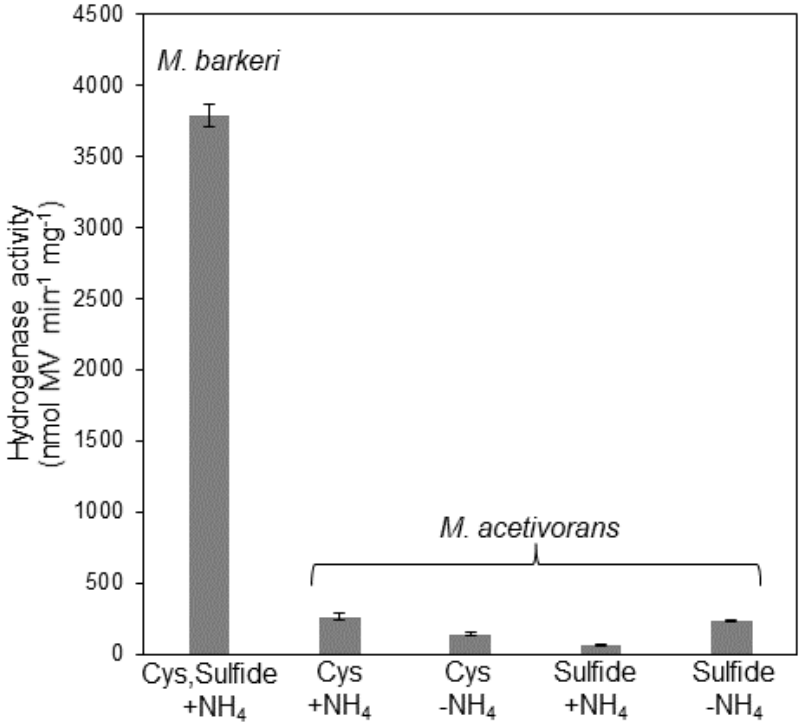

Figure 11. Hydrogenase assays of cell-free lysates. Specific activity is defined as nmol of methyl viologen reduced * min^{-1} * mg^{-1} of soluble protein. *M. barkeri* was grown non-diazotrophically with cysteine and sulfide. *M acetivorans* was grown diazotrophically ($-NH_4$) or nondiazotrophically ($+NH_4$) with cysteine or sulfide as indicated. All bars represent mean ± SD of triplicates, except *M. barkeri*, which was a duplicate.

Table 1. Strains and plasmids used in this study

Name	Description	Source or reference
	Strains	
E. coli		
DH5α	Cloning strain	NEB
WM4489	DH10β-derived host to boost copy number of pJK- and pDN-derived plasmids containing *oriV*	(Eliot *et al.*, 2008)
M. acetivorans		
WWM73	Δ*hpt*::P*mcrB-tetR*-ϕC31-*int*-attP	(Guss *et al.*, 2008)
DJL60	WWM73 Δ*iscSU2*::*pac-hpt*	(Deere *et al.*, 2020)
DJL63	WWM73 Δ*sufCB2*	This study
DJL91	WWM73 λattB::pDL243	This study
DJL92	WWM73 λattB::pDL244	This study
	Plasmids	
pDL243	pDL734 with sgRNA to target *isc1* for CRISPRi	This study
pDL244	pDL734 with sgRNA to target *isc2* for CRISPRi	This study
pDL245	pDL734 with faulty sgRNA meant to target *isc3* for CRISPRi	This study
pDL734	pDN203-derived vector for CRISPRi-dCas9 system, pDL238 analog with Cas9 mutated to dCas9	(Dhamad & Lessner, 2020), This study
pDN203	Vector for HDR CRISPR/Cas9 editing, contains sgRNA for *ssuC* gene	(Nayak & Metcalf, 2017)

Table 2. Acetylene reduction activity of lysates and proteins.

Sample	Nitrogenase activity[b]
WWM73, cysteine-grown	0.41
WWM73, sulfide-grown	1.06
A. vinelandii	14.23
MaNifHDK[a]	50.7

[a] Calculation based on mg NifDK; 3.04 mg NifH was added to 0.277 mg NifDK.
[b] Nitrogenase activity (nmol ethylene evolved min^{-1} mg^{-1} protein)

CONCLUSIONS

Methanosarcina acetivorans likely does not rely on a single pathway of Fe-S cluster biogenesis directly analogous to the systems found in bacteria and eukaryotes. Its genome encodes multiple homologs of genes predicted to function in Fe-S cluster assembly, and this complexity, along with the metabolic adaptability it may confer, can make genetic analysis challenging. The centrality of Fe-S proteins in the pathways of methanogenesis, together with methane's importance as both a fuel source and as a driver of anthropogenic climate change, make the study of Fe-S cluster biogenesis in methanogens a challenge worth pursuing. That these organisms may grant us a window into earlier life on Earth and a better understanding of how microbial life has evolved is further enticement, especially in light of the methanogens' status as the likely first nitrogen-fixing organisms.

This dissertation examined Fe-S cluster biogenesis in genus *Methanosarcina*, specifically *M. acetiovorans*, presenting a model in which ISC-type systems are used when cysteine is the sulfur source for growth, and SUF-type systems are used when the methanogen is growing with inorganic sulfide. This hypothetical model was first tested by evaluating the role of ISC-type systems for [Fe-S] assembly. Three such gene clusters were identified and the one believed to be the most highly expressed in wild-type *M. acetivorans* was deleted from the genome. Various aspects of growth were examined in this Isc2 deletion strain. **Deletion of the genes for IscS2 and IscU2 did not eliminate the ability to grow on cysteine, nor result in any serious growth defect under standard conditions for growing *Methanosarcina acetivorans,* but intracellular sulfur metabolism was altered.**

Related systems for Fe-S biogenesis and delivery were targeted for deletion, including ApbC, a predicted [Fe-S] carrier protein nearly universally encoded in genomes of microbes in

the domain Archaea. The more highly expressed of the two putative SUF systems in *M. acetivorans* was also deleted, using a new CRISPR/Cas9 system for genome editing in this methanogen that greatly facilitates the generation of markerless mutants that can be further mutated or complemented *in trans*. SUF systems are believed to be primordial in domain Archaea and are also nearly universally encoded by microbes in this lineage. Various growth conditions were tested for the ApbC and Suf2 deletion strains. **Neither ApbC nor the Suf2 system is essential in *M. acetivorans,* but ApbC is implicated in growth on different sulfur sources, especially thiosulfate, and possibly in growth on the methanogenic carbon substrate acetate The role of SUF systems in growth under these conditions is unknown.**

The final avenue of investigation presented in this dissertation dealt with nitrogen fixation in *M. acetivorans*. Nitrogenase is a highly complex assemblage of proteins binding a number of unique Fe-S clusters, which in bacteria are served by a dedicated system of [Fe-S] biogenesis, NIF, that is not encoded by diazotrophic methanogens. The genomic requirements for nitrogen fixation were tested using mutants generated for the earlier projects, as well as new strains subject to ISC gene repression using a recently created CRISPRi system for interference of transcription. **Nitrogen fixation in *M. acetivorans* relies on the products of the Isc2 gene cluster for optimal growth, but only when cysteine is the sulfur source, and nitrogenase activity can potentially serve as an important indicator for the cell's ability to assemble and deliver Fe-S clusters target apo-proteins.**

The results from this dissertation indicate that Fe-S cluster assembly in methanogens does not follow a simple schema, and that the genomic complexity of *Methanosarcina acetivorans* undergirds a metabolic flexibility that makes dissecting biosynthetic pathways challenging. They also serve as a reminder that bioinformatics, while important in guiding hypotheses and

interpreting large datasets, is not the final word in predicting metabolism in prokaryotes. A gene like ApbC or SUF systems may be nearly universally conserved in a lineage like the domain Archaea, but still be relatively dispensable in a given organism. Future studies of [Fe-S] biogenesis in *M. acetivorans* can make use of the strains generated and techniques demonstrated herein to create multiple mutations within a single strain, and test these mutant strains for their ability to assemble functional Fe-S protein complexes like nitrogenase. It is possible that all three putative ISC gene clusters and both putative SUF gene clusters could all be eliminated from this methanogen's genome without lethality, which would indicate the presence of some entirely unknown and previously undescribed system for Fe-S cluster biogenesis, perhaps revealing ancient pathways not yet conceived of by microbiologists.